Engineering Failure Analysis 130 (2021) 105798

Contents lists available at ScienceDirect

Engineering Failure Analysis

journal homepage: www.elsevier.com/locate/engfailanal

Review

Failures and leak inspection techniques of tube-to-tubesheet joints: A review

Dinu Thomas Thekkuden [a], Abdel-Hamid Ismail Mourad [a,b,c,*], Abdel-Hakim Bouzid [d]

[a] Mechanical Engineering Department, College of Engineering, United Arab Emirates University, Al-Ain, P.O. Box. 15551, United Arab Emirates
[b] National Water and Energy Center, United Arab Emirates University, Al Ain, P.O. Box. 15551, United Arab Emirates
[c] On Leave from Mechanical Design Department, Faculty of Engineering, El Mataria, Helwan University, Cairo, Egypt
[d] Ecole de Technologie Superieure, 1100 Notre-Dame Quest, Montreal, Quebec H3C 1K3, Canada

ARTICLE INFO

Keywords:
A review
Heat exchanger
Tube-to-tubesheet joints
Failure mechanisms
Leak inspection and prevention

ABSTRACT

The integral components of heat exchangers and in particular the tubes, tubesheets and tube-to-tubesheet joints have vital roles in the proper functioning of this equipment. Several frequent instances of heat exchanger premature failures at the tube-to-tubesheet joints reported in the past decades have resulted in a huge investment loss. As a counter measure, proper case studies of failure followed by maintenance are commonly practiced in the industry. Several accidents were originated from the failure of heat exchangers and therefore, failure analysis for the root cause is inevitable to take precautionary measures for avoiding similar catastrophes. Proper regular online and offline inspections of heat exchangers are useful to predict the effectiveness and performance of the heat exchanger. Many leak inspection techniques are currently in use to identify the leaks in and around the tube-to-tubesheet joints. Review articles addressing the importance of tube-to-tubesheet joints and problems are scanty. Therefore, this review discusses the major root causes of heat exchanger failures and recommended preventive remedial measures followed by the leak inspection techniques relevant to the heat exchanger tube-to-tubesheet joints. The information discussed in the article is promising for researchers and professionals working in the field of heat exchangers.

1. Introduction

There are several reported incidents of heat exchanger failures that caused the collapse of heat exchangers before completing the estimated lifetime in the past. These premature failures of heat exchangers cause interruptions in production resulting in huge financial losses. Malfunction of heat exchangers in thermal power plants, oil refineries and nuclear power plants causes a drastic effect on productivity and profit. The cost incurred during the repair of a heat exchanger fouling is around 0.25% of the gross domestic product in many countries. A pie chart indicating the expense due to fouling alone in different countries is shown in Fig. 1. Literatures of heat exchanger failures prove that the most critical part exposed to these failures is tube-to-tubesheet joints (TTJ) at the tube entrance. Many researchers have put efforts into conducting failure analyses of heat exchanger components and identifying the root causes.

* Corresponding author at: Mechanical Engineering Department, College of Engineering, United Arab Emirates University, Al-Ain, P.O. Box. 15551, United Arab Emirates.
E-mail address: ahmourad@uaeu.ac.ae (A.-H.I. Mourad).

https://doi.org/10.1016/j.engfailanal.2021.105798
Received 16 June 2021; Received in revised form 30 September 2021; Accepted 8 October 2021
Available online 12 October 2021

Nomenclature

AE	Acoustic emission
HSE	Health and Safety Executive
IOB	Iron oxidizing bacteria
LSR	Lowest stress ratio
MAWP	Maximum allowable working pressure
MIC	Microbiologically influenced corrosion
NDDCS	Natural draft dry cooling systems
PWHT	Post weld heat treatment
SCC	Stress corrosion cracking
SR	Stress ratio
SRB	Sulfate reducing bacteria
TDS	Total dissolved solids

These post analyses have been beneficial to engineers for taking preventive measures as early as in the initial stage of fabrication. However, many repeated premature failures of heat exchangers with similar root causes indicate the need for a comprehensive review covering the aspects of root causes and preventive techniques.

Heat exchanger tubes of ammonia evaporators installed at the coastal region in China with an estimated lifetime of 15 years failed due to a wall thinning phenomenon one year after commissioning [1]. Similar premature failures of evaporators have also been reported in polyurethane plants operating with o-dichlorobenzene and ammonia media where insufficient thermal treatment, stress corrosion cracking, and strain ageing embrittlement at the tube and shell sides have been identified as the main causes [2-6]. In Al Khafji plant, the stress corrosion cracking caused the rupture of tubes at the tube-to-tubesheet joints [7]. Welding, expansion, and a combination of welding and expansion commonly used to produce tube-to-tubesheet joints result in localized mechanical and thermal stresses at the joints. Stress corrosion attack in tube-to-tubesheet joints is a common phenomenon that is accelerated when highly stressed regions are in contact with corrosive media. According to Chang et al., parts of the tubes inserted in the tubesheet in multiple steam generators of nuclear power plants are exposed to guillotine cracks [8]. Karwoski et al. pointed out instances of shutdown in Main Yankee, Haddam Neck, Zion 1, Zion 2, Trojan, and San Onofre 1 reactors because of steam generator tube ruptures [9]. Within few months of commissioning, Sherritt International discovered corrosion in 165 out of 860 stainless tubes in a high-pressure still condenser used for ammonia recovery [10]. In this case, corrosion has only affected the joints produced by rolling expansion followed by seal welding, with the rest of the tube and tubesheet regions remaining unaffected. The failure analysis report of Guo et al. further validated this major finding stating that the SCC and weld micro fissures at the joint were the main reasons for the failure of stainless steel tube bundle in condensate/heavy gas oil heat exchanger in a petrochemical plant [11]. Xu et al. investigated a shell and tube heat exchanger for dimethyl to propylene in which the failure of the tube near the joint was observed during the operation soon after

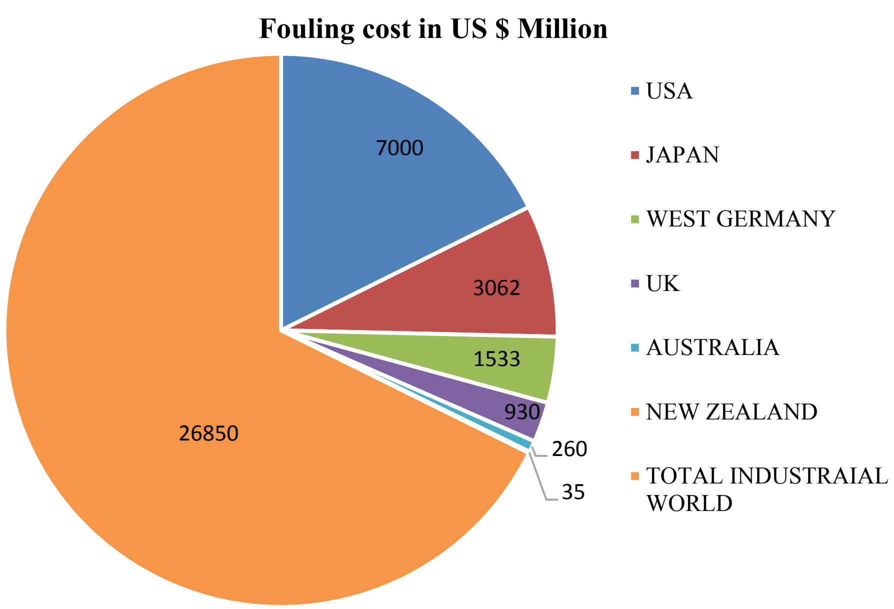

Fig. 1. Estimated fouling costs in different countries [16].

commissioning. In their study, the cracks generated at the tube and tubesheet region propagated as a result of stress corrosion cracking, thermal fatigue and localized corrosion [12].

Therefore, an inspection of tube-to-tubesheet expanded joints, tube-to-tubesheet welds, and shell joints is highly needed regularly based on the evidence. Brennenstuhl et al. reported that Microbially Influenced Corrosion (MIC) in stainless steel heat exchangers caused damage of approximately $55 million within 8 years [13]. Malik et al. has reported various failures and collapse of the boilers in a case study report [14]. The boilers in shoiba phase II, Al Jubail, Madina- Yanbu, Al Khafji plants had severe tube failures. In these plants, the flame impingement, creep, intergranular and transgranular SCC, scales, the presence of foreign elements S, V, Ca and K were the key causes. In most of the cases, the tube wall thickness at the affected regions reduced by 5–8% due to scale induced corrosion. Thinning of the tube making up to 65% loss due to corrosion at the tube-to-tubesheet welds led to the failure of vertical acid reboiler in Celanese Chemical Co. Nanjing, China. The strong welded or expanded joints gradually weakens causing leaks as a result of hot and localized corrosion. The use of tube end shields, plugs and collars are the remedies to cease specific tubes from the operation. The cracks at the seal expanded region in a shell and tube heat exchanger for dimethyl ether to propylene project is shown in Fig. 2. There are further instances where 50% of the tube thickness is corroded away from the parent material [15]. In this case, the chloride-induced crevice and pitting corrosion were observed in the stainless steel tubes near the region where the tubes were kept tightened using a rope during the transit or service period.

According to TEMA standard, seal welding and strength welding are required wherever tightness and leak-proof at tube-to-tubesheet joints are mandatory. In conventional cases, the gas tungsten arc welding process is commonly used for joining tube-to-tubesheet. The tube-to-tubesheet joints can be categorized according to the joining processes: (1) expansion joint, (2) welding joint, (3) joint with a combination of expansion and welding. Otegui and Fazzini found the emanated cracks from the tube-to-tubesheet joints in a heat exchanger (shell side: water at 121 bar and 246 °C; tube side: gas at 6 bar and 593–399 °C) [17]. Here, the SA-213T11 tube was expanded followed by welding against SA-336 F11 C12 tubesheet. The tubesheet was forged, quenched from 995 °C and tempered to 730 °C. The joint was post-weld heat treated (PWHT) to relieve the residual stress. The primary and secondary cracks were found to have originated from the bottom side of the weld between the tube-to-tubesheet interstice and propagated through the heat affected zone. The radial and circumferential cracks emanating from the tube-to-tubesheet are shown in Figs. 3 and 4. Leak through transverse cracks is shown in Fig. 5. Under the action of internal pressure, the secondary crack propagates from the exceeded critical crack sized cracks [18].

High mechanical loads, ineffective PWHT inducing the residual stresses are the factors propagating the cracks. The weld edge preparation is an important task prior to welding. The weld should be properly fused or else the plate can shear along the thickness [20]. Different geometrical conditions and orientation at the tubesheet have a crucial significance on the joint strength. Thekkuden et al. emphasized that the optimal expansion pressure and presence of grooves produce a leak-proof joint with adequate joint strength [21,22]. Wei and Ling proved that the welding on the geometry with the tube projected from the tubesheet provide greater pull-out strength and fatigue life when compared to welding on the flush joint and tubesheet with grooves [23]. Azevedo et al. investigated a collapsed heat exchanger in a styrene plant with benzene and water vapour as mediums. 45% of the total 1500 tubes failed due to cracks emanating from the tube surface and welded tube-to-tubesheet regions [24]. The cracks at the weld region are due to high carbon enrichment as the fraction of the carbides varying from 4% to 33%. Apart from the carbon embrittlement, the overload is also attributed to the brittle crack propagation caused by the jamming of the floating tubesheet during the maintenance operation [24]. The carbon embrittlement and overload increase the brittleness, which in fact, favour the crack initiation and propagation. According to Mcintyre, erosion-corrosion, mechanical and thermal fatigue, stress corrosion cracking and overheating are the major causes for the failure in heat exchangers [25]. Additional cases of premature heat exchanger failures, location of defects in and around tube-to-tubesheet joints, factors, period of service and preventive measures that signifies the importance of review are listed in Table 1.

In summary, improper design of the tubes and tubesheets, overheating, mal-operation, incorrect water-treatment, joint leaks, presence of oxygen, sulfur, chlorine and vanadium, high mechanical loads, improper post-weld heat treatment, high content of carbon, fouling and thermo-mechanical stresses are the causes for the failure of tube-to-tubesheet joints, tubes and tubesheet adjacent to tube-to-tubesheet joints. Even though there are recurrent cases of heat exchanger failures, there are no predication rules or methodology to

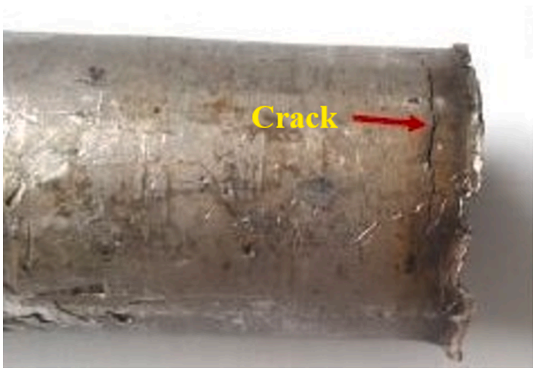

Fig. 2. Crack in the outer tube surface close to tube-to-tubesheet joints [12].

Fig. 3. Radial cracks at TTJ [17].

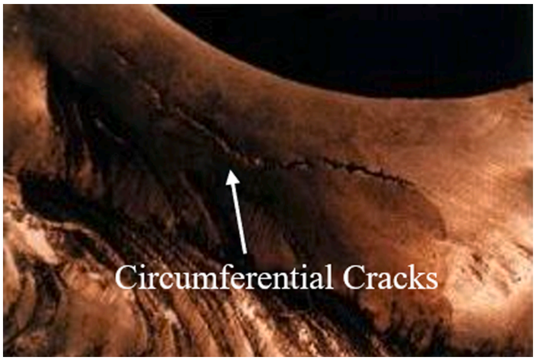

Fig. 4. Circumferential crack at TTJ [17].

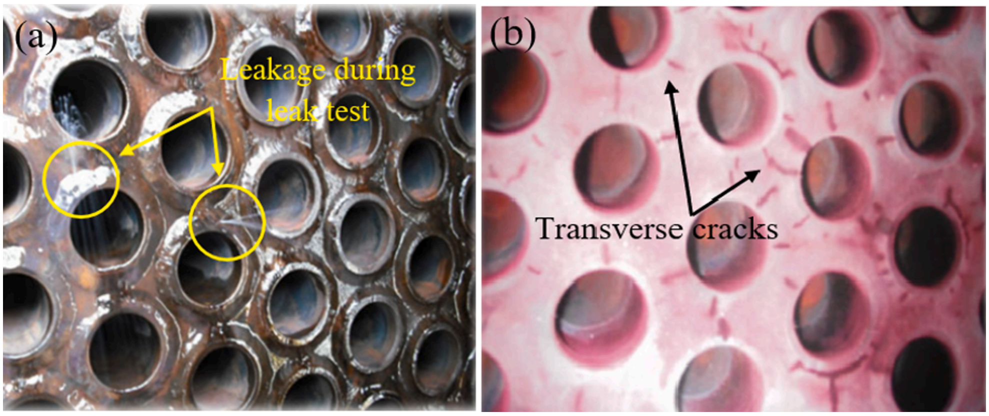

Fig. 5. Leak. (a) leak through cracks [19] (b) Transverse cracks [19].

completely avoid the failure of heat exchangers. The identification of the exact reasons that can lead to the collapse of the heat exchanger during the operation is very complex. Therefore, based on the frequent occurrences of failures and literature review, a comprehensive study of factors affecting the failure, preventive measures and leak inspection techniques focusing on the region around the tube-to-tubesheet joints is highly demanded. The main objective of the paper is to address the failure mechanisms associated with the tube-to-tubesheet joints, factors influencing the failures, preventive measures and leak inspection techniques.

Table 1
Details of premature failures of heat exchangers.

No.	Cases of heat exchanger failure	Location of failure	Period of service (months)	Material	Tube side medium	Application	Root causes	Counter measures
1	Failure analysis of titanium heater tubes and stainless steel heat exchanger weld joints in nitric acid loop [26]	Tube-to-tubesheet weld joints	13.7	• Titanium (tube) • SSL304 (Tubesheet)	• Nitric acid	• Nuclear spent fuel reprocessing	• Hydrogen-induced cracking • Intergranular corrosion	• Periodic inspection and removal of corrosion products
2	Fatigue cracking of a shell tube heat exchanger [27]	Tube-to-tubesheet welded joints	1	• SS 304 (Tube) • SA 516 gr.70 (Tubesheet)	• Water vapour	• Cool the steam	• Periodic load • Resonant vibration • Bad welds • Improper expansion position	• Improve the quality of welding and expansion
3	Cracking of heat exchangers with dissimilar weld [28]	Tube-to-tubesheet joints	Few hours into service	• SA 106 (Tube) • 2205 Duplex stainless steel (Tubesheet)	• Hydrogen sulfide	• Hydrogen sulfide application	• Sulphide stress corrosion	• Make environment free of water and water vapour
4	Korean nuclear power plant [29]	Tube and tubesheet joints	480	• Alloy 600 (Tube) • LA steel (Tubesheet)	• Hydrazine and Ammonia	• Steam generation	• Denting • SCC • Pitting	• Addition of boron - reduction of dissolved oxygen • Tube plugging - suppression of impurities • Temperature reduction of primary water • Crevice flushing –T102 addition - control of dissolved oxygen - power reduction to 85% - Na/Cl
5	Intergranular cracking at the weld joints of 347H boiler tubes [30]	Tube-to-tubesheet joints	5	• 347H austenitic stainless steel (Tube)	• Water	• Steam generation	• Formation of Cr carbides • Dissolution of Nb carbide in weld heat affected zone • High tensile stress	• Reduce the welding passes with no compromise on the joint strength
6	Premature Failure of Heat exchanger for Dimethyl ether to propylene in early startup operation [12]	Tube-to-tubesheet joints	0.26	• S30409 • (Tubes) • S30408II • (Tubesheet)	• Water + propylene	• Reactor	• Stress corrosion cracking • Polluted medium with catalyst and chloride content • 7High tensile stresses due to seal expansion process	• Reduce the chloride ion • Perform stress relieving operation
7	Failure of heat exchanger in a gas plant [19]	Tube-to-tubesheet joints	NIL	• ASTM A 179 (Tube) • ASTM A	• Steam	• Gas generation in gas plant	• Poor workmanship and welding	• Post weld heat treatment to reduce the residual stresses and detrimental

(continued on next page)

Table 1 (*continued*)

No.	Cases of heat exchanger failure	Location of failure	Period of service (months)	Material	Tube side medium	Application	Root causes	Counter measures
				• 387 grade 11 (Tubesheet)			• Stress corrosion cracking	effect of high temperature • Heat treatment softens the heat affected zone and restores the toughness • Qualify the welder using mock-up joint inspection prior to fabrication
8	Pin hole leakage of heat exchangers used for air conditioning [31]	Tubes	2	• Copper	• Halocarbon gas	• Air conditioning	• Ant-nest corrosion • Organic contaminants	• Use of lubrication oils with low carboxylic acid • Drying and sealing of the tubes • Removal of contaminants
9	Bursting of the spiral wound heat exchanger tubes in a nuclear power plant [32]	Tubes	NIL	• SS304L	• Deionized water	• Nuclear power generation	• SCC • High chloride content and hot alkaline environment	• Use corrosion resistant materials • Control the quality of the mediums
10	Perforation in methacrylic acid reboiler [33]	Tubes	120 (Expected life: 240 months)	• SS314	• Methacrylic acid	• Chemical plant	• Erosion	• Increase the tube side fluid velocity
611,111	Stress corrosion cracking of heat exchanger tubes [12]	Tubes	0.26	• Austenitic stain less steel	• Propylene	• Reactor	• Increased Chloride content • High tensile stress due to seal expansion	• Control the purity of the medium • Reduce the chloride ions
12	Leak in finned heat exchanger [34]	Tubes	During commisioning	• Copper		• Air conditioning	• Ant nest corrosion	• Use surface inhibitors and coatings • Control the humidity in the environment
13	Premature failure of Ammonia evaporators after 1 year of commission; expected with 15 years lifetime [1]	Tubes	12 (Expected life: 180 months)	• 10 Carbon steel (Tube) • 16MnIII • (Tubesheet)	• o-dichlorobenzene	• Ammonia evaporator	• Uniform corrosion and pitting due to high Cl−, S and CO2. • Erosion	• Control Chloride ions and water vapour from the upstream • Recommended expansion followed by seal welding • Cleaning during shut down
14	Frequent failure of heat exchanger in a nuclear power plant located in China [35]	Tubes	36	• ASME SB-338 Gr.2 Titanium (tube) • Carbon steel (Tubesheet)	• Seawater	• Cooling water system in nuclear power plant	• Fouling with sediments, rubber debris and sea shells in desalinated water • Fretting • Erosion	• Reduce the velocity to 2 m/s to prevent erosion • Removal of sediments during routine inspection • Filter the desalinated water from sea using a

(*continued on next page*)

Table 1 (*continued*)

No.	Cases of heat exchanger failure	Location of failure	Period of service (months)	Material	Tube side medium	Application	Root causes	Counter measures
							• Mechanical damage during installation	mesh size less than 10 mm
15	Leakage of heat exchanger in a Chinese nuclear power [36]	Tubes	36	• Titanium Gr.2 (tube) • Carbon steel (Tubesheet)	• Seawater	• Cooling water system in nuclear power plant	• Hydrogen assisted corrosion • Galvanic and crevice corrosion in the gaps between tube and tubesheet • Inward bulging of tubes due to hydrogen blistering	• Seal the gap at the tube-to-tubesheet joint location using a polymer resin seal
16	Ying-Yang corrosion in purified terephthalic acid dryer heat exchanger tubes [37]	Tubes	24	• 316L stainless steel (Tube)	• Steam	Purified terephthalicacid (PTA) dryer	• Pitting corrosion with Ying-Yang corrosion morphology	• Limit the chloride ion in NaOH alkaline wash liquor below 30 ppm to prevent pitting corrosion • Bromine ion containing catalysts should controlled in the oxidation unit • Monitoring the surface conditions of tube
17	Failure of heat exchanger in Ethylene plant [38]	Tubes	9	• 10 carbon steel (Tube)	• Steam	• Ethylene production	• Pitting and acidic corrosion • Presence of Cl^- and S ions • Caustic embrittlement • High pH fluctuation	• Reduce NaOH solution to less than 5% • Alkali liquor and phosphates can control the pH • Limit the presence of chloride ions
18	Failure of oil–gas separator vessel [39]	Tubes	3	• AISI 1045	• Crude oil	• Oil-gas separator vessel of desalination unit	• Localized corrosion due to hot corrosive gases such as H_2S, CO_2. etc. • Increased proportion of inorganic compounds	• Use protective coatings • Control temperature, addition of emulsifier and water to oil ratio
19	Failure of jacket pipe in a double pipe heat exchanger [40]	pipes	12(Expected life: 180 months)	• ASTM SA 106 gr. B	• unpolymerized ethylene gases + low-molecular-weight polyethylene oligomers	• Cool in the recycling of ethylene gases	• Uniform corrosion • Fouling • Erosion	• Descaling the inner side of pipes • Improve the quality of the cooling water • Upgrade the pipe materials
20	Cracking of plate heat exchanger [41]	Plates	172.6	• ASTM B265 Grade 1Titanium	• Sea water	• To decrease fresh water temperature	• Mechanical fatigue • Presence of titanium hydride	• Reduce the formation of titanium hydride

2. Root causes and preventive measures

2.1. Mechanical loads

2.1.1. Erosion – corrosion

The tube side and shell side heat transfer media flow continuously in a pressurized heat exchanger with a certain velocity depending on the required heat transfer rate. A considerable layer of metal in the form of ions or corroded metal products is removed from the metal surface because of the interaction of media in an erosion-corrosion process. As a consequence of tube thinning, the leak will be started. The main factors affecting the erosion-corrosion in heat exchangers are high velocity, turbulence, impingement and impingement angle, presence of solid sediment particles in nano and micro scale, particle size of impurities, tube bends, mechanical cleaning and presence of high chlorine content and vapours.

Anna Kosnica et al. claimed that the impurities at the nano and micro scale present in the medium can initiate the erosion along the tube walls and tube inlets at tube-to-tubesheet joints. The erosion increases with the larger particle size whereas the low mass of the nano particles reduces the erosion rate considerably [42]. Tube-to-tubesheet joints [43], tube bends [44] and the tube near baffles are the most affected structural parts due to the direct hitting of media with suspended particles at a higher impingement angle. Weimin et al. reported the catastrophic behaviour of erosion increases sharply with the decrease in the particle size [45]. But Habib et al. proved that the above particle size dependency on the erosion rate is valid only at a lower header inlet velocity whereas the particle size effect is negligible at higher inlet velocities [46]. Willem et al. found out that the influence of velocity on the erosion-corrosion is higher than on individual erosion or corrosion due to the combined effect of erosion and corrosion [47]. The debris is mostly accumulated on the tubesheet at the tube-to-tubesheet joints causing irregular velocity and turbulence. A fast streaming velocity causes oscillation in the tube resulting in the wear of tube and baffles while turbulence develops a local pressure surge and shear stresses carving out the material [48]. In addition, turbulence is also developed at the tube and shell inlets due to the splitting of media into small particles having localized velocities. The combination of turbulence and high localized velocities at a higher operating temperature has a synergistic effect on accelerating the damage of tube-to-tubesheet joints. Hot vapours and bursting of the bubbles at the tube entrance also accelerate the deterioration process. High pressure at a lower impingement angle exerted by water and air jet for flushing the scales out during a periodic inspection causes erosion [33]. Other than the velocity, the flow impingement angle and flow patterns are also found to affect the erosion corrosion-induced corrosion. Based on the experiments conducted by Khayatan et al., the particle force at various angles on the tubes depassivate layer from the metal and they concluded that the highest erosion rate is observed at the impingement angles ranging from 30° to 50° whereas the highest corrosion rate is observed at the impingement angles from 40° to 60° [49]. Frequent number of the impacts, high normal and low tangential stresses are the reasons for corrosion at a higher impingement angle. The schematic representation showing the erosion-corrosion is shown in Fig. 6. The erosion at the tube-to-tubesheet joints is depicted in Fig. 7.

Erosion due to low flow velocity and the presence of extraneous particles sedimented at the tube-to-tubesheet joint is one of the major reasons for the collapse of Cu-5Ni tubed heat exchanger in steam power plant [51]. High amount of solid sediments in crude methanol used as a process tube-side medium in a heat exchanger used for petrochemical refinery is the cause for the failure according to the analysis of Rezaei et al.[52]. Similarly, Kuznicka pointed out the main reasons for the premature failure of 9 out of 118 tubes in a heat exchanger that lasted less than 5 years are high presence of chlorine and solid sediments [53]. The failure analysis of heat exchanger failures by Ni et al. [33], Gong et al. [35], Gong et al. [40] from Table 1 proved erosion followed by corrosion as one of the major factors for the early failure of heat exchanger. Pandey found out the impingement caused by the sea water velocity exceeding 3.5 m/s and a considerable loss in the Fe content has caused the early failure of condenser in a crude distillation plant of petrochemical

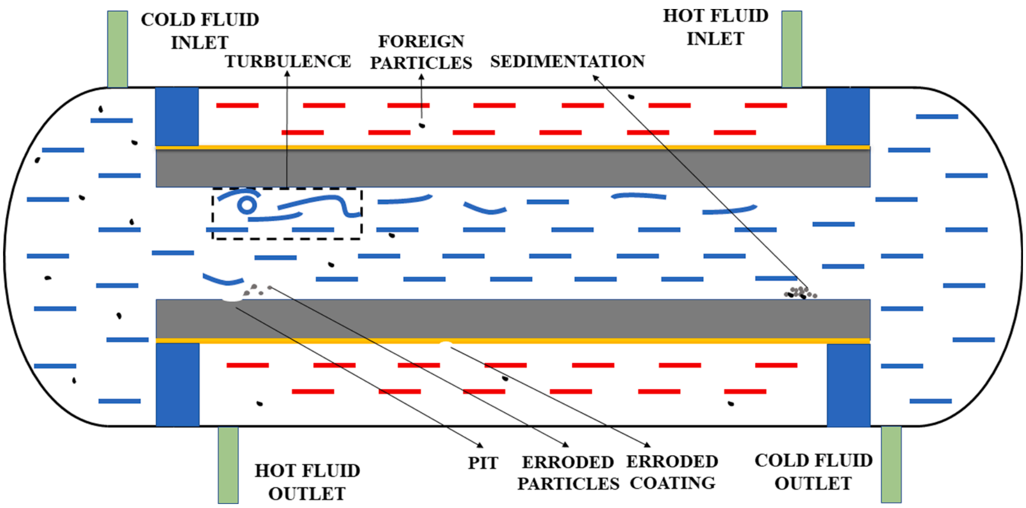

Fig. 6. Schematic representation showing factors affecting erosion-corrosion.

Fig. 7. Erosion at Tube-to-tubesheet [50].

refinery [54]. Li et al. concluded turbulence, velocity exceeding the threshold and suspended slit particles as the main reasons for the collapse of condenser in a 150 MW thermal power plant [55]. However, a synergistic effect of erosion and corrosion caused the complete degradation of finned tube heat exchanger at half of the threshod velocity [56]. Further, erosion-corrosion was the primary cause for the collapse of Al-Wajh multiple effect distillation condenser in a desalination unit [57].

Selecting the erosion resistant tube with protective coatings and tubesheet material prevents erosion-corrosion to a greater extent. Erosion-corrosion can be considerably reduced by choosing the materials with high hardness, stiffness and toughness [58-60]. Meuronen recommended 10CrMo910 chrome moly steel over 15Mo3 and St35.8 carbon steels due to high erosion resistance in the tube blanks exposed to moving air with solid particles [61]. CFD analysis based on near wall turbulence intensity is beneficial to predict the possibility for erosion-corrosion [62]. Lai and Bremhorst suggest using prismatic flow correcting devices to develop uniform axial flow preventing erosion-corrosion to a larger extent compared to deflectors and fences at the tube inlets in shell and tube heat exchangers [63]. Use of infiltration techniques and magnetic plugs, welding overlays, cathodic protection of materials can prevent erosion-corrosion. The carbide and nitride coatings on the slightly impaired tubes applied using any of the techniques such as high velocity oxy fuel, plasma coating, supersonic gas stream can effectively increase the life of the heat exchangers. Tungsten carbide coatings exhibit high erosion and corrosion resistance at extremely high temperatures while chromium carbide coatings are dominantly good against erosion at high temperatures. Titanium nitride is recommended for low impingement angle erosion protection. Similarly, ceramic coatings such as aluminum oxide-ceramic, chromium oxide-ceramic, zirconium oxide ceramics have unique characteristic to provide erosion protection in an acidic environment. Reducing the oxygen in the fluid and controlling the pH value of the fluid help to arrest erosion corrosion. Badr et al. recommended limiting the fluid velocity within the threshold in case particulates cannot be separated from the media completely [64].

2.1.2. Liquid droplet impingement erosion

Steam is produced from the water in the shell side of the steam generators using the heat produced in a nuclear reactor core. This steam may contain liquid droplets due to the insufficient temperatures required to convert to steam or environmental conditions. These liquid droplets in the steam passing through the tube and shell flowing at a velocity hit on the tube and tubesheet surface. This impingement of droplets on the tube and tubesheet with an impact pressure acting in a short time span of nano-seconds result in the erosion of metal from the hit region. This kind of erosion due to liquid droplet impingement is termed as liquid droplet impingement erosion. Pressure of liquid droplets in steam, density of drops, velocity of liquid drops, impact pressure greater than the stagnation pressure, impingement angle, surface roughness and hardness of tube and tubesheet material and specific locations such as inlet, vent tube and tube bends are the major factors influencing the liquid droplet impingement erosion. The liquid droplet erosion is different from the cavitation erosion, being the difference be, the liquid droplets in the gaseous flowing medium cause liquid droplet erosion while gas bubbles suspended in the flowing liquid phase cause the cavitation erosion. In both cases, the impact pressure is more than the stagnation pressure in the heat exchangers. The schematic representation differentiating liquid droplet impingement erosion and cavitation corrosion is shown in Fig. 8. The various stages in the liquid impingement erosion process involve the preliminary stage involving incubation, acceleration and steady maximum erosion rate followed by the final stage in which the erosion rate decelerates until reaching a terminal steady erosion rate [65]. This erosion is a time dependent process caused by the repetitive action of impingement by droplets. In the incubation stage, the impact pressure only increases the surface roughness by forming nano and micro pits without any indicative weight loss. After the initial stage, these micro pits coalesce aggravating the erosion process with a higher erosion rate. Before the final rupture, the erosion rate increases constantly for a long duration depending on the impact pressure followed by further deceleration. Two major force components, normal and shear as a result of impingement, play a critical role on the extent of degradation.

Ahmad et al. found that the 90° impingement angle has a devastating effect on the target surface since the normal component is the highest [66]. Ferng and Horng identified the steam inlet tube and vent tube as the critical parts in a heat exchanger that undergoes severe wall thinning due to steam impingement erosion [67]. Essentially, the density, impact pressure and acoustic velocity of the single droplet are the factors affecting the liquid droplet impingement erosion [68]. In addition, Fujisawa et al. found out the surface

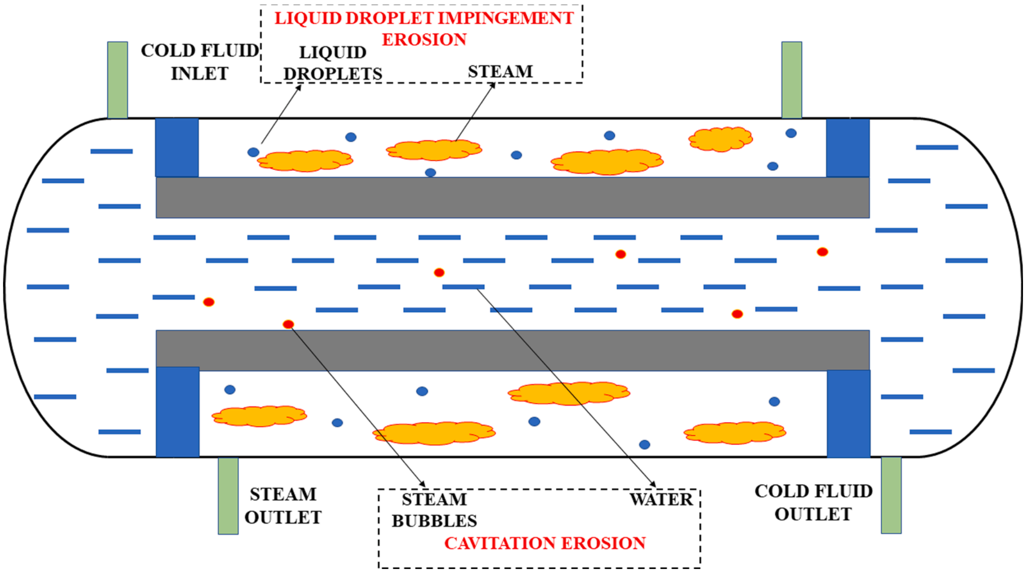

Fig. 8. Schematic representation differentiating liquid droplet impingement erosion and cavitation corrosion.

roughness of the tube wall affects the impingement erosion stages. As the surface roughness increases, the incubation period decreases and the erosion rate increases [69]. However, a liquid film on the rough surface acts as a smooth surface and effectively dampers the impingement erosion process [70,71]. Roughening of the surface and perforation are the end results of steam impingement and is therefore considered as a major defect in condensers. Kirols et al. agree on the fact that the initial surface roughness has a significant effect on the liquid droplet impingement erosion behaviour [72]. The material properties of tube and tubesheet are important design factors in preventing the liquid impingement erosion attack. In 1993, Nava et al. reported that the erosion-corrosion resistance decreases as the substrate hardness increases at high temperatures [73]. But the results of Fujisawa et al. contradict to above relation stating that the erosion rate decreases as the hardness and thin film layer increase [74]. The higher the hardness, the higher is the erosion resistance. The droplet impingement erosion is one of the common failure reasons in a steam generator of sodium-cooled fast reactor. The droplet impingement erosion can easily initiate leakage that results in a chemical reaction followed by high flame propagation. Xiong et al., identifying the impact of droplet impingement erosion, conducted a numerical analysis with moving particle semi-implicit method for all speeds on water, sodium and sodium hydroxide droplets and found the pressure load was independent of the droplet size [75].

Ranjbar found out the copper alloyed tubes at the inlet of tube-to-tubesheet joints in steam powerplant heat exchanger suffered dealloying and impingement attack at a low velocity medium flow filled with sediments after collecting extraneous particulates from the tubesheet [51]. Javidi et al. found liquid impingement erosion and water droplet erosion as the main causes for the damage of output nozzle of air cooled heat exchanger in a natural gas refinery [76]. Malik et al. reported a case study where the evaporator brass tubes in multiple effect distillation plant failed due to liquid impingement attack of flowing sea water exceeding 2 m/s [77]. Ke reported the failure of heat exchanger tubes in continuous catalytic reforming pre-hydrotreater was caused by liquid droplet impingement erosion and improper operating temperature [78].

As a precautionary method, the use of erosion resistant material with high hardness is widely preferred to prevent liquid droplet impingement erosion. An appropriate temperature should be maintained for the steam medium to be in the vapour state. Smith invented tube shields to protect the first few rows of tubes at the entrance that are exposed to impingement and erosion close to inlets [79].

2.1.3. Vibrational failures

The past evidence of heat exchanger inspection indicates the significance of controlling the vibration due to many reported vibration-induced heat exchanger failures. The main reasons for the formation of vibration-induced vibration are the accumulation of debris restricting the flow, turbulence, interactions of tube-to-tubesheet and tube-to-baffles and their clearances. Other common causes in the decreasing order of significance are vortex shedding [80], multi-phase buffeting, acoustic resonance [81], turbulence buffeting [82], hydraulic transients, environmental excitation and transmitted mechanical vibration.

The vibration imparted to the tubes from surrounding equipment or by the flow of the medium greater than 4 fps can initiate the failure. According to Goyder, the most influencing cause for the vibrational damage to the tubes is fluid-elastic instability [83]. The debris accumulated in the tube passage especially at the tube-to-tubesheet joints can cause a blockage disrupting the flow of source medium. Dole et al. reported the most susceptible region vulnerable to vibration-induced failures are tube-to-tubesheet region, pass partition lanes and U bends [84]. Moreover, excessive turbulence and vibration cause tube oscillations loosening the joint strength of expanded tube-to-tubesheet joints and mechanical wear between tube and baffles [48]. Apart from tubes adjacent to baffles, the U

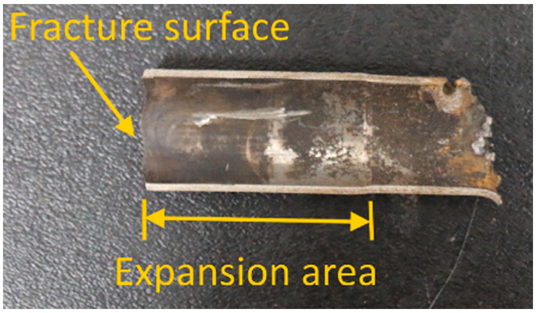

Fig. 9. Vibration induced fatigue defect at tube-to-tubesheet joint [27].

bends in the U tube heat exchanger are also most prone to vibration-assisted damages [85]. The mechanism of the failure by the high amplitude of the vibration is generally thinning at the point of contact, fatigue failure, fretting and failure at TTJ, cavitation, corrosion or fretting corrosion. The fretting wear in the tubes of steam generators and heat exchangers are caused by flow-induced vibration as a result of the dynamic interaction between the tubes and supports. Tube-to-tubesheet interactions, tube-to-baffle interactions, clearances, materials affect the fretting wear [86]. Moreover, the fretting causes easy removal of passive layer from the tube material, which forms the location for crevice corrosion and pitting [87]. Abrasive wear, spalling, debris reattachment are the most severe situations encountered as a result of fretting wear [88]. The failure of tube-to-tubesheet joint as a result of fatigue imparted by the vibration is shown in Fig. 9.

The major reason for the failure of heat exchanger tubes in process gas plant that cools the cracked gas from ethylene crackers is fretting as analyzed by Shahrani and Al-Subai [89]. As listed in Table 1, Liu et al. provided the effect of resonant vibration on the formation of fatigue crack on the welded tube-to-tubesheet joint that caused the failure of shell and tube heat exchanger after 30 days of operation [27]. Ma et al. also provided an evidence of the failure of titanium condensers in Yangzi Petrochemical Co. Ltd. due to fluid-induced vibration [90]. Jahangiri investigated a boiler that failed within 4 years but was expected to be in service for 30 years and the tubes at the tube entrance around the tubesheet cracked by the formation of vibrational bending stresses [91]. Fretting of the tube adjacent to anti-vibration bars was the root cause for the sudden shutdown of San onofre nuclear generating station-unit 3 [92].

As a preventive measure, it is recommended to select the tube, tubesheet and baffle material with high stiffness and modulus of elasticity because the vibration resistance is found to increase considerably with the stiffness [93]. For example, super-ferritic alloys are more vibrational resistant than titanium grade 2. However, crack free joints are to be ensured while fabricating the tube-to-tubesheet joints as they exhibit brittle nature during crack propagation [94,95]. A minimum tube wall thickness is recommended to prevent the vibrational defect caused by the supports. Though the excessive vibration has to be completely avoided, a controlled flow-induced vibration is effective in enhancing the convective heat transfer rate [96]. Anti-vibration bars or anti-vibration spacers are useful for suppressing vibrations. When the operating temperature increases above the transition temperature, the spacers expand exerting a lateral load on the tubes damping the flow-induced vibration [97]. Eisinger recommended to use innovative helical spacers [98]. The anti-vibration bars or mating materials significantly influence the wear modes. In addition, the clearance between the tube and baffles, baffle thickness, baffle pitch and forces between the tubes and baffles are to be under consideration in the design stage [83]. Eisinger and Sullivan recommended an optimum baffle location for suppressing the acoustic waves [99]. Guo et al. found the layer of scales formed on the tube and tubesheet surface due to the presence of elements in the material having an affinity towards oxygen reduces the wear rate considerably [92]. Mi et al. suggested specialized coating to prevent the lamination wear at high temperature due to fretting [100]. Lorenzo-Martin et al. reported that the heat treated Al_2O_3 deposited tubes were excellent in resisting the fretting wear compared to tubes with as-deposited Al_2O_3 and uncoated tubes. Pettigrew and Taylor recommend to use acceptance criteria based on maximum flow velocity, fretting wear depth on tube walls, tube-to-support clearance, shredding frequency, acoustic frequency and resonance parameter [101,102].

2.1.4. *Cleaning defect*

The main causes for the cleaning attributed defects are the use of over pressurized water jet, over pressurized air from sootblowers, impurities suspended in the water, density, volume and size of accumulates adhered on the tube inlets and tube sides, excessive velocity and high impact angle of cleaning medium, improper solvent, inappropriate cleaning procedure and presence of chemical residue. Cleaning process is performed during shutdown of the process plant to remove the mineral deposits, scales produced during operation. The accumulation of foreign particles in the form of dust, mold, soot and algae at the tube-to-tubesheet entrance and inner and outer surface of heat exchanger tubes hinders the smooth flow of process media. For these reasons, both internal and external cleaning are in practice. Trafczynski et al. explained an overall outline involved in the cleaning process, (a) isolating the heat exchanger from the heat exchanger networks (b) cleaning the heat exchanger using liquid wash followed by steaming (c) dismantling the tube bundles, cleaning the tubes and assembling back them to heat exchanger (d) checking the working of tubes by applying hydraulic pressure (e) disposing the waste collected after the cleaning process [103].

The outer tube surface is equally exposed to shell side fluid in the case of shell and tube heat exchangers. Therefore, fouling and rusting on the outer tube surface has the same adverse impact as of within the tube. Also, most of the accumulates are adhered to the tubesheet near the tube entrance. In such cases, manually or automated low pressurized high-volume water and high-pressure hand

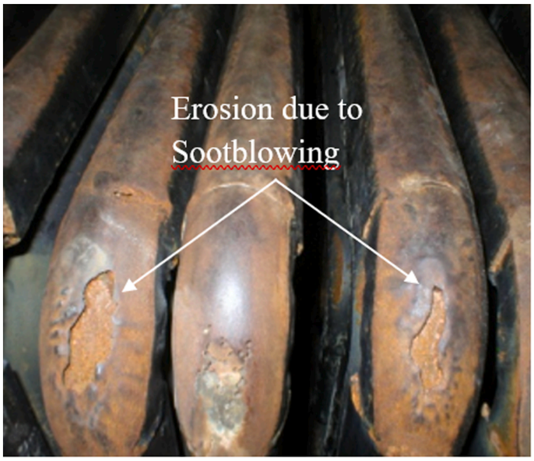

Fig. 10. Erosion due to sootblowing [104].

lancing are the techniques widely opted to clean the tubes and tubesheets. However, the cleaning processes with water expose the susceptibility to corrosion at the dents created previously by the fouling action. In the case of boilers, sootblowers with pressurized air are used for cleaning the tubes. Waclaw et al. explain the hardness, velocity, shape and impact angle of the solid particles suspended in the heat exchanger would potentially harm the tubes when subjected to sootblowing [104]. The damage caused by sootblowing is shown in Fig. 10. The cleaning process also causes a considerable reduction of the tube wall thickness. Chemical cleaning is also the best choice for cleaning and maintenance purposes. However, an improper solvent, inappropriate cleaning procedure and incomplete process leaving chemical residue accelerate the corrosion. The chemical cleaning process intended to deter corrosion on the affected parts often has an indirect effect on the surrounding materials. There is a high probability for the chemical solution in a vapour or liquid state to reach other regions. The chemicals sprayed on the parts in good condition can initiate the corrosion process. In such cases, control of the hotwell chemistry during the chemical cleaning process is important. As the accumulation of deposits and fouling are impossible to estimate unless the heat exchanger is dismantled and investigated, an incorrect strategy would end up in high economical loss.

Cleaning PIGS inserted into the pipes are effective in removing the deposits from the tube. These pigs exert a shear force along the inner surface of the tubes to wash out the fouling deposits. Barry and Robert patented an innovative cleaning PIG using hammer shock waves [105]. Ainslie et al. used ice plugging for heat exchanger applications and claimed to be an effective choice for complex geometrical tubes with bends [106]. In the case of accumulated hard deposits such as $CaCO_3$, SiO_2 partially or completely blocking the stream can be cleaned using hydro-drilling technology [107]. This robust technique is used for taking away the foul caused by oxides, calcium, sulfur or asphalt. Chemically cleaning using a mix of hydrochloric acid, dispersants and corrosion inhibitors is often used to clean away the settled mud or fouls. To predict the damages without dismantling the heat exchangers, online statistical monitoring approaches are highly advisable to predict the fouling deposits [108-112]. When the heat efficiency is impaired and the cleaning process is widely recommended, optimizing the cleaning schedule of heat exchangers in networks has a wide scope in saving energy and further reducing the loss [113-118].

2.1.5. Hydrogen embrittlement cracking

Hydrogen cracking in heat exchanger materials and tube-to-tubesheet joints is mainly due to the presence of hydrogen developed by chemical reaction or welding [119]. The intrusion of hydrogen, poor cathodic protection, heat treatments to increase the material strength, cold working process, high residual stress are the favouring conditions for hydrogen embrittlement cracking. The material turns brittle with an abrupt change in toughness, consequently, adding the risk of unexpected fracture. The small atomic hydrogen can intrude and change the crystal structure affecting the deformation process. High strength steels, titanium alloys, aluminium alloys are the most affected metallic materials. Increasing the material strength, cold working and residual stress impart hydrogen embrittlement. The process can cause a serious impact on the materials with poor cathodic protection. At lower voltages, monatomic hydrogen diffuses inside the material and forms the intermetallic phase on the surfaces further growing makes the metal brittle.

The hydrogen embrittlement cracks at the tube-to-tubesheet joint are commonly in the form of intergranular or transgranular cracks [120]. The reversibility and irreversibility of the hydrogen embrittlement process depend on materials. Hydrogen embrittlement is reversible on superferritic stainless steel and irreversible on titanium. The brittle nature of hydrogen embrittled material changes to ductile upon eliminating the hydrogen. Tube-to-tubesheet expanded or weld joints are the most critical regions exposed to hydrogen embrittlement cracking due to excessive residual stress present in these deformed regions. The stress state at these cracked joints is high that accelerates the failure process at a faster rate [121-123]. Onishi et al. emphasized the most prone area to hydrogen cracking is at the junction of the outer tube to tubesheet [124]. Fig. 11 illustrates the hydrogen-induced cracking at the weld heat affected zone and base metal zone in 9Cr–1Mo steel.

The horizontal heat exchanger with a floating tubesheet that operated only for 50,000 h failed due to hydrogen embrittlement

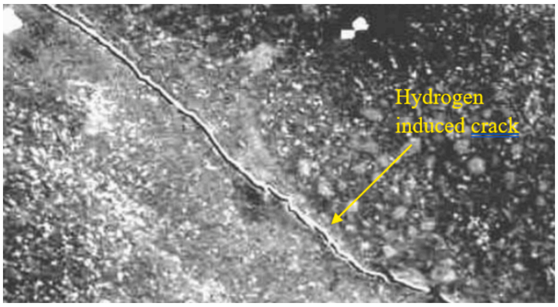

Fig. 11. Hydrogen-induced cracking in 9Cr–1Mo steel at HAZ / base metal boundary [125].

causing through-thickness cracks in 40% of tube-to-tubesheet weld joints [24]. Shalaby confirmed hydrogen embrittlement cracks at the Titanium tube ends fixed to Muntz tubesheet by the presence of granular features and deformed Ti grains [126]. As listed in Table 1, Shankar et al. investigated a 400 L capacity nitric acid loop after 10,000 h of operation due to leakage at the titanium tube to stainless steel tubesheet weld joints and concluded hydrogen embrittlement as the main cause for the collapse [26]. Similarly, diffused hydrogen in the titanium tube to carbon steel tubesheet was the reason for the failure of heat exchanger used as a cooling water system in a Chinese nuclear power plant [36].

Usage of dry electrodes, pre-weld and post-weld treatment and cleaning of joints are some of the remedies to prevent hydrogen embrittlement. NACE standard MR-01-75 and ISO 15156-1 provide guidelines about the hardness to be limited at the welded regions [127]. The preventive measure is to maintain the potential of the voltage greater than −750 millivolt.

2.2. Temperature

2.2.1. Thermal fatigue

Thermal cycling in a heat exchanger can result in thermal fatigue due to intensive induced thermal stresses. The problem aggravates across the length of the tube sections if there is an appreciable temperature gradient. The factors causing inappropriate thermal stresses and thermal gradients are localized heating due to blocks formed by sedimentation of muds and scales in the flow path, improper tube and shell side temperature, wetting of the heated regions and plugging.

According to the analysis conducted by Siamak and Stephan, the tube-to-tubesheet joints are the critical regions in a shell and tube heat exchanger with the highest thermal stresses [128]. Stephan reports the weldments in nuclear power plant piping are more sensitive to thermal gradients for crack development [129]. Rakesh and Soham pointed out the fact that the tube-to-tubesheet joint is most critically affected by thermo-structural fatigue rather than the shell-to-head joints [130]. According to Farrahi et al., 15% of plugging using plugs installed at the tube-to-tubesheet joint in the heat exchangers to temporarily cease the functioning of cracked tubes would result in an increase of 15 °C in the tubes [131]. Farrahi et al. reported that the tubesheet exposed to the shell side and at the weld toe in tube-to-tubesheet joints are the two major regions with the highest residual stress developed as a result of mechanical and thermal loads [132]. A high economical loss with an expensive replacement should be encountered in the case of a crack that propagates through the tubesheet ligaments. The presence of carbides and precipitates in the cracks is an indicator of the localized over-heating issue. Azevedo and Alves stated that the presence of graphite nodules and spherodized Fe_3C particles in ASTM A 178 grade tube in addition to the thick deposit of sulphur and magnesium on the tube proved the evidence of over-heating [133]. Fig. 12 shows the transgranular and wedge-shaped cracks propagated due to thermal fatigue at the heat recovery area tube walls. Apart from

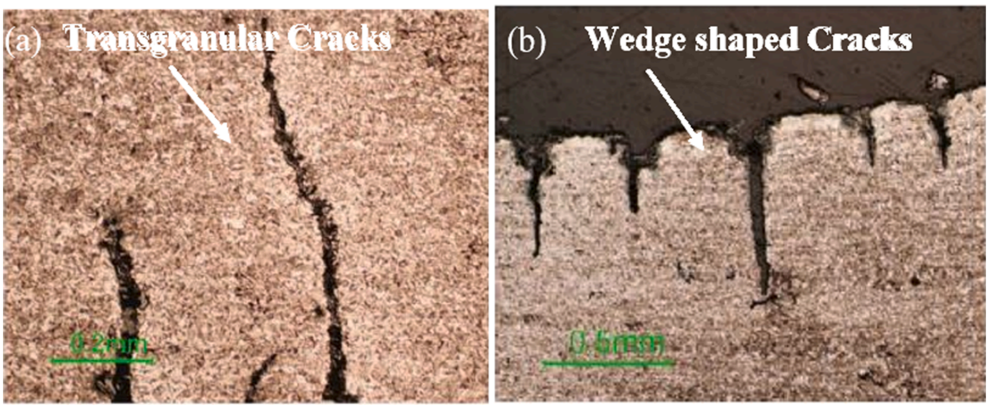

Fig. 12. Thermal fatigue cracks at the left-hand side of the heat recovery area. (a) Transgranular cracks (b) wedge-shaped cracks [142].

the above, the accumulation of foreign particles such as sediments, muds, scales on the tube surface interrupts the flow causing a blockage especially at the tube entrance (tube-to-tubesheet joint). This phenomenon increases the chance for localized heating in tube regions adjacent to blocked regions. Investigating the boilers, Dehnavi et al. reported that the scale formation at the stream side causes overheating while their excessive presence at the fire side results in wall thinning and high hoop stress [134]. Overheating of the tubes can cause swelling of the tubes, in which, the diameter of the tubes increase abnormally with a greater margin [20]. The pressure withstand ability of the heat exchanger tubes significantly reduces with the increase in the operating temperature resulting in lowering the stress values. Also, such expansion of welded tubes on the tubesheets exerts a tensile and shear stresses at the joints developing a mixed mode cracks [135-137]. In the work done by Dewa, the localized overheating that occurred at the tube bends led to the bursting [138]. Therefore, the improper tube-side and shell-side temperatures, wetting of the heated portions are a few reasons to cause thermal fatigue. The critical fatigue damage near the tubesheet holes in high temperature operated heat exchangers is 0.3 for the case investigated by Mao et al. [139], whereas the normal range lies in the range of 0.20 – 0.40 [140,141]. Every instance of transient temperature influence highlights the tubesheets and tube-to-tubesheet joints as critical zones exposed to thermal fatigue.

Zhu et al. emphasized the formation of cracks at the tube-to-tubesheet welded and expanded joints due to high operating temperature led to cease the operation of slurry oil steam generators [143]. Usman and Nusair, upon investigating a failed heat exchanger that lasted only for three and half months, found out thermal fatigue and localized heating as the main reasons for the collapse [144]. Ahmad et al., after the investigation of boilers in the Kapar power station situated in Malaysia, claimed thermal fatigue as the primary reason for the failure at the left-hand side of the heat recovery area tube [142].

To avoid thermal fatigue, special care should be taken to avoid rapid cooling and heating. This can be achieved by proper maintenance and regular inspection. Plugging, cutting and replacement of defective tubes should be considered. Identification of the possible sites that undergoes tube failure by cyclic loading is mandatory. Martens et al. suggest to conduct CFD analysis prior to fabrication for optimizing the operating parameter limits in order to avoid steam blanketing and short-term high temperature creep [145]. Martens et al. suggest to control the heat flux by proper regular inspection for extending the life of the heat exchanger [146]. Maintaining proper temperature by inspection, proper placement of feedwater stub, material choice can prevent thermal fatigue in heat exchangers.

2.2.2. Steam and water hammer

Water hammer is one of the common defects in boilers, steam generators and heat exchangers causing tubes to rupture due to factors such as high pressure surge, presence of slugs, blockage at the tube entrance and tubes, presence of condensed water droplets, volumetric difference between the steam and water, gas bubble collapse, increased inlet flow and decreased inlet water temperature. This usually ends in rupturing the tubes because of a high-pressure surge developed in the flow path due to sudden acceleration and deceleration of the working medium [147]. Any blockage in the tubes is enough for decelerating the flow of medium causing water hammer. Due to heat loss, the steam condenses to form water droplets. These water droplets accumulate to form a slug along the flow path that prevents the regular motion of the medium.

Sukamta et al confirm that the slugging initiates the water hammer in a horizontal pipe heat exchanger. The presence of slugs causes an abrupt change in the flow pattern. The transition slug flow and large scale slug flow pattern emphasizes the initiation of water hammer in heat exchangers [148]. Therefore, when an obstacle is encountered, the kinetic energy of the steam or liquid changes to pressure energy. The rupture not only causes an economical loss but also can cause personnel fatalities when busted. The bursting pressure, in such cases, is very high compared to the withstandable pressure. Since the chances for slug formation is high at the tube-to-tubesheet joint and due to direct impingement of process media on the tubesheet, the intensity of damage caused by water hammer is high on the tube-to-tubesheet joints. Hydraulic shock, thermal shock, flow shock and differential shock also causes water hammer. The hydraulic shock is generated by the abrupt rushing of the fluids into the tubes creating a sudden momentum. This can cause a tube slip from the expanded-welded joints causing mode II cracks in the weldments [149,150]. The slow opening of the valves to allow the water within the tubes is the remedy to prevent hydraulic shock. The difference in the volumetric capacity of steam and water during the condensation process can be extremely dangerous. Once the steam condenses to water droplets, these water droplets under high pressure rush into the defected region or voids along with the steam. Also, if the tubes contain bi-phases of steam and water inside the tube, the steam moves approximately 10 times faster than the water in a bi-phased system. Stefan claims the hammer process in bi-phase scenario is more complex to investigate due to gas bubble collapse [151]. The water can temporarily seal the path because of the formation of waves. Once the seal has been removed, a sudden surge forms which could cause the hammering action. The negative consequences of the water hammer are the collapsing of the piping, the build-up of the overpressure, the splitting, the crack forming, the fracturing of the joints, the breakdown of the tubing supports and attachments. The intensity of the water hammer can also trigger injuries to the personals. Priyankan et al. reveals the common dependency of inlet pressure and flow velocity to the condensation induced water hammer [152]. According to their experimental investigation, peak pressure magnitude increases with an increase in the inlet flow rate and decrease in the inlet water temperature.

The water hammer can be prevented by several methods. One way is to limit the fluid flow velocity less than the threshold. Elbows in the U tube heat exchangers can reduce the pressure waves, thus reducing the chance for water hammer. The shorter the tube, the lesser is the chance for the occurrence of water hammer. However, there will be a limitation in shortening the length of tubes in heat exchangers used for heavy applications. Swierzawski and Griffith proposed to use a flow restricting orifice in the inlet tube and to reduce the inlet water subcooling for preventing the water hammer [153]. Effective use of steam trap and condensate pumps removes the condensate from the stream [154]. An installed flash vessel that separates the steam and condensed fluid can mitigate the water hammer issue to a certain extent [155]. Increasing the inlet temperature and reducing the inlet flow rate are important steps towards mitigating the water hammer issue. Priyankan et al. recommend to maintain super-heated steam to possibly prevent the water hammer

[156]. WAHA3, which can model condenser induced water hammer, can be used effectively for estimating the magnitude of peak pressure [157,158]. Numerical analysis using WAHA can predict the slug formation, pressure surge and steam bubble condensation [159].

2.2.3. Freeze defect

Lack of thermal protection, malfunctioning of the thermal protective heating device, improper drainage of the unit, inadequate antifreeze solution concentrations, less tube spacing due to design fault, inappropriate fluid with less freezing point, irregular tube shapes and environmental temperatures are the reasons for freeze-up failure.

Freezing up of the tubes are commonly observed in evaporators and condensers whenever the temperature drops below the freezing point of the fluid. This defect is commonly seen in natural draft dry cooling systems (NDDCS) in cold countries. NDDCS are increasingly used in nuclear and thermal power plants. The freezing cold natural air considerably reduces the temperature of the flowing water at an increased heat transfer rate [160]. Thereby, if the water is the medium in the condenser, the formation of ice exerts more pressure than water on the tubes. This rise in pressure can cause line breaks and failure. For marine applications, low temperature operated LNG regasification is performed using sea water or water-glycol solutions [161,162]. Brenk et al. report, during LNG regasification using shell and tube heat exchanger, the ice formation intensifies if the temperature gradient between the freezing temperature of the heating fluid and boiling temperature of LNG is higher [163]. In addition, an irregular shape of the tubes also promotes the formation of ice slightly whereas increasing the tube spacing helps to mitigate the freezing process [163]. In the case of the evaporator, Schwartz emphasized that the collapse mainly occurs near the tubesheet [164].

Freezing of water residue remained in the tube bundles after the pressure leak test and the overloaded internal pressure were the causes for the failure of the heat exchanger investigated by Shuzhi [165].

Chen et al. recommended to adjust air flow control of louvers in air-cooled heat exchangers [166]. In addition, Kong et al. suggested to regulate the water flow rate and air flow rate simultaneously for an efficient anti-freezing effect [167]. Use of rolling type windbreaker [168], partial through-flow tower shell [169] and alteration of windbreaker configurations [170] are some of the effective anti-freezing techniques.

2.3. Corrosion

2.3.1. Pitting

Pitting is a form of localized corrosion characterized by the aspect ratio of the damage. ie, the depth of the hole will be deep with respect to the dimensions on the surface of the metal. Pitting in heat exchangers is caused by the presence of chlorine, sulphur and vanadium, oxides of manganese, calcium carbonate containing chlorine and an acidic environment.

The penetration rate and the growth in the case of pitting are tremendously high enough to perforate the tube and tubesheet wall. The defect is observed on the metals coated with a thin layer by surface treatment or by the reaction with the environment. The pits are formed mainly due to the presence of chlorine [171], sulfur, vanadium etc. The oxides of manganese, calcium carbonate containing chloride are found to have pitting action and the weight loss due to pits are often negligible. A localized pit is shown in Fig. 13. Once the localized pits are formed, there is a chance to have pH value so less as 2 within the crevices even though bases are used as the medium. The high potential difference at the crevice compared to the outer surface forms anode and cathode. Being surface area less in the crevice, the current density will be severe at the anode side which propels the galvanic corrosion. The high current density also aggravates the cracking process.

Ranjbar et al. assessed the failed admiralty brass oil heat exchanger used in an industrial unit and concluded under deposit pitting and dezincification as the major root causes [173]. Gong et al. found pitting and uniform corrosion on the tubesheet drilled holes in a steam generator that has been kept in the storage as a reserve tubesheet for nuclear power plant application [174]. Pitting is one of the reasons for the failure of heat exchanger in Korean nuclear power plant [29]. Pitting of ammonia evaporators after one year of commission due to the presence of chlorine, sulphur and carbon dioxide indicate the necessity of controlling the elements in process media [1]. Similarly, Gong et al. proved the pitting corrosion due to the presence of chlorine and sulphur in an ethylene plant [38].

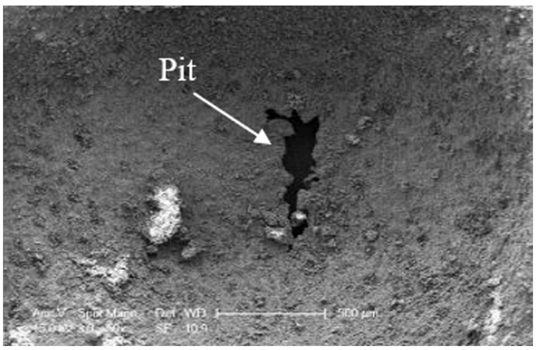

Fig. 13. Pits on the internal surface of the copper tubes [172].

Gong et al. reported pitting corrosion with Ying-Yang morphology in purified terephthalic acid dryer heat exchanger tubes [37].

The addition of Zirconium [175], chromium, molybdenum, nitrogen in alloys resists the pitting action. The pitting resistance equivalent number (PREN) formula developed by the Rockwell for the stainless steel to resist chloride pitting is provided in equation 1 [176,177].

$$PREN = wt.\%\ Cr + 3.3\ wt\%\ Mo + 16\ wt\%\ N \quad (1)$$

The higher the pitting resistance equivalent number, the higher will be the pitting resistance. The nitrogen and Molybdenum are 16 and 3.3 times effective than chromium. The nickel has little or no effect on chloride pitting resistance [178]. In contrast, Roland confirms that certain Nickel alloys that include NO 7208 have greater resistance to chloride pitting corrosion [179]. Zhang et al. found that a small percentage of nitrogen as shielding gas along with Argon in a gas tungsten arc welding at the tube-to-tubesheet joint improves the pitting corrosion resistance considerably [180]. In the case of dissimilar tube-to-tubesheet weld joints, the unmixed zone between the base metal and weld zone acts to have reduced pitting resistance [181]. Deen et al. suggest using quality water with reverse osmosis [171]. In addition, the qualification focus should be given to the presence of chlorine rather than the total dissolved solids (TDS) value. A chloride level below 50 ppm is highly recommended to avoid pitting corrosion. Hu et al. also recommend to compulsorily control the chloride ions and water vapour. During shut down, mechanical cleaning of the heat exchanger tubes could remove the under deposited corroded parts [1]. Therefore, a specialist should continuously monitor the essential parts and temperatures involved.

2.3.2. Sulphide attack

The brackish or sea water used as cooling water may contain sulphides, sulphur or polysulfides which are the propellants of corrosion in copper and copper alloys. These aggregation of suphur byproducts such as H_2S, SO_2, SO_3 from the untreated water on the metal gradually promotes the sulphide attack. Therefore, the main reasons causing sulphide attacks are the use of untreated water from lakes and sea having high presence of sulphur as a heat exchanger medium and chemically reacted byproducts.

The sulphide attacks the protective coating especially on the copper tubes and further, the presence of oxygen accelerates the cracking process. Due to sulphide attack, the erosion-corrosion, pitting, dealloying accelerate at a faster rate. The thick deposits of the products of sulphur over the tubes and fins can considerably reduce the heat transfer efficiency and the temperature of the tube wall. The corroded products are easily detachable from the metal leaving pits and holes due to different coefficients of thermal expansion. The sulfuric corrosion due to sedimentation of the sulphur compounds forms sulphide scale on the cracks and along the grain boundaries. Since the tube-to-tubesheet weld joints are numerous in the case of heat exchangers working in power plants, the chances for sulphide attack on the cracks at the weld joints are also high. Also, the metal sulphide formation rate is usually higher than the metal oxide formation rate.

Considerable reduction in the thickness of the tube wall is the end result that leads to bursting with leaks [182]. The chemical reactions due to the presence of S involving the production of acids can promote the sulfuric acid dew point corrosion [183]. The percentage composition of the sulphur is found to be more in many cases in the failed part upon inspection [184]. Fig. 14 shows the solid residue deposited on the tube-to-tubesheet joints of heat exchangers in sulfur recovery unit. Lins and Guimaraes emphasize the fact that the heat exchangers in sulfur recovery units are frequently forced to paralyze the activity due to corrosion caused by excessive sulfur byproducts such as H_2S, SO_2, SO_3 [185]. Farhat and Johnsen found excessive sulfur in the di-isopropanolamine solution passed to the shell side of the heat exchanger exposed over a long time resulted in wall thinning and stress corrosion cracking [186]. From Table 1, Corleto and Argade concluded sulphide-stress corrosion cracking as the main cause for the failure of heat exchanger failed immediately after being in service [28].

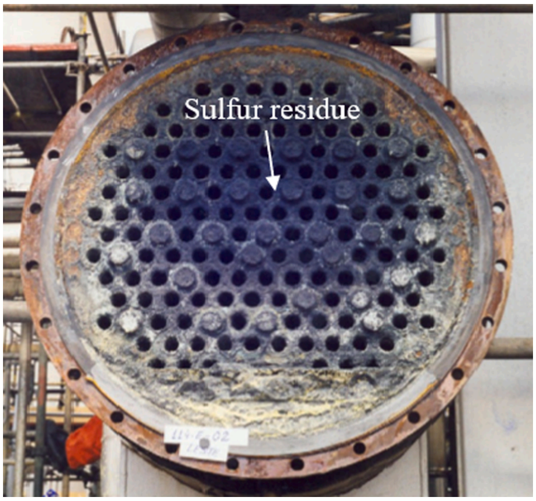

Fig. 14. A Solid residue deposited on the tube-to-tubesheet joints of heat exchangers in sulfur recovery unit [185].

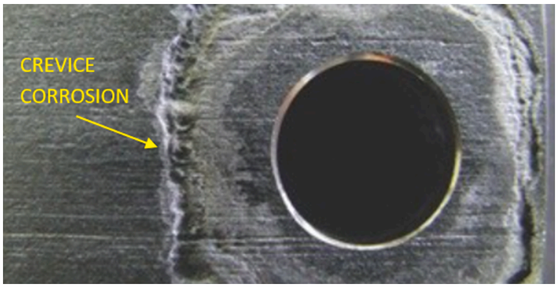

Fig. 15. Crevice corrosion around the tube [188].

A desulfurizer and correct monitoring of the sulphur content can restrict the accumulation of sulphur over the tube. The maintenance of high wall temperature and flue gas temperature can prevent sulfuric dew point corrosion. Materials with high corrosion resistance and proper controlling of the moisture help in reducing the impact of sulfuric corrosion. Daily flushing of the tubes with freshwater, preconditioning the tube surface by ferrous sulphate dosing to make corrosion resistant, changing the materials to titanium, stainless steels are the corrective measures.

2.3.3. Crevice corrosion

Crevice corrosion occurs due to differences in the pH values of tube and shell side fluids, high chloride ion concentration, presence of acids, formation of active anodic potentials, the composition of media and purpose of heat exchanger. Crevice corrosion undergoes three stages namely, incubation, initiation and propagation stage. Geometry, environment and environmental condition determine and alter the duration of the stages. The two mechanisms that state crevice corrosion are critical crevice corrosion theory and IR drop theory. The difference in the pH and the chloride ion concentration when reaching a critical state deteriorates the material from the crevice which leads to failure. The crevices sites turning anode and outside sites as cathode increase the anions influx rate to the crevice ultimately deteriorating the metal further and this forms the former theory. In the latter theory, due to factors like geometry, composition, concentration gradients, the potential difference arose between the crevice and exterior forms the active anodic potential. The IR drop is dominant in this case which finally results in crevice corrosion [187]. Crevice corrosion is also similar to pitting but occurs in the area that is shielded from the environment and thereby lesser the chance to flush away the corrosion products enclosed within the tightened crevices. As the cracks formed by the crevice corrosion are so tight, the pH value inside the cracks will be very less. This attack is very common in the tubesheets of condensers. Fig. 15 shows the crevice corrosion at the tube end.

The crevice corrosion occurs once the surface passive film is removed by other defects during the continuous operation of the heat exchanger. Crevice corrosion further intensifies the damage due to the propagation of the cracks in the depth direction [87]. Certain elements cause severe passivity breakdown at a higher temperature. Chlorine, added to feedwater for improving the quality, has a potential for passivity breakdown on stainless steel metals. Any small quantity of acid would be enough to accelerate the crevice corrosion attack in an uncontrollable manner [189]. Similarly, high content of sodium and potassium are the cause of crevice corrosion in 12CrMoV tubes [190]. The severity of crevice cracks turns out more if a piece of material drops down as a result of interactions of adjacent propagated crevice cracks. Highly hidden and secluded areas such as between tube and baffles, tube-to-tubesheet joint and portions in contact with stagnant mud or scales were observed as the region of attack.

The exchangers like distillate coolers, raw water heaters, ejector condensers using titanium in combination with alloy 904L tubes for tubesheets suffered crevice corrosion within one year of operation [191]. The defect originated at the bottom side of the tube holes and propagated towards the thickness affecting the TTJ. The failure of heat recovery heat exchanger in Al-Jubail plant was due to the accelerated corrosion at the crevices developed in the tube-to-tubesheet intersections [77].

Certain material properties and alloying elements have a crucial impact in providing resistance over crevice corrosion attacks. Inconel 686 and C-276 are highly preferred substitutes for Inconel 685 tubes in heat exchangers to prevent crevice corrosion [192]. To prevent the crevice attack, cathodic protection needs to be provided with aluminium alloy anodes but may result in hydriding. Maintaining the proper flow of medium with recommended adequate velocity can avoid and prevent crevice corrosion. ASTM G48 test is commonly used to measure crevice corrosion. The crevice corrosion resistance is more for the metals with higher critical crevice temperature (CCT). In general, the CCT above 25̊C is needed for the metals operating in the coastal or seawater applications.

2.3.4. Fouling

The fouling is termed as the deposition of undesired particles causing blockage along the path of the fluid flow or over the heat transfer surface, consequently, increasing the resistance to the medium flow ultimately resulting in a high pressure drop and thereby affecting the heat transfer rate significantly. A layout of fouling over the tube surface is demonstrated in Fig. 16. Sedimentation of muds, salts and contaminants from untreated media such as seawater, lake water and brine solution, high concentration of bacteria and fungi in heat transfer media, crystallization of soluble salts, presence of calcium carbonates, surface roughness, low inlet velocity, low tube wall temperature and concentrations of elements such as Cl, Va, Mo and O_2 promotes fouling. In general, the growth of fouling deposits undergoes initiation, transport, deposition, removal and ageing [193]. The fouling can be classified based on the mechanisms such as sedimentation, crystallization, chemical reaction and polymerization, organic material growth, coking, and corrosion

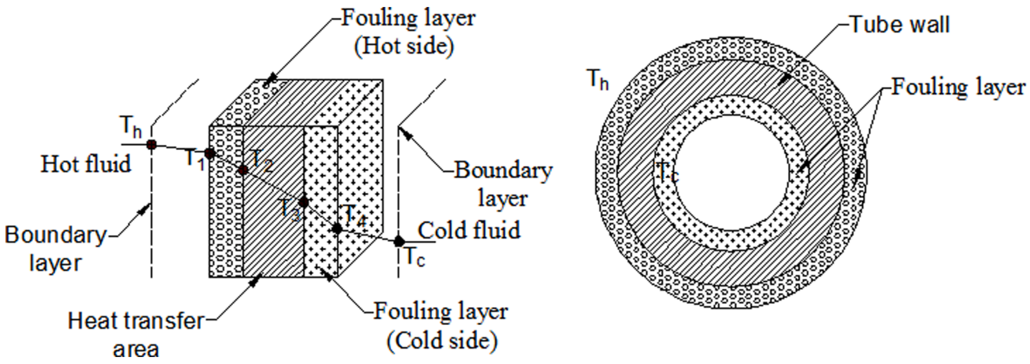

Fig. 16. Representation of fouling layer on the heat transfer surface.

[194,195].

Sedimentation of muds, minute particles, silts and contaminants from the process streams over the surface of tube and tubesheet settled by gravitation causes particulate fouling whereas the chemical reaction between the reactants in process media causes corrosion fouling. Precipitations formed by crystallization of soluble salts form scales on the tube and tubesheet surface promotes precipitation fouling. When the dissolved salts crystallize from the saturated solutions followed by precipitation on the heat transfer surface, sludges and scales develop at the surface. Concentrations of elements such as Cl, Va, Mo, O_2, in the medium have a significant effect on the fouling rate. David and Mohan experimented for the surface roughness with respect to fouling on Aluminium, Agion stainless steel, cold-rolled carbon steel and Stainless steel-Satin finish that are exposed to untreated lake water completely immersed in a tank over 90 days [196]. They found out that the surface roughness increases with days in an exposed condition. In addition, they found out that the material has a significant role in resisting fouling. Cold-rolled carbon steel, which is commonly used for tubes and tubesheets, was the most seriously affected by fouling imparting high surface roughness compared to the latter three materials [196]. This irregular surface imparts resistance to the fluid flow affecting the operation of heat exchanger. Albert et al. confirm that the roughness and flow constriction have a significant effect on the fouling resistance [197]. Apart from the fouling attributed surface roughness, the surface roughness in the bare metal acts as nucleation sites. The minute gaps on the roughened surface help the particles to stick strongly on the surface layer. Kazi et al. concluded that the fouling resistance is a function of fouling solution, surface temperature and thermal conductivity [198,199]. According to TEMA standard, physical considerations are fluid properties and propensity of the fluid, heat exchanger geometry and orientation, surface and fluid bulk temperature, local fluid velocities, heat transfer process, fluid treatment, cathodic protection and, economic considerations are the costs associated with cleaning, maintenance, operation and production, fluid pumping, shut down, out of service and tax rates [200]. Wang et al. found that the fouling resistance decreased with the increase in inlet velocity [201]. In contradiction, Trafczynski et al. reported that the fouling rate accelerates at a lower crude inlet velocity [202]. There is a high tendency for the foulants to adhere in the regions such as inlets and outlets where the velocity changes abruptly. Mengyan and Barry found the characteristic nature of fouling rate, ie., as velocity increases, fouling rate reaches maximum followed by a decrease towards zero [203]. Also, Al-Otaibi states the fouling resistance increases with increased tube wall temperature [204].

A layer formed over the tube surface contributes additional resistance to heat transfer resulting in the depreciation of thermal effectiveness of the heat exchanger [205]. Apparently, this causes an increase of the thermal loads greater than the anticipated value. According to Su et al., inorganic carbon and chloride elements accumulated from engine exhaust and atmospheric aerosol aggravate the pitting action in aircrafts' aluminium heat exchangers [206]. Lu et al. proved that the dissolved oxygen, hostile temperature and substrate have a critical role in the corrosion process initiated by fouling [207]. Mao et al. reported that the improper assessment of in-vessel retention of molten debris causes sustaining of residue pressure in the pressure vessel. An 8 MPa of such sustained pressure breaks through from the vessel by developing cracks in the weak and thinnest wall thickened regions [208]. Two cases of fouling reported by Gong et al. as mentioned in Table 1 proved the influence of sediments in untreated seawater in promoting the fouling followed by the collapse of the heat exchanger [35,40].

However, fouling can be prevented by taking into consideration of several factors. The properties of fluids, surface temperature, materials, purity of the fluid, surface roughness and geometry of the heat exchanger are a few factors influencing fouling resistances. A uniform and steady fluid flow can considerably reduce the fouling deposit. A high velocity fluid increases the thermal efficiency of the heat exchanger, reduces the fouling action and also helps to dislodge the fouling deposit from the heat transfer surface. The effective action of antifoulants decreases significantly with the temperature rise. This is due to the high corrosion rate, crystallization, polymerization and considerable increase in the scales developed. In terms of biological activity, the lower temperature would cease the reproduction and growth of organisms while higher temperature tends to kill certain bacteria. The selection of materials is vital to mitigate the fouling phenomenon. The brass and copper tubes in heat exchangers are less prone to corrosion compared to mild steel tubes due to dissolved oxygen by forming the protective CuO film further preventing the corrosion at 40 °C temperature [207]. Salamah and Abdullah suggest to use double perforated impingement plates instead of conventional impingement plates in heat exchangers to enhance the flow distribution and reduce the accumulation of fouling deposits [209]. Most of the additives to prevent fouling are hazardous to the environment, but Kazi et al. found additive gum arabic as an effective way to resist fouling without causing any harm to the environment [199]. David and Mohan recommend to perform surface preparations and coatings for mitigating fouling [210]. Al-Otaibi found that even the coated carbon tubes exhibit excellent fouling resistance over bare titanium tubes [204]. Cunault et al. recommend to use acidic or alkaline wash cycle and also inline gas rumbling to mitigate the biofilms adhered to the metal surface [211]. Both gas rumbling and reverse flow processes exert shear stresses along the surfaces of tube trajectory breaking down the fouling deposits [212]. To a greater extent, resistance to fouling can be enhanced at the design stage by selecting the optimum parameters, type of exchanger, omitting the factor promoting the fouling and by providing a provision for easy access to the heat exchanger parts for cleaning prescribed by Muller-steinhagen [16]. Use of projectiles [213-219], inserts [203,220-227], wire brushes and scrapers are online mechanical means of mitigating the fouling deposits. According to Ainslie et al., ice pigging, contributing 4 to 5% excess shear force, is effective in removing moderately adhered deposits [106]. Manual or semiautomatic water blast using high pressure jet upto 1500 bar is widely used cleaning process [16]. Nitrogen purging on the tubes [228,229], eliminating the present unsaturates, removing sulfur compounds by caustic scrubbing [230], desalting, use of antioxidants to cease polymerization, corrosion inhibitors and dispersion agents are effective to prevent chemical reaction fouling. Cathodic protection, corrosion inhibitors and surface treatments reduce corrosion fouling. The threshold chemicals, sequestering agents, distortion agents and dispersants can obstruct the crystallization process. Preheating of the natural water, chemical cleaning [231-234], usage of anti-corrosive coatings [235,236], usage of alternative corrosion resistant tube and tubesheet materials and materials exhibiting the biocide properties, application of epoxy coatings on the tube surface[237] are the preventive measures against Micro biologically induced corrosion. Boruff and Stoll signifies the use of continuous chlorination as a preventive measure to suppress the growth of microbial deposits [238]. During regular inspection in the maintenance shut downs, back flushing, jetting pressurized air, cleaning using brushes, moving rubber balls from one end of the tube to the end and scraping aids the mechanical cleaning processes for reducing the damage caused by fouling.

2.3.5. Microbiologically influenced corrosion

Microbiologically influenced corrosion (MIC) is very common in heat exchangers using seawater or freshwater as mediums for heat transfer. MIC is caused by the use of contaminated media containing microorganisms, microbial action, corrosive agents, befouling, inappropriate materials and the presence of organic acids. The non-purified water may be contaminated with microorganisms. In such cases, there is a high chance for the deterioration of the metal surface by microbial action. The limiting values of bacteria and fungi concentrations are $1x10^5$ cells/mL and $1x10^3$ cells/mL. MIC is caused by the synergistic effect of microbes, metabolites, metals and environment. As a result, the electrochemical reactions cause the formation of pits. After the bacterial actions, the waste getting accumulated in the pits accelerates further the cracking process. The corrosive agents and chemical compounds like organic acids, sulfur, iron are formed by the metabolic activities on nutrients and even the befouling can create the crevice. In general, the bacteria is broadly classified into aerobic bacteria and anaerobic bacteria based on the requirement of oxygen; rod shaped, spherical and filamentous based on the shape; heterotrophic and autotrophic based on the source of energy. The aerobic bacteria require oxygen to become active whereas the oxygen is toxic for anaerobic bacteria. Further, the microbes can be classified based on the type of electron acceptor in the absence of oxygen such as sulfate-reducing bacteria (SRB), iron-oxidizing bacteria (IOB), manganese reducing bacteria, nitrate-reducing bacteria, methanogenic bacteria, acid-producing bacteria, iron and sulfur-oxidizing bacteria. Some of the aerobic sulfate reducing bacteria are Thiobacillus thioparus [239 240], Thiobacillus concretivorus, Acidithiobacillus thiooxidans and anaerobic SRB are Desulfovibrio salixigens, Desulfovibrio vulgaris, Desulfovibrio desulfuricans, Desulfovibrio africanus, Desulfotomaculum orientis, Desulfotomaculum nigrificans. Aerobic bacteria oxidizing the manganese and Iron precipitating MnO_2 and Fe_2O_3 are Gallionella, Crenothrix, Ferrobacillus ferro-oxidants and Spaerotilus. Nitrate reducing bacteria in stagnant water produces HNO_3 that can potentially harm the metal. SRB turns the sulfates to sulfides and depolarizes the cathodic sites using hydrogen [241]. SRB commonly affects the alloys of iron, copper and aluminium. The sulfur-oxidizing bacteria produces sulfuric acid with low pH from the sulfides. Manganese reducing bacteria forms an insoluble MgO_2 layer over the metals. The MgO_2 layer turns permanganate under the chlorination process used for the removal of the slimes. The hydrochloric acid formed as a result can produce cracks. A low manganese concentration of about 20 ppb is sufficient to initiate the crack [178]. In all cases, the bacteria in the planktonic state stick to the surface developing a biofilm layer that constitutes bacteria, water, corroded products and extracellular polymeric substances [242]. Chitra et al. explain the formation of bio-films as follows: (1) Adhering of the planktonic cells to the metal surface, (2) irreversible attachment of bacterial cells through formation of extracellular polymeric substances, (3) formation of a biofilm layer, (4) maturation of a steady-state biofilm layer, (5) detachment of bacterial cells from the biofilm outer surface [243]. Microbiologically induced corrosion is a serious threat to heat exchangers operating in coastal regions.

Tube-to-tubesheet materials such as Nickel-chromium alloys, titanium, carbon steel, stainless steel, aluminum alloy, copper alloy, high nickel alloys, 6% Mo stainless steels can be easily affected by MIC. Microorganisms affect the corrosion by destroying protective surface coatings, crating corrosion cells, acid deposits and promoting anodic–cathodic reactions. The reactions are also temperature-dependent and often promotes between 4 °C and 60 °C.

Saarivirta et al. found microbiologically induced corrosion as the main reason for the premature failure of heat exchanger after 36 months of service [241]. Hussain reported SRB as the main reason for the failure of heat exchanger made of carbon steel tubes that lasted only for 9 months [244]. Meiying and Du claim that the synergistic action of SRB and IOB is the cause for the pitting action in the majority of the metals [245]. Microbiologically Induced Corrosion at tube-to-tubesheet joints is shown in Fig. 17.

Mechanical cleaning on regular basis and pigging operation could be beneficial to combat MIC. Also, the chemical treatment with biocides, anti-microbial agents and disinfectants can effectively control the population of bacteria. Reverse osmosis of the feed water is recommended. Skovhus et al. suggest to use coatings or linings, and corrosion monitoring and mitigating equipments as preventive measures [247]. Sharma recommended to use non-oxidizing biocide glutaraldehyde instead of chlorination to prevent bacterial build-

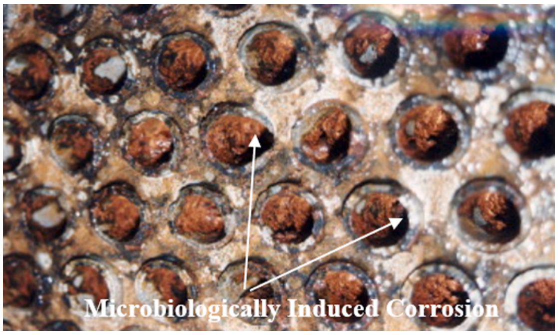

Fig. 17. Microbiologically Induced Corrosion at tube-to-tubesheet joints [246].

ups as chlorine changes the dissolved iron to solid iron aggravating the iron deposition on the surface [248]. The 25 °C CCT is required in the ASTM G48 test to resist the MIC.

2.4. Mutual effect of corrosion and stress

2.4.1. Stress corrosion cracking

Stress corrosion cracking (SCC) in the heat exchangers is caused by the plastic deformation in the fabrication of tube-to-tubesheet joints, fabrication techniques such as mechanical expansion and welding, thermal stresses due to thermal cycle, tube-to-tubesheet clearance, high weld hardness, presence of water or water vapour in H_2S environment, hydrogen, carbides and excessive elements such as sodium, calcium, chlorine and oxygen. The process of SCC is divided into three stages: initiation and propagation of the crack, steady-state crack propagation and final failure. In addition to residual stress and corrosive nature, temperature also plays a major role [249-255]. The SCC aggravates the crack propagation resulting in cracks [256,257]. Since the residual stresses are associated with the plastic deformation, major parameters such as tube yield stress, the initial clearance between tube and tubesheet are critical while fabricating tube-to-tubesheet joints. The stresses generated are usually less than the yield stress. In past studies, stress corrosion cracks have been propagated through the metal with either transgranular and intergranular morphology [258,259]. In another scenario, the hydrogen entraps in the localized stressed regions near the pits according to hydrogen-induced decohesion and hydrogen-enhanced local plasticity mechanisms [260]. Cracking initiates when the localized hydrogen exceeds a critical value [261]. In addition, the excessive carbides contributing to the hardness in the weld region also cause SCC [262]. The presence of excessive elements such as sodium, calcium, chlorine and oxygen can develop scales on the tube surface. Seawater, used in many heat exchangers, causes corrosion due to the high presence of chlorine [263]. These higher concentrations of foreign elements are added from the chemical agents such as caustic soda, phosphates and hydrazines added to the boiler feed water. The chemical reaction causes the formation of pits which are the initiation sites for the stress corrosion cracking [264]. The branching out of the cracks from the pits or initiation sites is the typical way to identify the stress corrosion cracking [264,265]. The crack propagation in the steam generators or heat exchangers consists of four stages, and they are corrosion, fatigue, SCC and the rupture stage. Fig. 18 demonstrates the schematic sketch indicating various combinations of the factors in forming corrosion, SCC and fatigue [266].

Stress corrosion cracking is very common at and around the tube-to-tubesheet joints in heat exchangers. The mutual synergistic

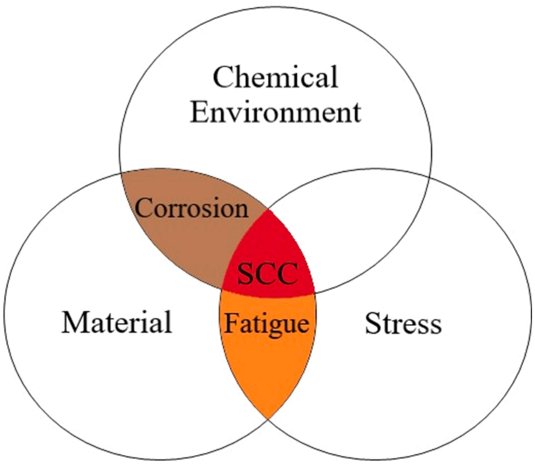

Fig. 18. Supporting factors causing Corrosion, SCC and Fatigue.

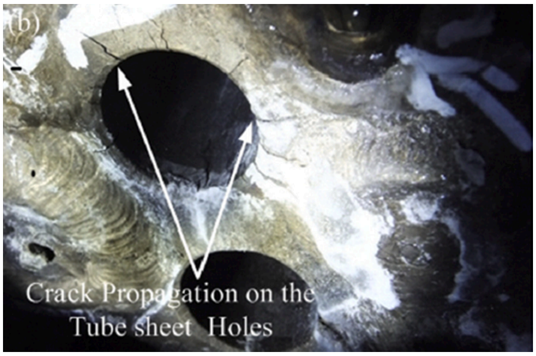

Fig. 19. SCC cracks at tube-to-tubesheet joints [281].

effect of tensile residual stresses and corrosive nature of heat transfer fluids is the reason for SCC in these specific locations [267-270]. Mechanical expansion of tube and thermal cycle contributed by welding induce mechanical and thermal residual stresses [271]. Apart from the tube-to-tubesheet joints, the SCC is also been observed in the transition zone between the expanded and unexpanded tube, U tube bends, baffle plates, bellows-type expansion joints, tube denting locations, sleeves and plugs [272]. It is evident that the plastically deformed tube wall thinning causes the development of residual stresses at the tube-to-tubesheet joints [273-276]. The microstructures of SCC generally indicate transgranular or intergranular cracks with a sharp cut passing through the grain and along the grain boundaries. The typical branched cracks are a characteristic of SCC [277]. The flat cleavage facet is the characteristic of the crack surface of the SCC failed specimen which was attributed by the brittleness at the particular exposed region [278,279]. In the condenser tubes, the SCC is observed on both sides of the tubes either on the water or steam side. Waterside stress corrosion cracking was less frequently observed than steam side attack. Though the SCC can occur anywhere along the condenser tube, it is frequently observed at locations such as tube inlet and fracture locations where the residual stress is very high as a result of the expansion process. The failures in waterside are assisted with fouling deposits which could act as an insulator causing overheating tremendously. The steamside corrosion cracking has intensified harmful effects over the tube if the presence of ammonia on stressed locations is very high.

Tawancy found out that the bent tube portions of the hydrocracker units made of 321 stainless steel are cracked due to polythionic acid-induced stress corrosion cracking. The polythionic acid is formed by condensation of the sulfur bearing scales developed on the inner side of the tubes in the presence of H_2S [280]. The polythionic acid produced as a result of sulfur inclusion in combination with mechanical or thermal load developed stress corrosion cracking ending up with failure [281]. The condenser tubes made of admiralty brass, brass, aluminium brass are often susceptible to waterside SCC. A similar finding was reported by Khalifeh et al in which the tubesheet near the weld joint was sensitized by overheating the wet carbonaceous deposits [281]. The deposits contained a high content of caustic and chlorides. Later, the cracks were propagated by the action of polythionic acids [281]. Corleto and Argade claim that the sulphide assisted stress corrosion cracking was the most serious problem in welded tube-to-tubesheet joints where the situation became more severe due to high weld hardness and presence of water/water vapour [28]. The massive impact of stress corrosion cracking can extend up to the bursting of the tube. Yang et al. investigated the bursted tubes in spiral wound heat exchangers used for nuclear power plant applications [32]. An excessive presence of the chloride ions in the untreated heat exchanger fluids and scales deposited in turn cause chloride stress corrosion cracking [282,283]. In general cases, the chloride stress corrosion increase with the temperature and chloride ion concentration. A few cases listed in Table 1 such as the collapse of steam generator in a Korean nuclear power plant reported by Hwang and Kim [29] and bursting of tubes in spiral-wound heat exchanger used for nuclear power plant reported by Gong et al. [32] are due to stress corrosion cracking. Stress corrosion cracking of heat exchanger tubes by the seal expansion process is reported by Xu et al. [12]. Adullah confirmed the poor workmanship in producing the tube-to-tubesheet welds of heat exchanger in gas plant resulted in SCC [19].

Fig. 19 shows the heat exchanger tubesheet affected by stress corrosion cracking.

The use of cupronickel, stainless steel, titanium in critical regions such as air removal regions can prevent the SCC. The less usage of ammonia and oxygen containing additives and flushing of the tube with water can considerably reduce the waterside SCC in condenser tubes. Shot peening imparts compressive stresses that neutralize the tensile residual stress in the tubesheet, thereby, reducing the necessary condition for SCC [284]. According to Parrott, the preventive steps to avoid the chloride stress corrosion cracking are to maintain the temperature below 115F and the chloride ion concentration below 50 ppm [285]. Stress relief treatments are advised by Duarte et al. to perform between the temperature 600–650 °C for the boiler tubes to avoid the accumulation of tensile stress due to forming actions [286]. Corleto and Argade recommended to avoid the presence of the water and water vapour in the H_2S environment in order to prevent embrittlement cracking [28]. Optimum residual stress is preferred at tube-to-tubesheet joints whereas the extremities will either lead to a leak or the formation of cracks. Turnbull and Zhou recommend lowering down the operating temperature for hindering the crack propagation [190].

2.4.2. Corrosion-Fatigue

Corrosion fatigue is defined as cracking produced by the combined action of fluctuating stress and a corrosive environment at lower stress levels or frequencies than would be required in the absence of a corrosive environment [287]. Mutual co-existence of cyclic

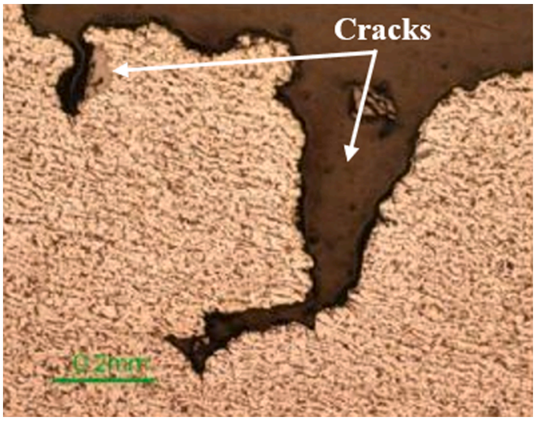

Fig. 20. Crack at the inner surface of the tube penetrating to outer surface [142].

loading, corrosive environment and high residual stresses is the favourable condition for corrosion fatigue. High residual stresses, stress intensity factors, loading frequency, operating temperature and pressure, corrosive agents and pH, flow-induced vibrations, thermal expansion and contraction are the factors affecting corrosion-fatigue.

The stress intensity factor, loading frequency, environment, mechanical and metallurgical properties are the parameters to be considered in the design stage of fabricating the heat exchangers. The thermal conductivity, pressure, temperature, concentration of corrosive particles and pH compromises the environmental factors. The mechanical loads in the heat exchanger components arise from flow-induced vibrations, thermal expansion and contraction, water hammer, etc. As a result of corrosion-fatigue, the endurance strength of the material drops significantly affecting the lifetime of the heat exchanger. Corrosion-fatigue defect is mostly common on tube-to-tubesheet joints, tubesheet and shell due to the comparatively high presence of residual stress. Corrosion aggravates in the cracks formed by thermal shock hindering the operation of heat exchangers. Round shaped cracks at the originating locations further penetrating as a transgranular crack is the typical characteristic of corrosion fatigue [142]. Fig. 20 shows the cracks propagated as a result of corrosion-fatigue. Since the endurance strength deteriorates, the damage ratio defined as the ratio of corrosion fatigue strength to air fatigue is limited for each of the materials. The damage ratio of mild steel, stainless steel and aluminium are 0.2, 0.5 and 0.4 respectively.

Corrosion fatigue initiating from the areas of dezincification was the sole reason for the failure of brass tubed oil lube cooler according to the failure analysis carried out by Ravindranath et al. [288]. Zahrani found corrosion fatigue was one of the root causes for the early failure of boiler feedwater heat exchanger made of 316Ti stainless steel that has reduced 65% to 70% of service life [289].

The preventive measures are to provide protective coatings, adding inhibitors, providing cathodic protection, inducing compressive stresses by shot peening.

Table 2 concludes the major root causes of failure mechanisms and their countermeasures based on the above discussions.

3. Quality inspection and assurance of tube-to-tubesheet joint

Qualification of tube-to-tubesheet joints is performed in the industries based on stringent policies and standards. The first step of the quality inspection starts with checking for the defects in the fabrication stage of tube, tubesheet and tube-to-tubesheet joint. The mock-up tube-to-tubesheet joint is prepared for determining the strength and characteristics of joints. The quality assurance of the structural components and joints using inspection techniques are mandatory. Many instances of leakage at the tube, tubesheet and tube-to-tubesheet joints as reported in the previous section prove the need for qualitative inspection. Table 3 illustrates the leak inspection techniques reported by the authors for analyzing the failures of tube-to-tubesheet joints in heat exchangers. Therefore, the major quality inspection techniques relevant to tube-to-tubesheet joints are described in the following section.

3.1. Leak test

The leak test is carried out to identify the location of the leak through the crack by measuring the flow of the testing medium. A change in the flow rate, variation in the maintained pressure or vacuum level are the main indicators of the presence of a defect. Ultrasonic detection, bubble test, gas leak testing, pressure change test, halogen diode detector probe test, helium mass spectrometer detector probe technique, helium mass spectrometer tracer probe method, helium mass spectrometer hood method, thermal conductivity detector probe test and eddy current testing are the leak tests that are explicitly used for identifying leaks in heat exchanger tube-to-tubesheet joints according to ASME section V standard. The pre-requisites for the leak test are that the area for the inspection should be free from any contaminants like oil, grease or paint and should be dry. For the same reason, it is recommended to perform the leak tests prior to the hydrostatic or hydro-pneumatic test.

Table 2
Causes and countermeasures of failure mechanisms.

No.	Defects	Susceptible regions	Causes	Countermeasures
1	Erosion – Corrosion	- Tube-to-tubesheet joints - Tubesheets - Tube inlets - Tube bends - Tube walls	- High fluid velocity - Presence of nano and micro solid sediment particles - Size of impurities - High chlorine content - Turbulence - Impingement with scale particles - Bursting of bubbles - Inlet fluid pressure	- Use of erosion resistant materials for tubes and tubesheets - Provide protective coating: carbide and nitride coatings, ceramic coatings - Use prismatic flow correcting devices - Improvise the shape and geometry of parts - Improve the design of inlet and outlet - Use infiltration technique and magnetic particles - Welding over the corroded cavity portions - Provide cathodic protection - Reduce oxygen and control the pH of media
2	Liquid Droplet Impingement Erosion	- Tubesheets - Tube entrance - Vent tubes - Tube ends - Nozzle	- High presence of liquid droplets in steam medium - Impact pressure greater than stagnation pressure - Impingement angle - Surface roughness - Low material hardness - Impact pressure - Density and velocity of liquid drops	- Use erosion resistant material with high hardness - Maintain and control the temperature of steam - Use tube shields
3	Vibrational Failures	- Tube-to-tubesheet joints - Pass partition lanes - U bends - Tube walls near baffles - Tubes near to anti-vibration bars	- Fluid elastic instability - Accumulation of debris - Turbulence - Flow induced vibration - Tube-to-tubesheet and tube-to-baffle interactions	- Use materials with high modulus of elasticity for tube and tubesheet - Increase the tolerance of tube wall thickness - Use anti-vibration bars or anti-vibration spacers - Provide proper clearance between tube and tubesheet and, tube and baffles - Provide coatings - Control shedding frequency, acoustic frequency and resonance parameter
4	Cleaning Defect	- Tube-to-tubesheet joints - Tubesheets - Tube walls	- Over pressurized water jet - Over pressurized air from sootblowers - Presence of impurities suspended in the water - Size, density and volume of accumulates adhered on the tube inlets - Excessive velocity and high impact angle of cleaning medium - Improper solvent - Inappropriate cleaning procedure and presence of chemical residue	- Use cleaning PIGS and hydro-drilling technique - Apply optimal pressurized cleaning medium - Use filtrated medium for cleaning - Adopt chemical cleaning instead of mechanical cleaning process
5	Hydrogen Embrittlement Cracking	- Tube-to-tubesheet welds	- Presence of excessive hydrogen - Intrusion or formation of hydrogen byproducts - Cold working - Heat treatments to enhance strength - Poor cathodic protection	- Use of dry electrodes - Perform preweld and postweld treatment - Cleaning of joints - Limit the hardness of the material based on NACE standard MR-01–75 and ISO 15156–1
6	Thermal Fatigue	- Tube-to-tubesheet welds - Tubesheets - Tubes near plugs - Tube bends - Shell-to-head joints	- High temperature gradient - Thermal stresses - Blockage by sediments, muds and scales - Improper tube and shell side temperatures - Wetting	- Periodically inspect temperature controlling devices to avoid rapid cooling and heating - Identification of possible sites prone to cyclic thermal loading and inspection - Regular quality inspections followed by proper maintenance

(*continued on next page*)

Table 2 (*continued*)

No.	Defects	Susceptible regions	Causes	Countermeasures
			- Plugging	- Plugging, cutting and replacement of tubes are mandatory
7	Steam and Water Hammer	- Tube-to-tubesheet joints - Tubesheets - Tube walls	- High pressure surge - Presence of slugs - Blockage - Condensed water droplets - Volumetric difference between steam and water - Gas bubble collapse - Increased inlet flow - Decreased inlet water temperature	- Limit the fluid flow velocity less than the threshold - Use elbows in U tube heat exchangers - Reduce the length of tube subjected to design considerations - Use flow restricting orifice in the inlet tube - Use of steam trap and condensate pumps removes the condensate - Increasing the inlet temperature and reducing the inlet flow rate - Maintain superheated steam - Use WAHA software for estimating peak pressure, slug formation, pressure surge and steam bubble condensation
8	Freeze Defect	- Tube-to-tubesheet joints - Tube walls	- Ambient temperature below the freezing point of fluid - Formation of ice - LNG gasification - Decreased tube spacing - Tube irregularity - Lack of thermal protection - Malfunctioning of the thermal protective heating device - Improper drainage - Inadequate antifreeze solutions	- Adjust air flow control of louvers in air cooled heat exchangers - Regulate the water flow rate and air flow rate periodically. - Use rolling type windbreaker - Use partial through-flow tower shell - Use alteration of windbreaker configurations
9	Pitting	- Tube-to-tubesheet welds - Tubesheets - Tube walls - Tube-to-tubesheet intersections	- Presence of elements such as chlorine, sulphur, vanadium etc. - Presence of calcium carbonate containing chloride - Formation of oxides of manganese - Acidic environment	- Add Zirconium, chromium, molybdenum in tube and tubesheet alloys - Use nitrogen as shielding gas with Argon in gas metal arc welding of tube-to-tubesheet joints - Enhance pitting resistance equivalent number of tube and tubesheet materials - Conduct reverse osmosis for the fed water - Reduce the chloride below 50 ppm - Control the chloride ions and water vapour - Regular checking of tube-to-tubesheet joints and temperature by a specialist
10	Sulphide attack	- Tube-to-tubesheet welds - Tube coatings - Tube walls	- Presence of sulphides and polysulphides - Formation of sulphur byproducts such as H2S, SO2 and SO3	- Use desulfurizer - Monitor the sulphur regularly - Maintenance of high wall temperature and flue gas temperature - Use corrosion resistant materials such as Titanium and Stainless steel. - Control the moisture content - Daily flushing of tubes with freshwater - Precondition the tube surface using ferrous sulphate
11	Crevice corrosion	- Tube-to-tubesheet intersections - Tube-to-baffle intersections - Tube-to-tubesheet welds - Tubesheets - Tubes adhered by scales and stagnant muds	- Difference in the pH - High concentration of chloride ion - Acidic fluids - Presence of active anodic potential - High concentration gradients	- Select materials with high critical crevice temperature. E.g., Inconel 686, C-276 - Provide cathodic protection - Regulate the flow of medium at a fixed velocity
12	Fouling	- Tube-to-tubesheet joints - Tubesheets	- Deposition of undesired particles causing blockage	- Use double perforated impingement plates for regulating the flow and reduce the accumulation

(*continued on next page*)

Table 2 (*continued*)

No.	Defects	Susceptible regions	Causes	Countermeasures
		- Tube inlets - Tube outlets - Tube walls	- Sedimentation of muds, salts, particles and contaminants - Crystallization of soluble salts - Presence of calcium carbonate - Use of untreated seawater, brine solution, aqueous solution with salts, caustic soda - High concentration of bacteria and fungi in water - Chemical reaction between reactants and, reactants and metals - Surface roughness - Low inlet velocity - Low tube wall temperature - High concentration of elements such as Chlorine, vanadium, Molybdenum and oxygen	- Use an additive gum Arabic - Perform surface preparations and coatings - Use acidic or alkaline wash cycle and inline gas rumbling - Design heat exchanger for easy cleaning process - Mechanical means of cleaning using projectiles, inserts, wire brushes and scrappers - Ice pigging - Water blast cleaning, Back flushing, Jetting pressurized air, Cleaning using brushes, Moving rubber balls and scraping - use antioxidants to cease polymerization, corrosion inhibitors and dispersion agents - Perform nitrogen purging, caustic scrubbing and desalting - Use threshold chemicals, sequestering agents, distortion agents and dispersants to obstruct the crystallization process - Chemical cleaning - Use alternative corrosion resistant tube and tubesheet materials - Application of epoxy coatings on the tube surface - Chlorination process
13	Microbiologically Influenced Corrosion	- Tubesheets - Tube walls - Tube coatings - Tube entrance - Tubes near to stagnant sedimentations	- Contamination of fluids with microorganisms - Microbial action - Presence of chemical compounds such as organic acids, sulphur and iron - Presence of corrosive agents - Befouling - Inappropriate selection of materials	- Mechanical cleaning on regular basis - Pigging operation - Perform chemical treatment with biocides - Use anti-microbial agents and disinfectants - Conduct reverse osmosis of the feed water - Use of coatings and linings - Periodic inspection of corrosion - Use non-oxidizing biocide glutaraldehyde instead of chlorination
14	Stress corrosion cracking (SCC)	- Tube-to-tubesheet welds - Tube-to-tubesheet expanded joints - Tube inlets - U tube bends - Baffle plates - Tube dents - Tubes near sleeves and plugs	- Plastic deformation in the fabrication of tube-to-tubesheet joints - Fabrication techniques such as mechanical expansion and welding - Fabrication techniques such as mechanical expansion and welding - Thermal stresses due to thermal cycle - Tube-to-tubesheet clearance - High weld hardness - Presence of water or water vapour in H2S environment and hydrogen, carbides - Excessive presence of elements such as sodium, calcium, chlorine and oxygen.	- Use of cupronickel, stainless steel, titanium - Reduce ammonia and oxygen containing additives - Flush the tube with fresh water - Use stress relief treatments to reduce the tensile stresses. Eg. Shot peening - Keep the chloride ion less than 50 ppm
15	Corrosion-Fatigue	- Tube-to-tubesheet joints - Tubesheets - Shell	- Combined action of fluctuating stress and corrosive environment - High residual stresses - Stress intensity factors - Loading frequency	- Provide protective coatings - Add inhibitors, - Providing cathodic protection - Inducing compressive stresses by shot peening

Table 3
Quality inspection techniques used for the failure analysis of tube-to-tubesheet joints.

Ref.	Author	Failure Location	Causes	LPI	Hydrostatic test	Helium test	UT	MPI	ET	RT
[290]	Sui et al.	TTJ	SCC	x	x					
[291]	Svensson and Catapano	TTJ	SCC	x	x	x	x			
[19]	Adullah and Ezuber	TTJ	SCC	x	x					
[17]	Otegui and Fazzini	TTJ	Over heating, Caustic stress corrosion					x		
[292]	Chen	TTJ	uniform corrosion	x						
[293]	Baboo	TTJ	Corrosion	x	x	x	x			
[294]	Mitra et al.	TTJ	SCC	x	x	x	x		x	x

LPI: Liquid Penetrant inspection; UT: Ultrasonic testing; MPI: Magnetic particle inspection; ET: Eddy current testing; RT: Radiographic testing

3.1.1. Ultrasonic detection

The pressure-based passive ultrasound method is widely adopted for detecting the leaks in the heat exchanger tubes [295]. The gases from the pressurized enclosed region travel to low-pressure regions through the cracks. These gases or liquids escaping from the enclosed tubes or shells turns turbulent and therefore, the fluid escaping from the leak produces a hissing sound. The ultrasonic leak detector scanned over the suspected parts detects the frequency of this hissing noise produced by the leakage. The ultrasonic leak detectors are designed to capture the sounds within specific frequencies ranging from 38 to 42 kHz [296]. Osama et al. confirmed that the frequency of measured leakage was always less than 50 Hz for the leakage in the pipelines [297]. The ultrasonic listening devices are run over the test region till the loudest point is reached. Listening rods, geophones [298] and acquaphones are the scanning devices used for ultrasonic detection [299]. Most of these devices use piezoelectric sensors and amplifiers for detecting sound and vibration [300,301]. Wireless sensor networks and radio frequency identification are equipped with data acquisition systems for monitoring the leakage [302]. The leakage level is estimated from the captured amplitude of the sound using leak noise correlator. However, the more leakage, the greater will be the ultrasound produced. The ultrasonic detection is suitable and reliable for tube-to-tubesheet joints due to the easiness of inspecting the exposed tubesheets at either end of shell and tube heat exchanger and scanning process. Given high significance to the tube-to-tubesheet welds, Guo et al. inspected the tube-to-tubesheet joints for defects using a phased array ultrasonic technique with appropriate phased array parameters and found porosities and lack of fusion flaws at the welded tube-to-tubesheet joints [303]. Yokell recommended ultrasonic inspection and helium leak sniffer test for inspecting and assuring the tightness of welded tube-to-cladded tubesheet [304]. Lillie applied ultrasonic and radiographic inspection in addition to helium leak test, liquid penetrant test and visual test for testing the butt welded 2 1/4 Cr-1 Mo steel tube-to-tubesheet in a sodium-cooled fast breeder reactor [305]. Pai et al. recommended to strictly use ultrasonic testing of tubes, tube-to-tubesheet weld joints and shell weld joints if radiography test is unavailable for evaluating the quality of welds in a 500MWE prototype fast breeder reactor [306]. Marino and Carminati proposed a methodology with an equipped data acquisition system to enhance the ultrasonic scanning and defect characterization explicitly for tube-to-tubesheet welds [307].Yoon et al. suggest ultrasonic testing over eddy current testing nuclear power plant steam generator tube and joints because the latter lacks the ability to accurately indicate the size of the defects [308]. Ultrasound leak detection at the tube-to-tubesheet joint is shown in Fig. 21.

Fig. 21. Ultrasound leak detection at the tube-to-tubesheet joint [309].

The gas flowing through the leaks will produce ultrasonic energy which can be detected by an ultrasonic leak detector. The sensitivity is limited to 10^{-3} Pa m^3/s, and due to the low value, it is not applicable to check the vessels containing hazardous liquids inside. In contrast to the above statement, Bergoglio and Mari have mentioned that the sensitivity of the acoustic leak detection systems goes up to 10^{-4} Pa m^3/s [310]. The detector which is capable of detecting the acoustic frequency ranging from 20 to 100 kHz is in practice for leakage detection [311]. The leakage should be less than $1x10^{-2}$ Pa m^3/s for acceptance [312]. According to UK Health and Safety Executive (HSE), the impact of the gas leaks can be classified into minor (gas leak <0.1 Kg/s); significant (0. 1 Kg/s < gas leak <1 Kg/s) and major (gas leak >1 Kg/s) [313]. The ultrasonic leak detector pigs are one of the newest techniques for determining the leaks in pipelines automatically. It uses hydrophones and specially developed software to detect the leak generated sounds. The pigs can print out the time at which the leak occurred, and the leak points will be traced by a magnetic marker system [314]. The technique can detect the leak irrespective of the gas or liquid. The technique is highly compatible with a vacuum and pressurized systems and the leaks at a greater distance can be easily detected. Due to high sensitivity, a chance for background noise interrupting the inspection is high [315].

3.1.2. Bubble testing

Holderness and Bruno found bubble testing as more effective over liquid penetrant test on seal welded followed by hydraulically expanded tube-to-tubesheet joints in SaskPower's Poplar River Power Station, where 43 leaked tube-to-tubesheet welded joints were identified using the former while only 30 leaked tube-to-tubesheet welded joints were detected by the liquid penetrant test [316]. Bubble testing is performed by either direct pressure technique or vacuum box method. In the direct pressure technique, the highly pressurized component with inert gas or air is soaked in a solution or liquid upon which the bubbles will form from the cracks. Bloomer experimentally confirmed that the bubble rate through the leaks increases rapidly with the increase of the gas throughput [317]. The pressure differential can start from 1 kg/cm^2 to 1.25 times the design pressure of the vessel. The upper range is 20 kg/cm^2. According to API 660 standard, the pneumatic pressure limits are between 50 kPa and 100 kPa for the bubble test [318]. If the tubes are welded to tubesheet, Yokell suggests pneumatic test pressure of 60 psig or 15% shell design pressure whichever is less [319]. After needed soak time, the soap solution has to be applied to the joints, and the temperature should be maintained in the range of 40̊F to 125̊F. The test can detect the leaks of the order of 10^{-5} pa m^3/s. From the vacuum box test, the leaks can be determined by observing the bubbles as same as that of the direct pressure test. The vacuum method is apt for the inspection of the components that are not subjected to be pressurized. The region where the soap is applied is made vacuum so that the atmospheric air from the other part leaks through and cracks can be located. The required vacuum can be established by any method such as vacuum pump, ejector, motor intake manifold or by any other method. For producing the vacuum in the region to be inspected, a vacuum box will be placed over the solution coated portion of the test surface. The partial pressure developed in the vacuum box should be maintained for at least 10 s. For both cases, the film formed from the bubble forming solution shall not break away from the area to be tested due to air drying or low surface tension. The minimum soak time required is 15 min. The solution used should be compatible with the temperature of the test conditions. The temperature of the test part shall be between 5 °C and 125 °C throughout the examination whereas the exceeded temperature are not permitted for the test. The solution can be applied by flowing, spraying or brushing. While immersed in the bath, continuous bubble forms at the leaked regions and the leakage can be verified. Massey and Jones used 15 psig pneumatic pressure and solution for conducting bubble test in order to qualify mockup expanded tube-to-tubesheet joints [320]. The bubble leak testing at the tube-to-tubesheet joints and tubes reveal the leaks and location instantaneously. Ayub was able to detect longitudinal cracks in tubes after conducting a quick soap based bubble test on the world's largest Ammonia heat pump (14 MWh) tubes [321]. Lesnjak et al. developed a system using the combined vacuum technique and spectrometry with helium detection for detecting the leaks by observing the

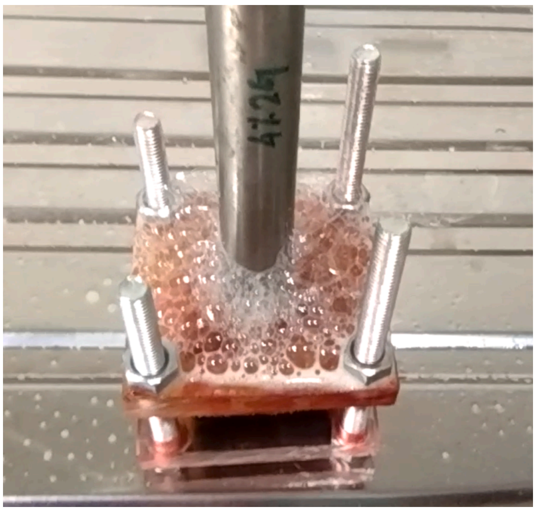

Fig. 22. Leak in a mockup tube-to-tubesheet joint detected using bubble test.

formation of bubbles [322]. Xu et al. designed an innovative hydrogen bubble based signal processing system using electromagnetic vortex flowmeter for the water leak detection in a steam generator devised for sodium-cooled fast reactors which is highly capable of detecting the water leak with an accuracy of 0.1 g/s [323]. These hydrogen bubbles are formed by a chemical reaction between liquid sodium and water when leaks are initiated. In such steam generators, hydrogen concentration detection method, an acoustic detection method and an electromagnetic detection method can be used to detect the leakage [324]. Leak identified by the author at 4% tube expansion in a mockup expanded tube-to-tubesheet joint using a bubble test is shown in Fig. 22.

3.1.3. Pressure change test

This technique detects the leakage rate over a period using pressure gauges from the enclosed components by measuring the variation in the pressure or vacuum. If there is any leak in the test specimen, the test specimen and a reference volume which will either be pressurizing or evacuating to an equal preset value will have a pressure difference. The valves provided and the sufficient time can stabilize the air inside. The transducer which is connected to both the test piece and reference volume having the differential pressure being zero initially shows up the difference between the pressure. Leakage testing devices based on the positive pressure differential are developed by Minor [325] and Bowling [326]. The difference in the pressure arises when there is any leakage in the test specimen.

3.1.4. Halogen diode detector testing

The testing involves collecting the air and tracer gas from the leakage through a tubular probe. The detector or the sniffer sucking the gas transfers to an instrument that is sensitive to the tracer gas. The halide gas is used as a tracer gas which is inserted into the component to be tested at a maximum of 25% of the designed pressure. The heated platinum element which acts as the anode in alkali-ion diode halogen leak detectors ionizes the halogen vapour and the ions get collected in the ion collector plate (cathode). The current proportional to ion formation is the indicator. In the case of electron capture halogen leak detectors, there will be a reduction in the concentration of the halogen ions due to electron capture that will be indicated on the meter. The affinity of particular molecular compounds for the low energy free electrons formed by the ionization of gas flow through an element with a weak radioactive tritium source is the principle of electron capture halogen leak detectors. Similar to halide gas and halogen leak detector, Samantray et al. suggested effectively use Bromine 82 radiotracer and NaI(Tl) scintillation detector for identifying leaks in heat exchangers [327]. Trichloromonofluoromethane (CCI_3F), Dichlorodifluoromethane (CCl_2F_2), Dlchloromonofluoromethane ($CHCl_2F$), Chlorodifluoromethane ($CH\ Cl\ F_2$), Dichlorotetrafluoroethane ($C_2Cl_2F_4$), Tetrafluoroethane ($C_2H_2F_4$), Dichloromethane (CH_2Cl_2), Sulfur Hexafluoride (SF_6) are some of the tracer gases used for leak detection [312].

The SF6 is recommended for the electron capture halogen leak detector whereas any tracer gas can be opted according to the sensitivity required in the case of alkali ion diode leak detector. The tracer gas concentration shall be a minimum of 10% by volume at the test pressure. For the test, the minimum time required to withstand the test pressure is 30 min but subjected to lower time when the testing components are evacuated partially before pressurization using halogen gas or else when using any special temporary device like leech box for testing short specimens. The method is suitable for tube inspection and tube-to-tubesheet joints according to ASME section V. The tube may contain cracks that can be detected by inserting a detector probe into the tube end held for a particular period. The examination should start from the uppermost portion of the tubesheet towards downwards. The Encapsulator method is used for inspecting tube-tubesheet joints. The encapsulator can be a funnel where its small end is connected to the detector probe and the big end to the tube-to-tubesheet joint. The detection time can be measured by the time taken for the indicated instrument response. The allowable rate for acceptance is $1x10^{-5}$ Pa m^3/s or below [312].

3.1.5. Helium leak test

In the case of helium leak test, Helium is generally used as the tracer gas supplied either to the tube or shell side. The leaks are identified using probes that are connected to the mass spectrometer leak detector and by sniffing the welds [315]. The helium leak tests can be performed using three methodologies; (1) inspecting component under vacuum, (2) inspecting component under pressurized condition, (3) combination of vacuum-pressurized conditions. Based on the types, helium tests are categorized into sniffer probe technique, tracer probe technique and hood method. In a helium leak test with sniffer probe, the helium leaked from the pressurized tube and tube-to-tubesheet joints is detected by sniffer probe whereas, in a helium leak test with tracer probe, the leak detector inserted through the tube-to-tubesheet joints to the vacuum tube detects the leaked in tracer gas from tracer probe. In a hood technique, the tested region is covered with a hood and pressurized tracer gas is either filled in the space between the test part and hood (Hood outside-in) or inside the tested region (Hood inside out). The leak is detected by a mass spectrometer leak detector placed in the evacuated region. Shriwardhankar et al. developed a leak testing system in vacuum mode with a leak detection rate of 6.66×10^{-9} Pa m^3/s for the steam generator in a fast breeder reactor [328]. Evacuating the inspecting tube and shell side to a vacuum level in the range of 10^{-3} to 10^{-4} mbar is required for achieving the sensitivity of 1.0×10^{-10} Pa m^3/s. Therefore, the vacuum process is an essential initial step for a successful helium leak test. In the experimental investigation on plate-fin heat exchangers by Jiang et al., a leak detection rate of 10^{-9} Pa.m^3/s was achieved [329]. Bergoglio and Mari mentioned the sensitivity of the mass spectrometer leak test using helium lies in the range of 10^{-12} Pa $m^3/s - 10^{-2}$ Pa m^3/s [310]. The helium sniffer probe technique contains a probe connected to the mass spectrometer leak detector. The test piece to be tested will be internally pressurized with helium or with the compounds containing helium. In the presence of cracks, the leaked helium to the atmosphere through the crack is detected by the sniffer probe. Goyal et al. used sniffer probe technique with a hood to apply 15 bar pressure for inspecting the leaks in plate fin heat exchangers [330]. In addition, they used spray probe technique with a hood for inspecting the leaks [330]. Palaniappan et al. used the hood method to detect the leaks in pressure vessels and pipelines in nuclear reactors [331].

Fig. 23. Hydrostatic testing of mock-up tube-to-tubesheet for leakage [320].

3.2. Hydrostatic testing

According to the TEMA RCB 1.31, the heat exchanger is to be hydraulically tested with water [332]. The shell side and tube side are to be tested separately in such a way that the leaks at the joints can be detected on either side of the tubesheet. The welded tube-to-tubesheet joints are required to be sufficiently cleaned before executing hydrostatic test. The minimum hydrostatic pressure shall be 1.5 times the design pressure at room temperature. The test pressure shall be held for at least 30 min. The preliminary procedure of hydrostatic test involves isolating the equipment and providing enough supports to withstand pressure. There should not have any open ends. The relief valve installed should avoid the over pressurization. The vents should be provided to release air from a high point and drain at the bottom to remove the liquid after the test. The air should be removed before the process. The overflow of the fluid should be ensured. The pressure has to be measured using two calibrated pressure gauges, and the indicated range must not exceed 150% of the test pressure. The pressure drops in the presence of leaks and cracks can be identified by visually inspecting the joints. The hydraulic fluid is water that is free from any chlorides or corrosive elements. Their presence beyond 30°C can induce corrosion and stress corrosion in austenitic steels. Hydrostatic tests are preferred to qualify the tube-to-tubesheet joints in heat exchangers operating at higher pressures [320]. The hydrostatic test is safe due to the incompressibility of water. Fig. 23 shows a setup for hydrostatic testing of mock-up tube-to-tubesheet joints.

3.3. Pneumatic testing

When the liquid cannot be tolerated as a test medium in the exchanger, the pneumatic test is preferred to qualify tube-to-tubesheet joints. As per ASME code - UG100 [334], those vessels in which the water cannot be filled and traces of water are not permitted can be tested pneumatically. The pneumatic test pressure shall be equal to the product of 1.1 times the maximum allowable working pressure (MAWP) and the lowest stress ratio (LSR) and need to make sure that the pressure applied should not exceed the maximum allowable working pressure set forth by the manufacturers. The pressure applied in the pneumatic testing is less than that of hydrostatic testing to prevent the explosion due to compressed air at the rupture [314]. The stress ratio (SR) is defined as the ratio of the stress at test temperature to the actual stress at design temperature. It is advised to maintain the temperature at least 30°F above the minimum design metal temperature to avoid brittle failures. Also, ASME code section VIII, Div.1 stated that the test pressure should not exceed 1.25 times the design pressure and the maximum pressure shall not exceed 150 psig. While performing the test, the pressure can be incremented in steps by one-tenth of the intended test pressure until the final pressure is reached. The pressure value equal to test pressure divided by 1.1 can be held for whole the inspection time. A safety valve is recommended to avoid over pressurization. Prabhat and Aravinda used the pneumatic testing apart from the bubble and helium leak test for testing the accessible welded parts in heat exchangers for fast breeder reactor [335]. Rakesh et al. used 0.2 MPa pneumatic pressure to qualify the welded tube-to-tubesheet joints before executing the expansion process [336]. Fig. 24 shows a setup for pneumatic testing of tube-to-tubesheet joints.

3.4. Acoustic emission testing

Acoustic emission testing is one of the non-destructive testing techniques used for detecting the flaws or cracks in tubes and tube-to-tubesheet joints. During the structural changes in the solid material, the transient elastic wave generates from the release of strain energy. When flaws are encountered, the acoustic emission (AE) count rate increases from the nominal warning the presence of a defect. The amplitude of the signal is related to the strain energy in the material. The time–amplitude plots during the inspection can plot the variation and are potentially good to find the defects. The phase transformation, crack growth, creep, stress rupture, deformation, corrosion, seismic activity releases the acoustic emission. The AE testing system consists of sensors, signal processing, recording equipment and display systems. The sources of noise such as splashing of the liquid, very high pressurizing rate, mechanical devices, electromagnetic interference, environmental disturbances hinder the testing. The frequency of the sensor depends on acoustic

Fig. 24. Pneumatic testing of mock-up tube-to-tubesheet joint [320].

attenuation, noise and vessel configuration. The preferred frequency range is 100 kHz to 400 kHz and the upper frequencies are needed if there are noises. MR lee and JH lee confirms that the signals corresponding to the gas turbulence have a narrow width between 130 and 250 kHz [337]. The noise level and the location of the sensors are critical in examining the leaks. Hanacek and Winkler, inspecting five heat exchangers in SAPHIR reactor, reported abnormal vibrations of tube bundle caused by the turbulent fluid flow to contribute to the main reason for high noise level [338]. Blaise et al. who devised a vibro-acoustic based approach for the detection of Nitrogen or water into a sodium circuit in a sodium cooled fast reactor, claimed the difficulty to detect the heat exchanger leaks close to turbines and pumps [339]. Nitrogen, an excellent tracer gas, is used for many leak testing systems [340]. Therefore, noise is the major drawback in acoustic-based detection systems. The location of the sensor depends on the vessel configurations and the area where the flaws have to be detected. A number of sensors can be incorporated for testing with maximum spacing not greater than 1.5 times the threshold distance. Pressurization is an important step in AE testing. The pressure will cause local yielding accompanied by acoustic emission. According to ASME BPVC section V, the test involves pressurizing the test coupon step by step to the full potential. In general, the pressure is incremented by 50%, 65%, 85% and 100% of the maximum test pressure. The holding period at each incremented stage is to be 10 min while for the final stage is to be 30 min. If the discontinuities are not exhibited by the first stage of the loading, the second stage is necessary starting from the 50% to 98%. For the AE testing of the in-service pressure vessels, the load which is the combined effect of pressure and temperature is to be applied from 90% of the total load till 110%, if possible with an intermediate stage of 100% and 105%. The hold time for the last stage is minimum 30 min while it is 10 min for the rest of the increments. Daniel and Michael have used the acoustic emission technique for determining scale failure in heat exchanger tubes subjected to dry and wet environments [341]. Based on the studies of Merheb et al., the acoustic emission technique has an inherent capability to monitor fouling in plate heat exchangers [342]. Han et al. used the AE technique for ensuring the integrity of 100E8 boiler tube-to-tubesheet joints after diagnosing with severe defects at the tubesheet [343].

3.5. Eddy current testing

Eddy current testing is practiced for detecting the flaws in heat exchanger tube-to-tubesheet joints and tubes during the production-line inspection, in-situ inspection and maintenance. A probe is inserted from one end of tube-to-tubehseet joint to the opposite tube-to-tubesheet joints covering the entire length of tube. The eddy currents generated by the electromagnetic coils produce a magnetic field around the flaw. This varied magnetic field will create reverse current across the coil which can be detected either from the voltage in the secondary coil or from the impedance variation in the original coil placed in the probe [344].

The probes used in eddy current testing are of two types namely, impedance and transmit-receive. The impedance probes induce the eddy current and, the distortion at the defects is used as a source to identify the flaws. The transmit-receive probes contain a separate transmitter and a receiver which is more flexible in design and application. Wijnants et al. emphasized that the main issue lies in the estimation of the depth of crevice by visual means after identifying the crevice corrosion attack in tubesheet and external surface of 25% tubes. Eddy current testing using a rotating probe that has been tuned to frequency with 90° phase shift between the external and internal defects was the solution used for measuring the extent of crevice penetration [345]. In addition, the testing frequency $f_{90} = 3\rho/t^2$ kHz can differentiate the defects in inner diameter and outer diameter with 90° phase angle where the ρ is the material resistivity and t is the tube wall thickness. A small phase angle criteria for internal tube defects, near to 90° for external tube defects and phase angle between the two extremes for through wall defects are opted for crack detection in an eddy current testing [346]. Finally, eddy current testing signals are compared with ASME depth curves to evaluate the depth of the cracks [312]. Out of three major types of probes used for eddy current testing, Hur et al. found plus point coil probe has better capability to detect circumferential and intergranular cracks than pancake and bobbin coil probe [347]. The study of Kim et al. suggested to use X-probe compared to bobbin and and rotating coils in the eddy current technique for inspecting steam generators in nuclear power plants [348]. Huang et al. recommended plugging to San Onofre 1 and Byron Unit 2 steam generator tubes after identifying the leakages successfully based on eddy current test results [349]. However, Tian et al. indicated a possible problem of wobbling of probes that are inserted using a gas pressure while performing eddy current testing of steam generators in Fast breeder reactor type nuclear power plant [350]. Mitra et al. conducted eddy current test and ultrasonic test in accordance with ASME III Class I to qualify the tube-to-tubesheet joints produced using gas tungsten inert gas welding for 500Mwe pool type sodium cooled fast reactor [351]. In their study, these tests are highly recommended to ensure the tightness and structural integrity of tube-to-tubesheet joints wherein the other case, any leak would result in the mixing of sodium and steam causing a drastic explosion due to chemical reaction.

3.6. Radiographic testing

Zscherpel et al. invented a prototype radiographic inspection setup using Gammamat B3 containing an Iridium 192 isotope and NDT film as a radiation source and detector respectively explicitly for tube-to-tubesheet joints [352]. Any leak through the tube-to-tubesheet joints in steam generators of prototype fast breeder reactor indicates potential hazard of sodium-water chemical reaction. To prevent catastrophic failure in such steam generators, Venkatraman et al. used projective magnification technique using microfocal radiography for monitoring the quality of tube-to-tubesheet joints. Shimizu et al. established a radiographic test for small internal diameter thick walled tube welded to tubesheet in steam generators of sodium cooled fast breeder reactor [353]. Thekkuden et al. used radiographic inspection for determining the internal porosities in the welded joints effectively [354,354]. Any manual errors in identifying the cracks from the radiographs can potentially reduce the lifetime of heat exchangers. Arunmuthu et al. proposed an image processing based solution using Butterworth band pass filter for enhancing the inspection of tube-to-tubesheet joints radiographs to avoid visual inspection of radiographs directly [356]. Similarly, Ding et al. and Zhao et al. invented an automatic digital radiographic imaging system for evaluating the welded tube-to-tubesheet joints [357,357]. This radiographic inspection is preferred for examining the presence of internal voids and porosities in tube-to-tubesheet weldments.

Conclusion

Major findings of the failure mechanisms, influencing factors, countermeasures and leak inspection techniques relevant to the tube-to-tubesheet joints are provided below.

Major influencing factors associated with the shell-side and tube-side process media are the usage of untreated water, presence of impurities and solid sediments, size and density of the particles, flow velocity exceeding the threshold, turbulence and impingement. In addition, the presence of elements such as sulphur, chlorine, vanadium, calcium, oxygen, manganese, calcium carbonates, crystallization of soluble salts and presence of corrosive agents in the medium and acidic media exhibits threat to the tube and tubesheet. These factors in the process media having direct contact with the tube-to-tubesheet joints are the major causes for erosion-corrosion, liquid droplet impingement erosion, fouling, microbiologically induced corrosion, crevice corrosion, sulphide attack, pitting and hydrogen embrittlement cracking. Temperature attributed defects such as steam and water hammer, thermal fatigue, freeze defect are mainly due to inconsistent temperature of the flowing medium and thermal stresses. The main causes for the irregular temperature are the accumulation of debris and sedimentations on the tube entrance near tube-to-tubesheet joint and tube walls, presence of slugs, blocks in the path, improper tube and shell side temperature by design fault, wetting of the heated regions, plugging, malfunctioning of thermal protective heating device, less thermal protection, use of inadequate antifreeze solution, less tube spacing, low freezing point of process media, irregular tube shapes. In addition, the formation and collapse of gas bubbles and condensation of water vapour can lead to the formation of cracks. High thermal residual stresses built-in at the tube-to-tubesheet welds by the tungsten inert gas welding initiates the cracking process. During the stage of maintenance, over pressurized water and air jet, contaminants in the cleaning medium, impact angle of cleaning jet, high velocity of jet are the major causes of mechanical cleaning related defects whereas the presence of chemical residue and influence of chemical reaction after chemical reactions exposes a serious threat to heat exchanger joints. Apart from the above, tube bends, inappropriate structural materials for tube and tubesheet and design faults are the structural concerns promoting cracks.

Treatment of process media using infiltration techniques and magnetic plugs, restricting the flow velocity within the threshold limit, prismatic flow correcting devices, flow restricting orifices, tube shields are recommended to considerably reduce the impact pressure and mechanical load exerted by the solid particulates in the medium onto tube-to-tubesheet and tube walls. Protective coatings using carbides, nitrides, ceramics, epoxy coatings, cathodic protection, weld cladding, welding overlays are recommended to prevent tube and tubesheet from chemically induced corrosion. Periodic cleaning of heat exchangers using cleaning pigs, hydro-drilling, projectiles, inserts, wire brushes, scrapers, flushing with water, online monitoring approaches and, chemical cleaning using non-oxidizing biocides, anti-microbial agents, disinfectants, antioxidants, corrosion inhibitors, threshold chemicals, sequestering agents, distortion agents and dispersion agents are required to mitigate fouling due to scales adhered to the tube-to-tubesheet joint and surface of the tubes and tubesheets. Structural materials for the tube and tubesheets should have high stiffness, pitting resistance equivalent number, higher critical crevice temperature above 25 °C, erosion resistance and, corrosion resistant elements such as zirconium, chromium, molybdenum and nitrogen are preferred to prevent erosion and corrosion related heat exchanger defects. Post weld treatment and shot peening of tube-to-tubesheet welds are advised to reduce the mechanical and thermal stresses imparted by the joint fabrication techniques such as expansion and welding process.

Leak tests are compulsory before the commissioning of heat exchangers, during operation and maintenance. Destructive and non-destructive testing procedures for heat exchanger tube-to-tubesheet joints are prescribed in ASME section V. The sensitivity of ultrasonic detection technique using listening rods, geophone or acquaphones has increased upto 10^{-4} Pa m^3/s while leakage within 1×10^{-2} Pa m^3/s is the acceptance criteria. API 660 standard recommends to apply pneumatic pressure between 50 kPa and 100 kPa for the bubble test and the lack of bubbles indicates quality weld joint without cracks. The acceptance rate for the halogen leak test is below 1x10^{-5} Pa m^3/s. The highest sensitivity of helium leak test reported in the literature is 10^{-12} Pa m^3/s. The hydrostatic pressure of 1.5 times the designed operating pressure is needed for qualifying the joint strength of tube-to-tubesheet joints where it is 1.1 times the maximum allowable operating pressure for pneumatic testing. A frequency range between 100 kHz and 400 kHz is preferred for acoustic emission testing, however surrounding noises affect the accuracy of both acoustic emission and ultrasonic testing. Eddy current is adopted for estimating the thinning of tubes by measuring the tube wall thickness. Radiographic inspection is widely preferred to inspect the presence of cracks and porosities at the exact location of tube or tube-to-tubesheet joint.

Declaration of Competing Interest

The authors declare that they have no known competing financial interests or personal relationships that could have appeared to influence the work reported in this paper.

Acknowledgement

We would like to acknowledge the fund provided by the United Arab Emirates University through the grant number 31R105-Research Center.

References

[1] S.M. Hu, S.H. Wang, Z.G. Yang, Failure analysis on unexpected wall thinning of heat-exchange tubes in ammonia evaporators, Case Stud. Eng. Fail. Anal. 3 (2015) 52–61, https://doi.org/10.1016/j.csefa.2015.01.002.
[2] S.K. Bhaumik, R. Rangaraju, M.A. Parameswara, T.A. Bhaskaran, M.A. Venkataswamy, A.C. Raghuram, R.V. Krishnan, Failure of reformer tube of an ammonia plant, Eng. Fail. Anal. 9 (2002) 553–561, https://doi.org/10.1016/S1350-6307(01)00039-5.
[3] S. Sivaprasad, S.K. Narang, R. Singh, Failure of high pressure ammonia line in a fertilizer plant – a case study, Eng. Fail. Anal. 13 (2006) 867–875, https://doi.org/10.1016/j.engfailanal.2005.07.003.
[4] S.A.J. Jahromi, M.M. AliPour, A. Beirami, Failure analysis of 101-C ammonia plant heat exchanger, Eng. Fail. Anal. 10 (2003) 405–421, https://doi.org/10.1016/S1350-6307(03)00016-5.
[5] H. Cui, W. Wang, A. Li, M. Li, S. Xu, H. Liu, Failure analysis of the brittle fracture of a thick-walled 20 steel pipe in an ammonia synthesis unit, Eng. Fail. Anal. 17 (2010) 1359–1376, https://doi.org/10.1016/j.engfailanal.2010.04.002.
[6] H. Abbasfard, M. Ghanbari, A. Ghasemi, S. Ghader, H.H. Rafsanjani, A. Moradi, Failure analysis and modeling of super heater tubes of a waste heat boiler thermally coupled in ammonia oxidation reactor, Eng. Fail. Anal. 26 (2012) 285–292, https://doi.org/10.1016/j.engfailanal.2012.06.012.
[7] N. Asrar, A.U. Malik, S. Ahmed, Overheating and fuel ash corrosion failure of boiler tubes in swcc power plants, in: Proceeding Second Acquir. Exp. Symp. Desalin. Plants O&M, 1997.
[8] K.S. Chang, Y.C. Kweon, H.J. Kang, S.J. Lee, Y.S. Lee, J.J. Moon, M.K. Lee, J.H. Jeong, S.H. Yang, A study on the regulatory approach of KNGR multiple failure events, Korea Institute of, Nucl Saf (2000).
[9] K. Karwoski, L. Miller, N. Morgan, Regulatory perspective on steam generator tube operating experience, in: Nucl. Press. Equip. Expert. Regul. Symp., 2005.
[10] T.M. Ahmed, A. Alfantazi, J. Budac, G. Freeman, Failure analysis of 316L stainless steel tubing of the high-pressure still condenser, Eng. Fail. Anal. 16 (2009) 1432–1441, https://doi.org/10.1016/j.engfailanal.2008.09.015.
[11] C. Guo, C.J. Han, Y.M. Tang, Y. Zuo, S.Z. Lin, Failure analysis of welded 0Cr13Al tube bundle in a heat exchanger, Eng. Fail. Anal. 18 (2011) 890–894, https://doi.org/10.1016/j.engfailanal.2010.11.003.
[12] S. Xu, C. Wang, W. Wang, Failure analysis of stress corrosion cracking in heat exchanger tubes during start-up operation, Eng. Fail. Anal. 51 (2015) 1–8, https://doi.org/10.1016/j.engfailanal.2015.02.005.
[13] A.M. Brennenstuhl, P.E. Doherty, P.J. King, T.G. Dunstall, The effects of biofouling on the corrosion of nickel heat exchanger alloys at Ontario Hydro, Microbially Influ. Corros. Biodeterior. NJ Dowling, MW Mittelman, JC Danko, Eds.(Knoxville, TN Univ. Tennessee, 1990). (1991) 4–25.
[14] A.U. Malik, I. Andijani, M. Mobin, F. Al-muaili, M. Al-hajri, Corrosion of Boiler Tubes Some Case, Symp. A Q. J. Mod. Foreign Lit. (n.d.) 739–763.
[15] A.K. Sinha, Aspects of failure of condenser tubes and their remedial measures at power plants, 2010, pp. 1–20.
[16] H. Müller-Steinhagen, M.R. Malayeri, A.P. Watkinson, Heat exchanger fouling: mitigation and cleaning strategies, 2011.
[17] J.L. Otegui, P.G. Fazzini, Failure analysis of tube-tubesheet welds in cracked gas heat exchangers, Eng. Fail. Anal. 11 (2004) 903–913, https://doi.org/10.1016/j.engfailanal.2004.01.003.
[18] M. El-Sayed, A. El Domiaty, A.-H.-I. Mourad, Fracture assessment of axial crack in steel pipe under internal pressure, Procedia Eng. 130 (2015) 1273–1287.
[19] S. Adullah, H.M. Ezuber, Repair of tube–tubesheet weld cracks in a cracked gas/steam heat exchanger, J. Fail. Anal. Prev. 11 (2011) 611–617.
[20] K.K. Parthiban, Case studies in failures in boilers, n.d.
[21] D.T. Thekkuden, A-H.I. Mourad, A.-H. Bouzid, Impact of grooves in hydraulically expanded tube-to-tubesheet joints, in: ASME 2020 Press. Vessel. Pip. Conf., American Society of Mechanical Engineers Digital Collection, 2020.
[22] D.T. Thekkuden, A-H.I. Mourad, A.-H. Bouzid, T. Darabseh, Impact of expansion pressure on wall thinning and contact pressure for hydraulically expanded tube-to-tubesheet joints: Numerical analysis, in: 2020 Adv. Sci. Eng. Technol. Int. Conf., IEEE, 2020: pp. 1–6.
[23] X.L. Wei, X. Ling, Investigation of welded structures on mechanical properties of 304L welded tube-to-tubesheet joints, Eng. Fail. Anal. 52 (2015) 90–96.
[24] C.R.F. Azevedo, F. Beneduce Neto, S.D. Brandi, A.P. Tschiptschin, Cracking of 2.25Cr-1.0Mo steel tube/stationary tube-sheet weldment of a heat-exchanger, Eng. Fail. Anal. 15 (2008) 695–710, https://doi.org/10.1016/j.engfailanal.2007.06.013.
[25] K.B. Mcintyre, A review of the common causes of boiler failure in the sugar industry, Proc S Afr Sug Technol Ass. 76 (2002) 355–364. https://doi.org/10.1.1.381.5850.
[26] A.R. Shankar, R. Sole, K. Thyagarajan, R.P. George, U.K. Mudali, Failure analysis of titanium heater tubes and stainless steel heat exchanger weld joints in nitric acid loop, Eng. Fail. Anal. 99 (2019) 248–262, https://doi.org/10.1016/j.engfailanal.2019.02.016.
[27] L. Liu, N. Ding, J. Shi, N. Xu, W. Guo, C.M.L. Wu, Failure analysis of tube-to-tubesheet welded joints in a shell-tube heat exchanger, Case Stud, Eng. Fail. Anal. 7 (2016) 32–40, https://doi.org/10.1016/j.csefa.2016.06.002.
[28] C.R. Corleto, G.R. Argade, Failure analysis of dissimilar weld in heat exchanger, Case Stud Eng. Fail. Anal. 9 (2017) 27–34, https://doi.org/10.1016/j.csefa.2017.05.003.
[29] S.S. Hwang, H.P. Kim, SCC analysis of Alloy 600 tubes from a retired steam generator, J. Nucl. Mater. 440 (2013) 129–135, https://doi.org/10.1016/j.jnucmat.2013.04.061.
[30] H. Lee, J. Jung, D. Kim, K. Yoo, Failure analysis on welded joints of 347H austenitic boiler tubes, Eng. Fail. Anal. 57 (2015) 413–422.
[31] L. Cozzarini, L. Marsich, C. Schmid, Ant-nest corrosion failure of heat exchangers copper pipes, Eng. Fail. Anal. 109 (2020), 104387, https://doi.org/10.1016/j.engfailanal.2020.104387.
[32] X.L. Yang, Y. Gong, Q. Tong, Z.G. Yang, Failure analysis on abnormal bursting of heat transfer tubes in spiral-wound heat exchanger for nuclear power plant, Eng. Fail. Anal. 108 (2020), 104298, https://doi.org/10.1016/j.engfailanal.2019.104298.

[33] T.W. Ni, J.L. Fei, S.H. Wang, Y. Gong, Z.G. Yang, Failure analysis on unexpected perforation of heat exchanger tube in methacrylic acid reboiler of specialty chemical plant, Eng. Fail. Anal. 108 (2020), 104267, https://doi.org/10.1016/j.engfailanal.2019.104267.
[34] H. Peltola, M. Lindgren, Failure analysis of a copper tube in a finned heat exchanger, Eng. Fail. Anal. 51 (2015) 83–97.
[35] Y. Gong, Z. Yang, J. Yuan, Failure analysis of leakage on titanium tubes within heat exchangers in a nuclear power plant. Part II: Mechanical degradation, Mater. Corros. 63 (2012) 18–28.
[36] Z. Yang, Y. Gong, J. Yuan, Failure analysis of leakage on titanium tubes within heat exchangers in a nuclear power plant. Part I: Electrochemical corrosion, Mater. Corros. 63 (2012) 7–17.
[37] Y. Gong, Z.-G. Yang, X.-H. Meng, Failure analysis of one peculiar 'Yin-Yang'corrosion morphology on heat exchanger tubes in purified terephthalic acid (PTA) dryer, Eng. Fail. Anal. 31 (2013) 203–210.
[38] Y. Gong, C. Yang, C. Yao, Z. Yang, Acidic/caustic alternating corrosion on carbon steel pipes in heat exchanger of ethylene plant, Mater. Corros. 62 (2011) 967–978.
[39] F. Nasirpouri, A. Mostafaei, L. Fathyunes, R. Jafari, Assessment of localized corrosion in carbon steel tube-grade AISI 1045 used in output oil–gas separator vessel of desalination unit in oil refinery industry, Eng. Fail. Anal. 40 (2014) 75–88.
[40] Y. Gong, X.-L. Yang, S.-H. Wang, Z.-G. Yang, Failure analysis on leaked jacket pipe of double-pipe heat exchanger in high-pressure polyethylene facility, Int. J. Press. Vessel. Pip. 187 (2020), 104166.
[41] A.S. Pelliccione, R. SantAnna, M.H.S. Siqueira, A.F. Ribeiro, J.E. Ramos, O.P. Silva, M.F. Pimentel, Failure analysis of a titanium plate heat exchanger – Mechanical fatigue, Eng. Fail. Anal. 105 (2019) 1172–1188, https://doi.org/10.1016/j.engfailanal.2019.07.059.
[42] A. Kosinska, B.V. Balakin, P. Kosinski, Theoretical analysis of erosion in elbows due to flows with nano- and micro-size particles, Powder Technol. 364 (2020) 484–493, https://doi.org/10.1016/j.powtec.2020.02.002.
[43] K. Bremhorst, P. Flint, The effect of flow patterns on the erosion-corrosion of shell and tube heat exchangers, Wear 145 (1991) 123–135, https://doi.org/10.1016/0043-1648(91)90243-N.
[44] J. Liu, W. BaKeDaShi, Z. Li, Y. Xu, W. Ji, C. Zhang, G. Cui, R. Zhang, Effect of flow velocity on erosion–corrosion of 90-degree horizontal elbow, Wear 376 (2017) 516–525.
[45] W. Gao, Y. Li, L. Kong, Numerical investigation of erosion of tube sheet and tubes of a shell and tube heat exchanger, Comput. Chem. Eng. 96 (2017) 115–127.
[46] M.A. Habib, H.M. Badr, S.A.M. Said, R. Ben-Mansour, S.S. Al-Anizi, Solid-particle erosion in the tube end of the tube sheet of a shell-and-tube heat exchanger, Int. J. Numer. Methods Fluids. 50 (2006) 885–909.
[47] W. Faes, S. Lecompte, Z.Y. Ahmed, J. Van Bael, R. Salenbien, K. Verbeken, M. De Paepe, Corrosion and corrosion prevention in heat exchangers, Corros. Rev. 37 (2019) 131–155.
[48] U. Klein, A. Zunkel, A. Eberle, Breakdown of heat exchangers due to erosion corrosion and fretting caused by inappropriate operating conditions, Eng. Fail. Anal. 43 (2014) 271–280.
[49] N. Khayatan, H.M. Ghasemi, M. Abedini, Synergistic erosion-corrosion behavior of commercially pure titanium at various impingement angles, Wear (2017), https://doi.org/10.1016/j.wear.2017.03.016.
[50] Six causes of heat exchanger tube failure, (n.d.). https://www.fluiddynamics.com.au/case-studies-1/six-causes-of-heat-exchanger-tube-failure.
[51] K. Ranjbar, Effect of flow induced corrosion and erosion on failure of a tubular heat exchanger, Mater. Des. 31 (2010) 613–619.
[52] M. Rezaei, Z. Mahidashti, S. Eftekhari, E. Abdi, A corrosion failure analysis of heat exchanger tubes operating in petrochemical refinery, Eng. Fail. Anal. 119 (2021), 105011.
[53] B. Kuznicka, Erosion – corrosion of heat exchanger tubes, Eng. Fail. Anal. 16 (2009) 2382–2387, https://doi.org/10.1016/j.engfailanal.2009.03.026.
[54] R.K. Pandey, Failure analysis of refinery tubes of overhead condenser, Eng. Fail. Anal. 13 (2006) 739–746, https://doi.org/10.1016/j.engfailanal.2005.02.016.
[55] Y. De Li, N. Xu, X.F. Wu, W.M. Guo, J.B. Shi, Q.S. Zang, Failure analysis of the condenser brass tube in 150MW thermal power units, Eng. Fail. Anal. 33 (2013) 75–82, https://doi.org/10.1016/j.engfailanal.2013.04.026.
[56] J.M.A. Van der Horst, C.R. Sloan, Erosion-corrosion of finned heat exchanger tubes, in: Erosion, Wear, Interfaces with Corros., ASTM International, 1974.
[57] T.L. Prakash, A.U. Malik, Investigations on the failure of al-wajh multieffect desal condenser tubes, (n.d.).
[58] A.-H.I. Mourad, A. El-Domiaty, Notch radius and specimen size effects on fracture toughness of low alloy steel, Procedia Eng. 10 (2011) 1348–1353.
[59] A.-H.I. Mourad, A. El-Domiaty, Y.J. Chao, Fracture toughness prediction of low alloy steel as a function of specimen notch root radius and size constraints, Eng. Fract. Mech. 103 (2013) 79–93.
[60] A-H.I. Mourad, J. Altarawneh, A. El Domiaty, Y.J. Chao, Fracture toughness determined from full-scale pipe, in: ASME 2012 Press. Vessel. Pip. Conf., American Society of Mechanical Engineers Digital Collection, 2012, p. 125–130.
[61] V. Meuronen, Erosion durability of steels in steam boiler heat exchanger tubes, Wear 240 (2000) 164–167.
[62] S. Nešić, Using computational fluid dynamics in combating erosion-corrosion, Chem. Eng. Sci. 61 (2006) 4086–4097, https://doi.org/10.1016/j.ces.2006.01.052.
[63] J.C.S. Lai, K. Bremhorst, Control of corrosion-erosion of tube inlets of shell and tube heat exchangers, Wear 54 (1979) 101–112.
[64] H.M. Badr, M.A. Habib, R. Ben-mansour, S.A.M. Said, S.S. Al-anizi, Erosion in the tube entrance region of an air-cooled heat exchanger, Int. J. Impact Eng. 32 (2006) 1440–1463, https://doi.org/10.1016/j.ijimpeng.2005.01.008.
[65] F.J. Heymann, Conclusions from the ASTM interlaboratory test program with liquid impact erosion facilities, Elsi. (1979) 20_1-20_10.
[66] M. Ahmad, M. Casey, N. Sürken, Experimental assessment of droplet impact erosion resistance of steam turbine blade materials, Wear 267 (2009) 1605–1618.
[67] Y.-M. Ferng, C.-T. Horng, Prediction of possible wear sites on the shell wall of feedwater heater due to droplet impingement using CFD models, Nucl. Eng. Des. 237 (2007) 1560–1568.
[68] F.J. Heymann, High-speed impact between a liquid drop and a solid surface, J. Appl. Phys. 40 (1969) 5113–5122.
[69] N. Fujisawa, S. Takano, K. Fujisawa, T. Yamagata, Experiments on liquid droplet impingement erosion on a rough surface, Wear 398 (2018) 158–164.
[70] K. Fujisawa, T. Yamagata, N. Fujisawa, Damping effect on impact pressure from liquid droplet impingement on wet wall, Ann. Nucl. Energy. 121 (2018) 260–268.
[71] K. Fujisawa, T. Yamagata, N. Fujisawa, Liquid droplet impingement erosion on groove roughness, Nucl. Eng. Des. 330 (2018) 368–376.
[72] H.S. Kirols, D. Kevorkov, A. Uihlein, M. Medraj, The effect of initial surface roughness on water droplet erosion behaviour, Wear 342 (2015) 198–209.
[73] J.G.C. Nava, F.H. Stott, M.M. Stack, The effect of substrate hardness on the erosion-corrosion resistance of materials in low-velocity conditions, Corros. Sci. 35 (1993) 1045–1051.
[74] N. Fujisawa, T. Yamagata, S. Takano, K. Saito, R. Morita, K. Fujiwara, F. Inada, The influence of material hardness on liquid droplet impingement erosion, Nucl. Eng. Des. 288 (2015) 27–34.
[75] J. Xiong, S. Koshizuka, M. Sakai, H. Ohshima, Investigation on droplet impingement erosion during steam generator tube failure accident, Nucl. Eng. Des. 249 (2012) 132–139, https://doi.org/10.1016/j.nucengdes.2011.08.048.
[76] M. Javidi, M.A. Sadeghi, R. Jafari, A.A. Hoodi, Failure analysis of an air-cooled heat exchanger in natural gas dehydration unit, Eng. Fail. Anal. 115 (2020), 104678.
[77] A.U. Malik, S.A. Al-Fozan, F. Al-Muaili, Corrosion of heat exchanger in thermal desalination plants and current trends in material selection, Desalin. Water Treat. 55 (2015) 2515–2525.
[78] C. Ke, Failure Analysis of Feed Heat Exchanger of CCR Pre-hydrotreater, Corros. Prot, Petrochemical Ind, 2012.
[79] H.E. Smith, Heat exchanger impingement protection, (1979).
[80] G.V. Patil, M.A. Dharap, R.I.K. Moorthy, Estimation of Fretting Wear-Limited Life of a Shell and Tube Heat Exchanger Tubes: Analytical Formulation, Computer Implementation and Qualification Against Actual Reported Failure, J. Fail. Anal. Prev. 17 (2017) 581–594, https://doi.org/10.1007/s11668-017-0279-2.
[81] T.A. Fiorentin, A. Mikowski, O.M. Silva, A. Lenzi, Noise and vibration analysis of a heat exchanger: a case study, Int. J. Acoust. Vib. 22 (2017) 270–275.

[82] G.V. Patil, M.A. Dharap, R.I.K. Moorthy, Analytical Reconstruction of Failure of a Shell and Tube Heat Exchanger, J. Fail. Anal. Prev. 17 (2017) 126–135, https://doi.org/10.1007/s11668-016-0219-6.
[83] H.G.D. Goyder, Flow-induced vibration in heat exchangers, Chem. Eng. Res. Des. 80 (2002) 226–232.
[84] R. Dole, S. Sridhar, S. Vivekanand, Mitigate vibration issues in shell-and-tube heat exchangers, Hydrocarb. Process, 2015.
[85] K.P. Singh, Predicting flow induced vibration in u-bend regions of heat exchangers: an engineering solution, J. Franklin Inst. 302 (1976) 195–205.
[86] P.L. Ko, Heat exchanger tube fretting wear: review and application to design, J. Tribol. 107 (1985) 149, https://doi.org/10.1115/1.3261010.
[87] Z.D. Fan, J.S. Du, Z.B. Zhang, Y.C. Ma, S.Y. Cao, K. Niu, C.X. Liu, Internal leakage of plate heat exchangers caused by cooperation of pitting, crevice corrosion, and fretting, Eng. Fail. Anal. 96 (2019) 340–347.
[88] C. Lorenzo-Martin, O.O. Ajayi, K. Hartman, S. Bhattacharya, A. Yacout, Effect of Al2O3 coating on fretting wear performance of Zr alloy, Wear 426 (2019) 219–227.
[89] S. Shahrani, S. Al-Subai, Failure analysis of heat exchanger tubes, J. Fail. Anal. Prev. 14 (2014) 790–800.
[90] Q.-L. Ma, H. Xu, Z.-W. Wang, F. Hou, L.-Y. Xu, Failure analysis and critical manufacturing technology research on titanium condensers, Eng. Fail. Anal. 12 (2005) 432–439.
[91] M.R. Jahangiri, Failure analysis of Type 304 stainless steel tubes in an energy production plant heat exchangers, J. Press. Vessel Technol. 133 (2011).
[92] X. Guo, P. Lai, L. Tang, J. Lu, J. Wang, L. Zhang, Fretting wear of alloy 690 tube mated with different materials in high temperature water, Wear 400 (2018) 119–126.
[93] R.L. Coit, C. Peake, A. Lohmeier, Design and manufacturing of large surface condensers – problems and solutions, Proc. Am. Power Conf. Volume XXV (1966) 469–483.
[94] A.-H.I. Mourad, M.G. Alghafri, O.A. Abu Zeid, Stable crack extension through AISI 4340 steel: Experimental investigation, in, Key Eng. Mater., Trans Tech Publ (2004) 207–212.
[95] A-H.I. Mourad, E. Elghandour, F.A. Kolkailah, Mixed mode stable crack extensions through stiffened specimens, 1999.
[96] L. Cheng, T. Luan, W. Du, M. Xu, Heat transfer enhancement by flow-induced vibration in heat exchangers, Int. J. Heat Mass Transf. 52 (2009) 1053–1057.
[97] M.T. Krawchuk, A. Girshik, Anti-vibration spacers used in tubular type heat exchangers, (1996).
[98] F.L. Eisinger, Prevention and cure of flow-induced vibration problems in tubular heat exchangers, (1980).
[99] F.L. Eisinger, R.E. Sullivan, Suppression of acoustic waves in steam generator and heat exchanger tube banks, J. Press. Vessel Technol. 125 (2003) 221–227.
[100] X. Mi, Z.B. Cai, X.M. Xiong, H. Qian, L.C. Tang, Y.C. Xie, J.F. Peng, M. Zhu, Investigation on fretting wear behavior of 690 alloy in water under various temperatures, Tribol. Int. 100 (2016) 400–409.
[101] M.J. Pettigrew, C.E. Taylor, Vibration analysis of shell-and-tube heat exchangers: an overview—Part 2: vibration response, fretting-wear, guidelines, J. Fluids Struct. 18 (2003) 485–500.
[102] M.J. Pettigrew, C.E. Taylor, Vibration analysis of shell-and-tube heat exchangers: an overview—Part 1: flow, damping, fluidelastic instability, J. Fluids Struct. 18 (2003) 469–483.
[103] M. Trafczynski, M. Markowski, K. Urbaniec, P. Trzciński, S. Alabrudzinski, W. Suchecki, Estimation of thermal effects of fouling growth for application in the scheduling of heat exchangers cleaning, Appl. Therm. Eng. 116103 (2020).
[104] W. Wojnar, Erosion of heat exchangers due to sootblowing, Eng. Fail. Anal. 33 (2013) 473–489.
[105] P.L. Barry, R.W. Vowles, Method of cleaning pipes and tubes by pigging using water hammer shock waves, (1988).
[106] E.A. Ainslie, G.L. Quarini, D.G. Ash, T.J. Deans, M. Herbert, T.D.L. Rhys, Heat exchanger cleaning using ice pigging, in: Heat Exch. Fouling Clean. VIII. Proc Int Conf Heat Exch. Fouling Cleaning, Schladming, Austria, 2009: pp. 433–438.
[107] B.J. Larson, Optimum Heat Exchanger Performance Depends On Clean Tubes, (n.d.).
[108] J. Loyola-Fuentes, R. Smith, Classification and estimation of unmeasured process variables in crude oil pre-heat trains subject to fouling deposition, Comput. Chem. Eng. 106779 (2020).
[109] B. Chen, D. Callens, P. Campistron, E. Moulin, P. Debreyne, G. Delaplace, Monitoring cleaning cycles of fouled ducts using ultrasonic coda wave interferometry (CWI), Ultrasonics 96 (2019) 253–260.
[110] Y. Shi, J. Wang, Z. Liu, On-line monitoring of ash fouling and soot-blowing optimization for convective heat exchanger in coal-fired power plant boiler, Appl. Therm. Eng. 78 (2015) 39–50.
[111] J. Li, Z. Zhai, J. Wang, S. Huang, On-line fouling monitoring model of condenser in coal-fired power plants, Appl. Therm. Eng. 104 (2016) 628–635.
[112] D.C. Pham, G. Mercère, R. Ouvrard, T. Poinot, H. Pálsson, Fouling detection in a parallel flow heat exchanger via a Roesser model identification procedure, IFAC-PapersOnLine. 50 (2017) 12866–12871.
[113] H.H. Chin, B. Wang, P.S. Varbanov, J.J. Klemeš, M. Zeng, Q.-W. Wang, Long-term investment and maintenance planning for heat exchanger network retrofit, Appl. Energy. 279 (2020), 115713.
[114] F.L. Santamaria, S. Macchietto, Integration of optimal cleaning scheduling and control of heat exchanger networks under fouling: MPCC solution, Comput. Chem. Eng. 126 (2019) 128–146.
[115] R. Al Ismaili, M.W. Lee, D.I. Wilson, V.S. Vassiliadis, Heat exchanger network cleaning scheduling: From optimal control to mixed-Integer decision making, Comput. Chem. Eng. 111 (2018) 1–15.
[116] R. Al Ismaili, M.W. Lee, D.I. Wilson, V.S. Vassiliadis, Optimisation of heat exchanger network cleaning schedules: Incorporating uncertainty in fouling and cleaning model parameters, Comput. Chem. Eng. 121 (2019) 409–421.
[117] F.L. Santamaria, S. Macchietto, Integration of optimal cleaning scheduling and flow split control for crude oil fouling mitigation in the operation of refinery heat exchanger networks, Comput. Aided Chem. Eng. (2018) 1087–1092.
[118] S. Sanaye, B. Niroomand, Simulation of heat exchanger network (HEN) and planning the optimum cleaning schedule, Energy Convers. Manag. 48 (2007) 1450–1461.
[119] S. Addepalli, D. Eiroa, S. Lieotrakool, A.-L. François, J. Guisset, D. Sanjaime, M. Kazarian, J. Duda, R. Roy, P. Phillips, Degradation study of heat exchangers, Procedia Cirp. 38 (2015) 137–142.
[120] A.S. El-Amoush, Hydrogen induced cracking and pitting of brass heat exchanger tube, Mater. Sci. Technol. 24 (2008) 711–717.
[121] A.-H.I. Mourad, S.K. Maiti, Influence of state of stress on mixed mode stable crack growth through D16AT aluminium alloy, Int. J. Fract. 72 (1995) 241–258.
[122] A-H.I. Mourad, Effect of stress state on mode II stable crack extension, in: Key Eng. Mater., Trans Tech Publ, 2005: pp. 1604–1610.
[123] A.-H.I. Mourad, Pure shear stable crack growth through compact-tension-shear specimen in plane state of stress, Strength Fract. Complex. 2 (2004) 111–125.
[124] K. Onishi, M. Yano, T. Hoshika, T. Haruna, Results Of An Investigation Into The Localized Hydrogen Embrittlement Of Titanium Heat Exchanger Tubes In A Wastewater Environment, in: Corros. 2007, OnePetro, 2007.
[125] R.K. Dayal, N. Parvathavarthini, Hydrogen embrittlement in power plant steels, Sadhana. 28 (2003) 431–451.
[126] H.M. Shalaby, Failure investigation of Muntz tubesheet and Ti tubes of surface condenser, Eng. Fail. Anal. 13 (2006) 780–788.
[127] N.S. MR, MR 01-75. Revision 1980 in, Mater. Require Ments, Sulfide Stress Crack. Resist. Met. Mater. Oil F. Eguipment.-7975. 31 (n.d.).
[128] S. Hoseinzadeh, P.S. Heyns, Thermo-structural fatigue and lifetime analysis of a heat exchanger as a feedwater heater in power plant, Eng. Fail. Anal. 104548 (2020).
[129] S. Courtin, High cycle thermal fatigue damage prediction in mixing zones of nuclear power plants: engineering issues illustrated on the FATHER case, Procedia Eng. 66 (2013) 240–249.
[130] R. Patil, S. Anand, Thermo-structural fatigue analysis of shell and tube type heat exchanger, Int. J. Press. Vessel. Pip. 155 (2017) 35–42.
[131] G.H. Farrahi, M. Chamani, A. Kiyoumarsioskouei, A.H. Mahmoudi, The effect of plugging of tubes on failure of shell and tube heat exchanger, Eng. Fail. Anal. 104 (2019) 545–559.
[132] G.H. Farrahi, K. Minaii, M. Chamani, A.H. Mahmoudi, Effect of residual stress on failure of tube-to-tubesheet weld in heat exchangers, Int. J. Eng. 32 (2019) 112–120.

[133] C.R.F. Azevedo, G.S. Alves, Failure analysis of a heat-exchanger serpentine, Eng. Fail. Anal. 12 (2005) 193–200.
[134] F. Dehnavi, A. Eslami, F. Ashrafizadeh, A case study on failure of superheater tubes in an industrial power plant, Eng. Fail. Anal. (2017), https://doi.org/10.1016/j.engfailanal.2017.07.007.
[135] S.K. Maiti, G.K. Kishore, A.-H.I. Mourad, Bilinear CTOD/CTOA scheme for characterisation of large range mode I and mixed mode stable crack growth through AISI 4340 steel, Nucl. Eng. Des. 238 (2008) 3175–3185.
[136] A.-H.I. Mourad, S.K. Maiti, Mode I and mixed-mode stable crack extensions through stiffened three-point bend specimens, Fatigue Fract. Eng. Mater. Struct. 18 (1995) 645–652.
[137] A.-H.I. Mourad, S.K. Maiti, Influence of state of stress on mode I and mixed mode stable crack growth through stiffened TPB specimens, Acta Mech. Solida Sin, Off. J. Chinese Soc. Theor. Appl. Mech. 8 (1995) 99–102.
[138] D.N. Adnyana, Failure of Heat Exchanger Return Bend Due to Long-Term Localized Overheating [Kerusakan pada Pipa Belokan U Alat Penukar Kalor akibat Panas Berlebih secara Lokal dalam Jangka Panjang], Metalurgi. 34 (2019) 19–30.
[139] J. Mao, D. Tang, S. Bao, L. Luo, Z. Gao, High temperature strength and multiaxial fatigue life assessment of a tubesheet structure, Eng. Fail. Anal. 68 (2016) 10–21.
[140] J. Mao, J. Zhang, W. Wang, Y. Liu, Creep-Fatigue Life Prediction of Stop and Regulating Valves on the Intermediate-Pressure Section of a 1000MW Steam Turbine, in: Turbo Expo Power Land, Sea, Air, American Society of Mechanical Engineers, 2013: p. V07AT27A002.
[141] J. Mao, W. Wang, Y. Liu, J. Zhang, Multiaxial creep-fatigue life prediction on the rotor of a 1000MW supercritical steam turbine, in: Turbo Expo Power Land (Ed.), Sea, American Society of Mechanical Engineers, Air, 2012, pp. 277–283.
[142] J. Ahmad, J. Purbolaksono, L. C, Thermal fatigue and corrosion fatigue in heat recovery area wall side tubes, Eng. Fail. Anal. 17 (2010) 334–343. https://doi.org/10.1016/j.engfailanal.2009.06.014.
[143] L.K. Zhu, L.J. Qiao, X.Y. Li, B.Z. Xu, W. Pan, L. Wang, A.A. Volinsky, Analysis of the tube-sheet cracking in slurry oil steam generators, Eng. Fail. Anal. 34 (2013) 379–386, https://doi.org/10.1016/j.engfailanal.2013.08.007.
[144] A. Usman, A.N. Khan, Failure analysis of heat exchanger tubes, Eng. Fail. Anal. 15 (2008) 118–128.
[145] D. Martens, M. Porter, S. McGuffie, J. Wheeler, A Means of Avoiding Sulfur Recovery Reaction Furnace Fired Tube Boiler Failures, ASME 2009 Press. Vessel. Pip. Div. Conf. (2009) 1–12. https://doi.org/10.1115/PVP2009-78073.
[146] D.H. Martens, C.S. Hsieh, C.. Brzon, Analysis of Tubesheet Stresses in a Sulfur Recovery Unit, in: ASME 1996 Press. Vessel. Pip. Conf., USA, 1996.
[147] The number one problem in a steam system-Water Hammer, (n.d.). https://www.swagelok.com/~/media/Distributor Media/C-G/Chicago/Services/ES - Waterhammer_BP_11.ashx (accessed August 29, 2017).
[148] S. Sukamta, I. Indarto, P. Purnomo, T.A. Rohmat, Experimental Investigation of slugging as initiating water hammer phenomena through indirect contacts steam condensing in a horizontal pipe heat exchanger, Int. J. Technol. 6 (2015) 909–915.
[149] A.-H.I. Mourad, S.K. Maiti, Mode II stable crack growth, Fatigue Fract. Eng. Mater. Struct. 19 (1996) 75–84, https://doi.org/10.1111/j.1460-2695.1996.tb00933.x.
[150] S.K. Maiti, A.-H.I. Mourad, Criterion for mixed mode stable crack growth—II. Compact tension geometry with and without stiffener, Eng. Fract. Mech. 52 (1995) 349–378.
[151] S. Dirndorfer, Steam condensation induced water hammer in a vertical up-fill configuration within an integral test facility: experiments and computational simulations, (2017).
[152] P. Datta, A. Chakravarty, K. Ghosh, A. Mukhopadhyay, S. Sen, A. Dutta, P. Goyal, I. Thangamani, Modeling and analysis of condensation induced water hammer, Numer. Heat Transf. Part A Appl. 74 (2018) 975–1000.
[153] T.J. Swierzawski, P. Griffith, Preventing water hammer in large horizontal pipes passing steam and water, (1990).
[154] A. SOURCEBOOK, Improving Steam System Performance: A Sourcebook for Industry, (n.d.).
[155] J.R. Risko, Stop Knocking Your Condensate Return, Chem. Eng. 112 (2016) 27.
[156] P. Datta, A. Chakravarty, K. Ghosh, A. Mukhopadhyay, S. Sen, A. Dutta, P. Goyal, A numerical analysis on the effect of inlet parameters for condensation induced water hammer, Nucl. Eng. Des. 304 (2016) 50–62.
[157] I.F. Barna, A.R. Imre, G. Baranyai, G. Ézsöl, Experimental and theoretical study of steam condensation induced water hammer phenomena, Nucl. Eng. Des. 240 (2010) 146–150.
[158] I. Tiselj, A. Horvat, G. Černe, J. Gale, I. Parzer, B. Mavko, M. Giot, J.M. Seynhaeve, B. Kucienska, H. Lemonnier, WAHALoads-two-phase flow water hammer transients and induced loads on materials and structures of nuclear power plants: WAHA3 code manual, 2004.
[159] I. Tiselj, C.S. Martin, Slug modeling with 1D two-fluid model, Kerntechnik. 77 (2012) 101–107.
[160] W. Wang, Y. Kong, X. Huang, L. Yang, X. Du, Y. Yang, Anti-freezing of air-cooled heat exchanger by switching off sectors, Appl. Therm. Eng. 120 (2017) 327–339.
[161] Z. Rogala, A. Brenk, Z. Malecha, Theoretical and numerical analysis of freezing risk during LNG evaporation process, Energies 12 (2019) 1426.
[162] M. Chorowski, P. Duda, J. Polinski, J. Skrzypacz, LNG systems for natural gas propelled ships, in: IOP Conf. Ser. Mater. Sci. Eng., IOP Publishing, 2015: p. 12089.
[163] A. Brenk, J. Kielar, Z. Malecha, Z. Rogala, The effect of geometrical modifications to a shell and tube heat exchanger on performance and freezing risk during LNG regasification, Int. J. Heat Mass Transf. 161 (2020), 120247.
[164] M.P. Schwartz, Four Types of Heat Exchanger Failures, n.d. http://www.deppmann.com/home/wp-content/uploads/2016/10/4-Types-of-Heat-Exchanger-Failures-article.pdf.
[165] Z. Shuzhi, Fracture failure analysis of heat exchangertube bundle, Refin Chem. Ind. (2012) 5.
[166] L. Chen, L. Yang, X. Du, Y. Yang, Anti-freezing of air-cooled heat exchanger by air flow control of louvers in power plants, Appl. Therm. Eng. 106 (2016) 537–550.
[167] Y. Kong, W. Wang, L. Yang, X. Du, Energy efficient strategies for anti-freezing of air-cooled heat exchanger, Appl. Energy. 261 (2020), 114468.
[168] X. Yang, H. Wei, R. Jin, L. Yang, X. Du, Y. Yang, Anti-freezing of air-cooled heat exchanger with rolling-type windbreaker, Int. J. Heat Mass Transf. 136 (2019) 70–86.
[169] H. Ma, F. Si, K. Zhu, J. Wang, Utilization of partial through-flow tower shell to cope with the excess cooling capacity of dry cooling tower in extremely cold days with crosswind, Int. J. Therm. Sci. 136 (2019) 70–85.
[170] L. Chen, L. Yang, X. Du, Y. Yang, Performance improvement of natural draft dry cooling system by interior and exterior windbreaker configurations, Int. J. Heat Mass Transf. 96 (2016) 42–63.
[171] K.M. Deen, M.A. Virk, C.I. Haque, R. Ahmad, I.H. Khan, Failure investigation of heat exchanger plates due to pitting corrosion, Eng. Fail. Anal. 17 (2010) 886–893.
[172] S. Lee, J. Kim, J. Koo, Investigation of pitting corrosion of a copper tube in a heating system, Eng. Fail. Anal. 17 (2010) 1424–1435, https://doi.org/10.1016/j.engfailanal.2010.05.002.
[173] K. Ranjbar, A. Taghavian, M. Amra, Failure assessment of an admiralty brass oil exchanger tubes, J. Fail. Anal. Prev. 20 (2020) 218–225.
[174] Y. Gong, M.-Y. Du, F.-Q. Ma, G.-Q. He, Y. Xue, C.-S. Jiao, X.-L. Yang, R.-B. Li, X.-Q. Liu, X.-L. Xu, Failure analysis and prevention of corrosion occurring during storage on steam generator tube sheet for advanced PWR, Part I: Root causes analysis, Eng. Fail. Anal. 116 (2020), 104710.
[175] C. Cao, D. Chen, J. Ren, J. Shen, L. Meng, J. Liu, Improved strength and enhanced pitting corrosion resistance of Al-Mn alloy with Zr addition, Mater. Lett. 255 (2019), 126535.
[176] E.M. Westin, S. Hertzman, Element distribution in lean duplex stainless steel welds, Weld. World. 58 (2014) 143–160.
[177] D.H. Kang, H.W. Lee, Study of the correlation between pitting corrosion and the component ratio of the dual phase in duplex stainless steel welds, Corros. Sci. 74 (2013) 396–407.

[178] D. Janikowski, Selecting tubing materials for power generation heat exchangers, 2003. http://www.plymouth.com/media/13960/Sel Tubing Mat for Pwr Gen _SW Chem_.pdf.
[179] R.T. Loto, Comparative study of the pitting corrosion resistance, passivation behavior and metastable pitting activity of NO7718, NO7208 and 439L super alloys in chloride/sulphate media, J. Mater. Res. Technol. 8 (2019) 623–629.
[180] Z. Zhang, H. Jing, L. Xu, Y. Han, L. Zhao, J. Zhang, Influence of microstructure and elemental partitioning on pitting corrosion resistance of duplex stainless steel welding joints, Appl. Surf. Sci. 394 (2017) 297–314.
[181] H. Xu, M.J. Xu, C. Yu, H. Lu, X. Wei, J.M. Chen, J.J. Xu, Effect of the microstructure in unmixed zone on corrosion behavior of 439 tube/308L tube-sheet welding joint, J. Mater. Process. Technol. 240 (2017) 162–167.
[182] Q. Ding, X.F. Tang, Z.G. Yang, Failure analysis on abnormal corrosion of economizer tubes in a waste heat boiler, Eng. Fail. Anal. 73 (2017) 129–138, https://doi.org/10.1016/j.engfailanal.2016.12.011.
[183] Z. Liang, Q. Zhao, Failure analysis of spiral finned tube on the economizer, Eng. Fail. Anal. 28 (2013) 208–214, https://doi.org/10.1016/j.engfailanal.2012.10.010.
[184] H.M. Shalaby, K. Ravindranath, N. Tanoli, B. Al-Wakaa, Failure of 321 stainless steel heater tube in heavy crude oil, Case Stud Eng. Fail. Anal. 9 (2017) 1–8, https://doi.org/10.1016/j.csefa.2017.04.004.
[185] V.F.C. Lins, E.M. Guimarães, Failure of a heat exchanger generated by an excess of SO2 and H2S in the sulfur recovery unit of a petroleum refinery, J. Loss Prev. Process Ind. 20 (2007) 91–97.
[186] H. Farhat, R. Johnsen, Hydrogen sulfide tube failure in a seawater heat exchanger, Mater. Perform. 56 (2017) 42–45.
[187] G.F. Kennell, R.W. Evitts, K.L. Heppner, A critical crevice solution and IR drop crevice corrosion model, Corros. Sci. 50 (2008) 1716–1725, https://doi.org/10.1016/j.corsci.2008.02.020.
[188] Pitting Corrosion vs. Crevice Corrosion: Identifying the Differences, (n.d.). https://thailand.swagelok.com/en/Blog/Oil_and_Gas_Applications/Pitting_Corrosion_vs_Crevice_Corrosion#.
[189] A. Gagliardi, A. Lanzutti, M. Simonato, R. Furlanetto, M. Magnan, F. Andreatta, L. Fedrizzi, Failure analysis of a plate heat exchanger used in a blast chiller, Eng. Fail. Anal. 92 (2018) 289–300.
[190] S.-T. Tu, H. Zhang, W.W. Zhou, Corrosion failures of high temperature heat pipes, Eng. Fail. Anal. 6 (1999) 363–370.
[191] S. Narain, S.H. Asad, Corrosion Problems in Low-Temperature Desalination Units, Acom No. 2-93 6. (1993).
[192] S.R. Allahkaram, P. Zakersafaee, S.A.M. Haghgoo, Failure analysis of heat exchanger tubes of four gas coolers, Eng. Fail. Anal. 18 (2011) 1108–1114.
[193] M. Awais, A.A. Bhuiyan, Recent advancements in impedance of fouling resistance and particulate depositions in heat exchangers, Int. J. Heat Mass Transf. 141 (2019) 580–603.
[194] J. Taborek, Fouling: the major unsolved problem in heat transfer, Chem. Eng. Prog. 68 (1972) 59–67.
[195] A. Belmiloudi, Heat Transfer: Theoretical Analysis, Experimental Investigations and Industrial Systems, BoD–Books on Demand, 2011.
[196] D.J. Kukulka, M. Devgun, Fouling surface finish evaluation, Appl. Therm. Eng. 27 (2007) 1165–1172, https://doi.org/10.1016/j.applthermaleng.2006.02.041.
[197] F. Albert, W. Augustin, S. Scholl, Roughness and constriction effects on heat transfer in crystallization fouling, Chem. Eng. Sci. 66 (2011) 499–509.
[198] S.N. Kazi, G.G. Duffy, X.D. Chen, Mineral scale formation and mitigation on metals and a polymeric heat exchanger surface, Appl. Therm. Eng. 30 (2010) 2236–2242.
[199] S.N. Kazi, K.H. Teng, M.S. Zakaria, E. Sadeghinezhad, M.A. Bakar, Study of mineral fouling mitigation on heat exchanger surface, Desalination 367 (2015) 248–254.
[200] T.E.M. Association, Standard of tubular exchanger manufacturers association, The association (1952).
[201] F. Wang, Y. He, S. Tang, Z. Tong, Parameter study on the fouling characteristics of the H-type finned tube heat exchangers, Int. J. Heat Mass Transf. 112 (2017) 367–378, https://doi.org/10.1016/j.ijheatmasstransfer.2017.04.107.
[202] M. Trafczynski, M. Markowski, K. Urbaniec, Monitoring of important variables affecting the formation of fouling in crude oil heat exchangers, Chem. Eng. Trans. 70 (2018) 1921–1926.
[203] M. Yang, B. Crittenden, Fouling thresholds in bare tubes and tubes fitted with inserts, Appl. Energy. 89 (2012) 67–73.
[204] D.A. Al-Otaibi, M.S.J. Hashmi, B.S. Yilbas, Fouling resistance of brackish water: comparision of fouling characteristics of coated carbon steel and titanium tubes, Exp. Therm. Fluid Sci. 55 (2014) 158–165.
[205] C.B. Panchal, J.G. Knudsen, Mitigation of water fouling: technology status and challenges, Adv. Heat Transf. 31 (1998) 431–474.
[206] J. Su, M. Ma, T. Wang, X. Guo, L. Hou, Z. Wang, Fouling corrosion in aluminum heat exchangers, Chinese J. Aeronaut. 28 (2015) 954–960.
[207] L. Ren, Y. Cheng, Q. Wang, X. Tian, J. Yang, D. Zhang, Relationship between corrosion product and fouling growth on mild steel, copper and brass surface, Colloids Surfaces A Physicochem. Eng. Asp. 591 (2020), 124502.
[208] J.F. Mao, J.W. Zhu, S.Y. Bao, L.J. Luo, Z.L. Gao, Creep deformation and damage behavior of reactor pressure vessel under core meltdown scenario, Int. J. Press. Vessel. Pip. 139 (2016) 107–116.
[209] S.S. Al-Anizi, A.M. Al-Otaibi, Double perforated impingement plate in shell-and-tube heat exchanger, Heat Transf. Eng. 30 (2009) 885–894.
[210] D.J. Kukulka, M. Devgun, Fluid temperature and velocity effect on fouling, Appl. Therm. Eng. 27 (2007) 2732–2744.
[211] C. Cunault, Y. Coquinot, C.H. Burton, S. Picard, A.M. Pourcher, Characteristics and composition of fouling caused by pig slurry in a tubular heat exchanger–recommended cleaning systems, J. Environ. Manage. 117 (2013) 17–31.
[212] A.E. Zohir, The influence of pulsation on heat transfer in a heat exchanger for parallel and counter water flows, New York Sci. J. 4 (2011) 61–71.
[213] M.S. Abd-Elhady, M.R. Malayeri, M.R. Jalalirad, Intensification of the cleaning action of structurally different projectiles by multiple injections and changing injection rate, Desalination 337 (2014) 52–59.
[214] M.R. Jalalirad, M.S. Abd-Elhady, M.R. Malayeri, Cleaning action of spherical projectiles in tubular heat exchangers, Int. J. Heat Mass Transf. 57 (2013) 491–499.
[215] M.R. Jalalirad, M.R. Malayeri, R. Preimesser, Online cleaning of tubular heat exchangers in water service systems using projectiles, Desalin. Water Treat. 51 (2013) 780–785.
[216] M. Muñoz Sellarès, Utilization of various projectiles to mitigate fouling in tubular heat exchangers, 2010.
[217] P.L. Barry, R.W. Vowles, Cleaning of tubes using projectiles, 1990.
[218] M.R. Malayeri, M.R. Jalalirad, Abatement of deposit formation in aqueous systems using various projectiles, Desalin. Water Treat. 55 (2015) 2931–2938.
[219] M.S. Abd-Elhady, M.R. Malayeri, Fouling mitigation in tubular exchangers using various projectiles: deposit removal mechanisms, Chem. Eng. Technol. 38 (2015) 2226–2234.
[220] S.P. Hinge, A.W. Patwardhan, Thermal-hydraulic performance of an annular pipe with square wire coil inserts using computational fluid dynamics, Ind. Eng. Chem. Res. 59 (2019) 3887–3903.
[221] A. Krueger, F. Pouponnot, Heat exchanger tube insert–an update in new application with trouble shooting aspects in crude unit, residue service, reboilers, U tubes, in: Proc. ECI Conf. Heat Exch. Fouling Cleaning-Challenges Oppor. Irsee, Ger., 2005.
[222] D.P. Ubale, Heat transfer enhancement in heat exchanger using twisted-tape inserts: a review, in: Int. Conf. Ideas, Impact Innov. Mech. Eng., 2017: pp. 425–428.
[223] A.T. Wijayanta, M. Aziz, K. Kariya, A. Miyara, Numerical study of heat transfer enhancement of internal flow using double-sided delta-winglet tape insert, Energies 11 (2018) 3170.
[224] G. Liu, C. Yang, J. Zhang, H. Zong, B. Xu, J. Qian, Internal flow analysis of a heat transfer enhanced tube with a segmented twisted tape insert, Energies 13 (2020) 207.
[225] A.T. Wijayanta, B. Kristiawan, M. Aziz, Internal flow in an enhanced tube having square-cut twisted tape insert, Energies 12 (2019) 306.
[226] S.W. Hong, A.E. Bergles, Augmentation of laminar flow heat transfer in tubes by means of twisted-tape inserts, 1976.
[227] M.M. Abu-Khader, An overview on tube inserts configurations and performances in tubular exchangers, World J. Eng., 2016.

[228] M.F. Saffiudeen, F.T. Mohammed, A. Syed, A case study on procedure standardization of heat exchanger retubing in KSA oil and gas industries, J. Fail. Anal. Prev. 20 (2020) 1451–1455.
[229] T.L. Hardenburger, M. Ennis, Nitrogen, Kirk-Othmer Encycl. Chem. Technol., 2000.
[230] R.K. Shah, B. Thonon, D.M. Benforado, Opportunities for heat exchanger applications in environmental systems, Appl. Therm. Eng. 20 (2000) 631–650.
[231] C. Goujon, T. Pauporté, A. Bescond, C. Mansour, S. Delaunay, J.-L. Bretelle, Effects of curative and preventive chemical cleaning processes on fouled steam generator tubes in nuclear power plants, Nucl. Eng. Des. 323 (2017) 120–132.
[232] H. Kawamura, K. Fujiwara, H. Kanbe, H. Hirano, H. Takiguchi, K. Yoshino, S. Yamamoto, T. Shibata, K. Ishigure, Applicability of chemical cleaning process to steam generator secondary side, (II) effect of chemical cleaning on integrity of SG tubing under accelerated IGSCC conditions, J. Nucl. Sci. Technol. 42 (2005) 275–288.
[233] K. Fujiwara, H. Kawamura, H. Kanbe, H. Hirano, H. Takiguchi, K. Yoshino, S. Yamamoto, T. Shibata, K. Ishigure, Applicability of chemical cleaning process to steam generator secondary side,(IV) Comprehensive applicability evaluation of chemical cleaning and its effect on integrity of other structural materials other than steam generator tubes, J. Nucl. Sci. Technol. 43 (2006) 1344–1358.
[234] H. Kawamura, K. Fujiwara, H. Kanbe, H. Hirano, H. Takiguchi, K. Yoshino, S. Yamamoto, T. Shibata, K. Ishigure, Applicability of chemical cleaning process to steam generator secondary side,(III) effect of chemical cleaning on long term integrity of steam generator tube after chemical cleaning process, J. Nucl. Sci. Technol. 43 (2006) 655–668.
[235] A.P.I. Popoola, O.E. Olorunniwo, O.O. Ige, Corrosion resistance through the application of anti-corrosion coatings, Dev. Corros. Prot. 2 (2014) 241–270.
[236] R. Mansour, A.M. Elshafei, Role of microorganisms in corrosion induction and prevention, Biotechnol. J. Int. (2016) 1–11.
[237] G. Tang, K. Zhang, Z. Yan, L. Ma, X. Huang, A self-curing, thermosetting resin based on epoxy and organic titanium chelate as an anticorrosive coating matrix for heat exchangers: preparation and properties, Prog. Org. Coatings. 102 (2017) 225–230.
[238] C.S. Boruff, K.E.S. Pekin III, Intermittent chlorination of condenser water, Ind. Eng. Chem. 24 (1932) 398–400.
[239] J.F. Blais, R.D. Tyagi, J.C. Auclair, Bioleaching of metals from sewage sludge: microorganisms and growth kinetics, Water Res. 27 (1993) 101–110.
[240] E.H. Valdebenito-Rolack, T.C. Araya, L.E. Abarzua, N.M. Ruiz-Tagle, K.E. Sossa, G.E. Aroca, H.E. Urrutia, Thiosulphate oxidation by Thiobacillus thioparus and Halothiobacillus neapolitanus strains isolated from the petrochemical industry, Electron. J. Biotechnol. 14 (2011) 7–8.
[241] E. Huttunen-Saarivirta, M. Honkanen, T. Lepistö, V.-T. Kuokkala, L. Koivisto, C.-G. Berg, Microbiologically influenced corrosion (MIC) in stainless steel heat exchanger, Appl. Surf. Sci. 258 (2012) 6512–6526.
[242] F.M. AlAbbas, R. Bhola, J.R. Spear, D.L. Olson, B. Mishra, Electrochemical characterization of microbiologically influenced corrosion on linepipe steel exposed to facultative anaerobic Desulfovibrio sp, Int J Electrochem Sci. 8 (2013) 859–871.
[243] S. Chitra, B. Anand, R. Vaidiyanathan, V. Balasubramanian, A review on microbial mediated corrosion on mild steel by inactivating the extracellular polysaccharide secreted by aerobic/anaerobic microorganism, Chem Sci Rev Lett. 3 (2014) 56–62.
[244] H.H. Almahamedh, Microbiologically Influenced Corrosion of Heat Exchanger Tubes, in: Corros. 2014, NACE International, 2014.
[245] M. Lv, M. Du, A review: microbiologically influenced corrosion and the effect of cathodic polarization on typical bacteria, Rev. Environ. Sci. Bio/Technology. 17 (2018) 431–446.
[246] J. Starosvetsky, D. Starosvetsky, R. Armon, Identification of microbiologically influenced corrosion (MIC) in industrial equipment failures, Eng. Fail. Anal. 14 (2007) 1500–1511.
[247] T.L. Skovhus, R.B. Eckert, E. Rodrigues, Management and control of microbiologically influenced corrosion (MIC) in the oil and gas industry—Overview and a North Sea case study, J. Biotechnol. 256 (2017) 31–45.
[248] P. Sharma, Microbiological-influenced corrosion failure of a heat exchanger tube of a fertilizer plant, J. Fail. Anal. Prev. 14 (2014) 314–317.
[249] M.N. Nazarova, R.R. Akhmetov, S.A. Krainov, Temperature factors effect on occurrence of stress corrosion cracking of main gas pipeline, in: IOP Conf. Ser. Earth Environ. Sci., IOP Publishing, 2017: p. 62011.
[250] J. Nakano, T. Sato, C. Kato, M. Yamamoto, T. Tsukada, Y. Kaji, Effects of temperature on stress corrosion cracking behavior of stainless steel and outer oxide distribution in cracks due to exposure to high-temperature water containing hydrogen peroxide, J. Nucl. Mater. 444 (2014) 454–461.
[251] Y. Zhong, C. Zhou, S. Chen, R. Wang, Effects of temperature and pressure on stress corrosion cracking behavior of 310S stainless steel in chloride solution, Chinese J Mech. Eng. 30 (2017) 200–206.
[252] T. Prosek, A. Iversen, C. Taxen, D. Thierry, Low-temperature stress corrosion cracking of stainless steels in the atmosphere in the presence of chloride deposits, Corrosion 65 (2009) 105–117.
[253] G. Hinds, A. Turnbull, Threshold temperature for stress corrosion cracking of duplex stainless steel under evaporative seawater conditions, Corrosion 64 (2008) 101–106.
[254] H. Hayashibara, M. Mayuzumi, Y. Mizutani, Effects of temperature and humidity on atmospheric stress corrosion cracking of 304 stainless steel, in: Corros. 2008, NACE International, 2008.
[255] L.Y. Huang, H.Q. Zhu, F.F. Zhang, X.W. Wang, Effect of temperature on the stress corrosion cracking of 304L austenitic stainless steels in alkaline solution, in, Mater. Sci. Forum, Trans Tech Publ (2015) 354–357.
[256] L. Cizelj, B. Mavko, H. Riesch-Oppermann, A. Briicker-Foit, Propagation of stress corrosion cracks in steam generator tubes, Int. J. Press. Vessel. Pip. 63 (1995) 35–43.
[257] K.I. Shin, J.H. Park, H.-D. Kim, H.-S. Chung, Simulation of stress corrosion crack growth in steam generator tubes, Nucl. Eng. Des. 214 (2002) 91–101, https://doi.org/10.1016/S0029-5493(02)00018-3.
[258] K. Thulukkanam, Heat Exchanger Design Handbook, Second Edition, 2013. https://doi.org/10.1201/b14877.
[259] A. Khalifeh, Stress corrosion cracking damages, in: Fail. Anal., IntechOpen, 2019.
[260] I.M. Robertson, The effect of hydrogen on dislocation dynamics, Eng. Fract. Mech. 68 (2001) 671–692.
[261] A. Fragiel, S. Serna, J. Malo-Tamayo, P. Silva, B. Campillo, E. Martínez-Martínez, L. Cota, M.H. Staia, E.S. Puchi-Cabrera, R. Perez, Effect of microstructure and temperature on the stress corrosion cracking of two microalloyed pipeline steels in H2S environment for gas transport, Eng. Fail. Anal. 105 (2019) 1055–1068.
[262] L. Dong, C. Ma, Q. Peng, E.-H. Han, W. Ke, Microstructure and stress corrosion cracking of a SA508-309L/308L-316L dissimilar metal weld joint in primary pressurized water reactor environment, J. Mater. Sci. Technol. 40 (2020) 1–14.
[263] Y.A. Alzafin, A.-H.I. Mourad, M. Abou Zour, O.A. Abuzeid, A study on the failure of pump casings made of ductile Ni-resist cast irons used in desalination plants, Eng. Fail. Anal. 14 (2007) 1294–1300.
[264] M.A. Rao, R.S. Babu, M.V.P. Kumar, Stress corrosion cracking failure of a SS 316L high pressure heater tube, Eng. Fail. Anal. 90 (2018) 14–22.
[265] J.S. Corte, J.M.A. Rebello, M.C.L. Areiza, S.S.M. Tavares, M.D. Araujo, Failure analysis of AISI 321 tubes of heat exchanger, Eng. Fail. Anal. 56 (2015) 170–176.
[266] J. Hu, F. Liu, G. Cheng, Z. Zhang, Determination of the critical crack length for steam generator tubing based on fracture-mechanics-based method, Ann. Nucl. Energy. 38 (2011) 1900–1905, https://doi.org/10.1016/j.anucene.2011.05.009.
[267] H. Panahi, A. Eslami, M.A. Golozar, A.A. Laleh, An investigation on corrosion failure of a shell-and-tube heat exchanger in a natural gas treating plant, Eng. Fail. Anal. 104918 (2020).
[268] A. Pola, M. Gelfi, L.E. Depero, R. Roberti, Study of annealing temperature effect on stress-corrosion cracking of aluminum brass heat-exchangers tubes by microdiffraction experiments, Eng. Fail. Anal. 15 (2008) 54–61.
[269] A. Ahmadi, M. shayegani Akmal, A. Pasha, S. Yareie, Failure analysis of cracked 2.25 Cr–1.0 Mo steel tubes of an oil refinery boiler, Eng. Fail. Anal. 110 (2020) 104435.
[270] Y. Li, Z. Liu, E. Fan, Y. Huang, Y. Fan, B. Zhao, Effect of cathodic potential on stress corrosion cracking behavior of different heat-affected zone microstructures of E690 steel in artificial seawater, J. Mater. Sci. Technol. (2019).
[271] S. Xu, Y. Zhao, Using FEM to determine the thermo-mechanical stress in tube to tube-sheet joint for the SCC failure analysis, Eng. Fail. Anal. 34 (2013) 24–34, https://doi.org/10.1016/j.engfailanal.2013.07.011.

[272] D.R. Diercks, W.J. Shack, J. Muscara, Overview of steam generator tube degradation and integrity issues, Nucl. Eng. Des. 194 (1999) 19–30, https://doi.org/10.1016/S0029-5493(99)00167-3.
[273] A.H. Bouzid, A.-H.I. Mourad, A. El Domiaty, Influence of Bauschinger effect on the residual contact pressure of hydraulically expanded tube-to-tubesheet joints, Int. J. Press. Vessel. Pip. 146 (2016) 1–10, https://doi.org/10.1016/j.ijpvp.2016.07.002.
[274] A.-H. Bouzid, M. Kazeminia, Effect of reverse yielding on the residual contact stresses of tube-to-tubesheet joints subjected to hydraulic expansion, in: ASME 2015 Press. Vessel. Pip. Conf., American Society of Mechanical Engineers Digital Collection, 2015.
[275] N.E. Laghzale, A.-H.I. Mourad, Theoretical analysis of hydraulically expanded tube-to-tubesheet joints with linear strain hardening material behavior, J. Press. Vessel Technol. 131 (2009) 61202–61208, https://doi.org/10.1115/1.4000197.
[276] N.E. Laghzale, A.-H.I. Mourad, Effect of creep on the residual stresses in tube-to-tubesheet joints, J. Press. Vessel Technol. 132 (2010) 61210, https://doi.org/10.1115/1.4001218.
[277] S.H. Khodamorad, N. Alinezhad, D.H. Fatmehsari, K. Ghahtan, Stress corrosion cracking in Type 316 plates of a heat exchanger, Biochem. Pharmacol. 5–6 (2016) 59–66, https://doi.org/10.1016/j.csefa.2016.03.001.
[278] A.I. Aljoboury, A.-H.I. Mourad, A. Alawar, M. Abou Zour, O.A. Abuzeid, Stress corrosion cracking of stainless steels recommended for building brine recirculation pumps, Eng. Fail. Anal. 17 (2010) 1337–1344, https://doi.org/10.1016/j.engfailanal.2010.03.008.
[279] Y.A. Alzafin, A.-H.I. Mourad, M.A. Zour, O.A. Abuzeid, Stress corrosion cracking of Ni-resist ductile iron used in manufacturing brine circulating pumps of desalination plants, Eng. Fail. Anal. 16 (2009) 733–739, https://doi.org/10.1016/j.engfailanal.2008.06.013.
[280] H.M. Tawancy, Failure of hydrocracker heat exchanger tubes in an oil refinery by polythionic acid-stress corrosion cracking, Eng. Fail. Anal. 16 (2009) 2091–2097.
[281] A.R. Khalifeh, A.D. Banaraki, H. Daneshmanesh, M.H. Paydar, Stress corrosion cracking of a circulation water heater tubesheet, Eng. Fail. Anal. 78 (2017) 55–66, https://doi.org/10.1016/j.engfailanal.2017.03.007.
[282] S.M.R. Ziaei, J. Mostowfi, M. Golestani, S.A.R. Ziaei, Failure analysis: chloride stress corrosion cracking of AISI 316 stainless steel downhole pressure memory gauge cover, Eng. Fail. Anal. (2013), https://doi.org/10.1016/j.engfailanal.2013.06.022.
[283] Y. Li, N. Xu, X. Wu, J. Shi, L. Zhang, M. Zhao, Q. Zang, Failure analysis of the 304 stainless steel tube in a gas analyzer, Eng. Fail. Anal. 20 (2012) 35–42, https://doi.org/10.1016/j.engfailanal.2011.10.004.
[284] H.S. Alkhaldi, A.I.O. Zaid, S.M. Alkhaldi, Shot peening as a process for improving fatigue life, strength and enhancing the resistance to stress corrosion cracking, Int. J. Sci. Eng. Res. 8 (2017) 584.
[285] R. Parrott, H. Pitts, H.D. Hill, Chloride stress corrosion cracking in austenitic stainless steel, Heal. Saf. Lab. Heal. Saf. Exec. Buxton, UK. (2011).
[286] C.A. Duarte, E. Espejo, J.C. Martinez, Failure analysis of the wall tubes of a water-tube boiler, Eng. Fail. Anal. 79 (2017) 704–713, https://doi.org/10.1016/j.engfailanal.2017.05.032.
[287] A.S.M. Handbook, Failure analysis and prevention, ASM Int. 11 (1986).
[288] K. Ravindranath, N. Tanoli, H. Gopal, Failure investigation of brass heat exchanger tube, Eng. Fail. Anal. 26 (2012) 332–336, https://doi.org/10.1016/j.engfailanal.2012.07.018.
[289] E.M. Zahrani, Premature failure of grade-316Ti stainless steel tubing in a boiler feed-water heat exchanger in a steel complex, J. Fail. Anal. Prev. 21 (2021) 61–73.
[290] R. Sui, Y. Zhao, B. Ge, W. Wang, Failure analysis of leakage at tube-to-tubesheet joints of a waste heat boiler, Eng. Fail. Anal. 129 (2021), 105639.
[291] E. Svensson, M. Catapano, Evaluation of the Tube to Tubesheet Joining Process in an AL6XN® Feedwater Heater, in: ASME Power Conf., American Society of Mechanical Engineers, 2017: p. V001T05A006.
[292] C.K. Chen, Failure analysis of corroded tube–tubesheet in an oxy-chlorination reactor, J. Fail. Anal. Prev. 7 (2007) 6–11.
[293] P. Baboo, High pressure vessel leakage in urea plants, GSJ 9 (2021).
[294] T.K. Mitra, A. Pai, P. Kumar, Challenges in manufacture of PFBR steam generators, Energy Procedia 7 (2011) 317–322.
[295] C. Moon, W.C. Brown, S. Mellen, E. Frenz, D.J. Pickering, Ultrasound techniques for leak detection, SAE Technical Paper, 2009.
[296] P. Tashian, Successful Leak Detection using Ultrasonics, AccuTrack® Ultrason. Instruments.[Online]. Available Http//Superiorsignal. Com/Resources/Useful-Articles/104-Successful-Leakdetection-Using-Ultrasonics.[Accessed 25-May-2020]. (n.d.).
[297] O. Hunaidi, A. Wang, M. Bracken, T. Gambino, C. Fricke, Detecting leaks in water distribution pipes, Institute for Research in Construction, National Research Council of Canada, 2000.
[298] P. Martínez-Garzón, M. Bohnhoff, G. Kwiatek, G. Zambrano-Narváez, R. Chalaturnyk, Microseismic monitoring of CO2 injection at the penn west enhanced oil recovery pilot project, canada: Implications for detection of wellbore leakage, Sensors 13 (2013) 11522–11538.
[299] O. Hunaidi, W. Chu, A. Wang, W. Guan, Detecting leaks in plastic pipes, Journal-American Water Work. Assoc. 92 (2000) 82–94.
[300] P. Razi, F. Taheri, A vibration-based strategy for health monitoring of offshore pipelines' girth-welds, Sensors. 14 (2014) 17174–17191.
[301] R. Bates, M. Battistin, S. Berry, A. Bitadze, P. Bonneau, N. Bousson, G. Boyd, G. Bozza, O. Crespo-Lopez, E. Da Riva, Implementation of ultrasonic sensing for high resolution measurement of binary gas mixture fractions, Sensors 14 (2014) 11260–11276.
[302] A.S. Almazyad, Y.M. Seddiq, A.M. Alotaibi, A.Y. Al-Nasheri, M.S. BenSaleh, A.M. Obeid, S.M. Qasim, A proposed scalable design and simulation of wireless sensor network-based long-distance water pipeline leakage monitoring system, Sensors 14 (2014) 3557–3577.
[303] W. Guo, S. Qian, Z. Ling, D. Hou, Research on phased array ultrasonic technique for testing tube to tube-sheet welds of heat exchanger, in: Press. Vessel. Pip. Conf., American Society of Mechanical Engineers, 2016: p. V005T10A003.
[304] S. Yokell, Assuring tube-to-tubesheet joint tightness and strength, J. Press. Vessel Technol. 134 (2012).
[305] A.F. Lillie, High quality tube-to-tubesheet joints-when, where and why, Rockwell International Corp., Canoga Park, CA (USA). Energy Systems Group, 1979.
[306] A. Pai, T.K. Mitra, S. Prasath, S. Athmalingam, T. Loganathan, P. Kumar, Quality control & quality assurance for tube to tubesheet joints and shell weld joints of straight tube design decay heat exchangers for 500mwe prototype fast breeder reactor, (n.d.).
[307] A. Marino, M. Carminati, Enhanced inspection of tube to tube-sheet welds in heat exchanger and JTFA for defect characterisation, 2006.
[308] B.S. Yoon, S.H. Yang, Y.S. Kim, H.J. Lee, Steam generator tube inspection of nuclear power plants using ultrasonic testing, Wear 20 (2006).
[309] A.S. Bandes, Ultrasound Leak Tests on Heat Exchangers, (n.d.). https://www.airbestpractices.com/technology/instrumentation/ultrasound-leak-tests-heat-exchangers#:~:text=By%3A Alan S.&text=Typically%2C ultrasound leak detection is,rate below 1x10-3 std.
[310] M. Bergoglio, D. Mari, Leak rate metrology for the society and industry, Measurement 45 (2012) 2434–2440.
[311] C. Moon, W.C. Brown, S. Mellen, D. Lovelace, Ultrasound techniques for leak detection in vehicle and pressure vessel production lines, Noise-Con 2008 (2008).
[312] 2015 ASME Boiler & Pressure Vessel Code section v, 2015th ed., NY, 2015. https://doi.org/https://doi.org/10.1016/B978-032303506-4.10361-X.
[313] E. Sizeland, Ultrasonic devices improve gas leak detection in challenging environments., World Oil. (2014) 133-135,[Accessed: 25-May-2020]. https://www.emerson.com/documents/automation/article-ultrasonic-leak-detection-in-challenging-environments-rosemount-en-72564.pdf.
[314] M. Stewart, Pipeline Pigging, in: Surf. Prod. Oper. Vol. IIIFacility Pip. Pipeine Syst., 2016: pp. 897–960.
[315] K. Boving, Ultrasonic Leak Detection, in: NDE HandbookNon-Destructive Exam. Methods Cond. Monit., 1989: pp. 148–158. http://scholar.google.com/scholar?hl=en&btnG=Search&q=intitle:NDE+Handbook#2.
[316] D. Holderness, J. Bruno, Effective expansion and repair of tube-to-tubesheet joints in a high pressure feedwater heater, Power Conf. (2010) 201–205.
[317] R.N. Bloomer, Leak detection and measurements by vacuum bubblers, Vacuum 23 (1973) 239–244, https://doi.org/10.1016/0042-207X(73)90070-5.
[318] Shell-and-Tube Heat Exchangers, ANSI/API Standard 660, American Petroleum Institute, Washington, DC, 2007.
[319] S. Yokell, Pressure testing feedwater heaters and power plant auxiliary heat exchangers, J. Press. Vessel Technol. 133 (2011).
[320] K.M. Massey, M.W. Jones, Tube Pullout Testing Experience, in: Proc. ASME 2012 Power Conf., California, USA, 2012: pp. 1–9. https://doi.org/10.1115/ICONE20-POWER2012-55186.
[321] Z. Ayub, World's largest ammonia heat pump (14 MWh) for district heating in Norway—a case study, Heat Transf. Eng. 37 (2016) 382–386.

[322] A. Lešnjak, J. Tušek, B. Arsenijevič, J. Gasperič, K. Gudek, A. Vučajnk, LEAK TESTING UNDER WATER, in: 8th Int. Conf. Slov. Soc. Non-Destructive Test., Citeseer, 2005: pp. 369–374.
[323] W. Xu, K.J. Xu, J.P. Wu, X.L. Yu, X.X. Yan, W. Xiong, Floor noise based bubble detection method in sodium using EVFM, Nucl. Eng. Des. 355 (2019), 110287, https://doi.org/10.1016/j.nucengdes.2019.110287.
[324] W. Xu, K.J. Xu, J.P. Wu, C.C. Wang, Bubble detection in sodium flow using EVFM and correlation coefficient calculation, Ann. Nucl. Energy. 129 (2019) 472–481, https://doi.org/10.1016/j.anucene.2019.02.015.
[325] B.H. Minor, Method for leak detection in heat transfer systems, 2011.
[326] M. Bowling, Leakage testing method for a plate heat exchanger, 2000.
[327] J.S. Samantray, S. Goswami, V.K. Sharma, J. Biswal, H.J. Pant, Leak detection in a high-pressure heat exchanger system in a refinery using radiotracer technique, J. Radioanal. Nucl. Chem. 302 (2014) 979–982.
[328] R.M. Shriwardhankar, P.B. Patil, M. Limaye, Development of helium leak testing system and procedure for testing welds of steam generator, Energy Procedia 7 (2011) 638–644.
[329] Q. Jiang, M. Zhuang, Q. Zhang, Z. Zhu, M. Geng, L. Sheng, P. Zhu, Experimental study on the thermal hydraulic performance of plate-fin heat exchangers for cryogenic applications, Cryogenics (Guildf). 91 (2018) 58–67.
[330] M. Goyal, A. Chakravarty, M.D. Atrey, Experimental investigations and validation of two dimensional model for multistream plate fin heat exchangers, Cryogenics (Guildf). 82 (2017) 83–91.
[331] M. Palaniappan, P.V. Thomas, B.S.C. Rao, R. Chandramohan, Mass spectrometer helium leak testing of large volume pipelines and pressure vessels of a nuclear power plant, Int. J. Press. Vessel. Pip. 73 (1997) 39–44.
[332] TEMA heat exchanger, 1999.
[333] ASME, ASME boiler & pressure vessel code: VIII, division 1, Rules for construction of pressure vessels, ASME 2010 (2010) 1–746.
[334] P. Kumar, A. Pai, An overview of welding aspects and challenges during manufacture of Intermediate Heat Exchangers for 500MWe Prototype Fast Breeder Reactor, Procedia Eng. 86 (2014) 173–183, https://doi.org/10.1016/j.proeng.2014.11.026.
[335] R. Kaul, N.G. Muralidharan, T. Jayakumar, K.V. Kasiviswanathan, B. Raj, R.K. Dayal, V.R. Raju, J.B. Gnanamoorthy, S. Pattu, Failure analysis of carbonate reboiler heat exchangers, Eng. Fail. Anal. 2 (1995) 165–174.
[336] M.-R. Lee, J.-H. Lee, Development of leak detection system of heat exchanger using acoustic emission technique, in: Proc. KSME Conf., The Korean Society of Mechanical Engineers, 2001: pp. 65–71.
[337] L. Hanacek, H. Winkler, Inspection of the heat exchangers of the reactor saphir by Acoustic Emission, Zeitschrift Fuer Werkstofftechnik. 15 (1984) 246–250.
[338] B.K. Guépié, E. Grall-Maës, P. Beauseroy, I. Nikiforov, F. Michel, Reliable leak detection in a heat exchanger of a sodium-cooled fast reactor, Ann. Nucl. Energy. 142 (2020), 107357.
[339] G. Jean-Luc, J. Eric, L. Francois, H. Joel, Detecting leaks in a heat exchanger in operation, (1987).
[340] D. Renusch, M. Schütze, Experience with the use of the acoustic emission technique for monitoring scale failure in wet and dry environments, Mater. High Temp. 22 (2005) 35–45.
[341] B. Merheb, G. Nassar, B. Nongaillard, G. Delaplace, J.C. Leuliet, Design and performance of a low-frequency non-intrusive acoustic technique for monitoring fouling in plate heat exchangers, J. Food Eng. 82 (2007) 518–527.
[342] Y.-L. Han, S.-Q. Zhang, S.-J. Zheng, W.-G. Zhu, B. Zhang, Failure analysis and acoustic emission tests of an in-service waste heat boiler, Eng. Fail. Anal. 13 (2006) 683–697.
[343] V.S. Cecco, F.L. Sharp, Transmit-receive eddy current probes for heat exchanger inspection, in, Non-Destructive Test., Elsevier (1988) 2581–2590.
[344] G.H. Wijnants, H.J. Abbink, W.R. Buist, EVALUATION BY EDDY CURRENT TECHNIQUES OF COPPER FILLED CORROSION CREVICES IN HEAT EXCHANGERS, in: Non-Destructive Testing'92, Elsevier, 1992: pp. 381–384.
[345] V.S. Cecco, F.L. Sharp, Recent advances in probe design for eddy current testing of heat exchangers, NDT Int. 23 (1990) 361, https://doi.org/10.1016/0308-9126(90)90917-D.
[346] D.H. Hur, M.S. Choi, D.H. Lee, S.J. Kim, J.H. Han, A case study on detection and sizing of defects in steam generator tubes using eddy current testing, Nucl. Eng. Des. 240 (2010) 204–208.
[347] K. Kim, K. Min, C. Kim, J.-G. Kim, M. Jhung, Detectability evaluation of the loose parts in steam generator by eddy current testing techniques, Nucl. Eng. Technol. 50 (2018) 1160–1167.
[348] T. Huang, G. Zhang, F. Liu, Design, manufacturing and repair of tube-to-tubesheet welds of steam generators of CPR1000 units, Nucl. Eng. Des. 333 (2018) 55–62.
[349] S. Tian, Z. Chen, M. Ueda, T. Yamashita, Signal processing schemes for Eddy Current Testing of steam generator tubes of nuclear power plants, Nucl. Eng. Des. 245 (2012) 78–88.
[350] T.K. Mitra, A. Pai, P. Kumar, Design and manufacture of tube to tubesheet joints of steam generator for 500 MWe Prototype Fast Breeder Reactor, 2009.
[351] U. Zscherpel, U. Ewert, P. Rost, M. Schmid, K. Spartiotis, A. WARRIKHOFF, X-ray Endoscopy for Inspection of Tube-to-Tube Sheet Welds in Heat Exchangers, in: 18th World Conf. Nondestruct. Test., Citeseer, 2012: pp. 16–20.
[352] S. Shimizu, T. Aota, M. Araki, Internal welding of tube-to-tubesheet joints of steam generator for sodium-cooled fast breeder reactor, FAPIG (Tokyo) (1975) 2–8.
[353] D.T. Thekkuden, A-H.I. Mourad, J.V. Christy, A.H. Idrisi, Assessment of Weld Quality Using Control Chart and Frequency Domain Analysis, in: ASME 2018 Press. Vessel. Pip. Conf., American Society of Mechanical Engineers, 2018: p. V06BT06A004-V06BT06A004.
[354] D.T. Thekkuden, A. Santhakumari, A. Sumesh, A.-H.I. Mourad, K. Rameshkumar, Instant detection of porosity in gas metal arc welding by using probability density distribution and control chart, Int. J. Adv. Manuf. Technol. 95 (2018) 4583–4606.
[355] K. Arunmuthu, T. Saravanan, J. Philip, T. Jayakumar, B. Raj, Image processing of radiographs of tube-to-tubesheet weld joints for enhanced detectability of defects, Insight-Non-Destructive Test. Cond. Monit. 50 (2008) 298–303.
[356] W. Zhao, K. Ding, G. Chen, A method of x-ray digital imaging automatic inspection on tube to tube sheet welded joints based on VC++, in, Citeseer (2008).
[357] K.-Q. DING, G. CHEN, L.-H. LIANG, B.-N. SHOU, S.-Q. LING, Digital Radiographic Imaging and Automatic Detection System for Welded Joint of Tube and Tube Sheet [J], Nondestruct. Test. 6, 2009.